

Excited-state locked amino analogues of the Green Fluorescent Protein chromophore with a giant Stokes shift

Snizhana O. Zaitseva,¹ Dilara A. Farkhutdinova², Nadezhda S. Baleeva,¹ Alexander Yu. Smirnov,¹ Marina B. Zagudaylova,¹ Aleksander M. Shakhov³, Artyom A. Astafiev^{3,2}, Mikhail S. Baranov,^{*1,4} and Anastasia V. Bochenkova^{*2}

ELECTRONIC SUPPLEMENTARY INFORMATION

Contents

1. Solvatochromic properties of the synthesized compounds	S2
2. Synthesis	S7
3. X-Ray results	S21
4. Copies of ^1H and ^{13}C NMR spectra	S22
5. Computational results	S71

¹ Institute of Bioorganic Chemistry, Russian Academy of Sciences, Miklukho-Maklaya 16/10, 117997 Moscow, Russia. baranovmikes@gmail.com

² Department of Chemistry, Lomonosov Moscow State University, Leninskie Gory 1/3, 119991 Moscow, Russia. bochenkova@phys.chem.msu.ru

³ Semenov Institute of Chemical Physics of RAS, Moscow, Russia

⁴ Pirogov Russian National Research Medical University, Ostrovitianov 1, Moscow 117997, Russia

1. Solvatochromic properties of the synthesized compounds

UV-VIS spectra were recorded with a Varian Cary 100 spectrophotometer. Fluorescence excitation and emission spectra were recorded with Agilent Cary Eclipse fluorescence spectrophotometer. The fluorescence quantum yield of compounds were measured according to the approaches presented in literature⁵.

Quantum yield was calculated by the formula:

$$\Phi_x = \Phi_{st} \times \frac{F_x}{F_{st}} \times \frac{f_{st}}{f_x} \times \frac{n_x^2}{n_{st}^2} \quad (1)$$

F is the area under the emission peak, f is the absorption factor, n is the refractive index of the solvent, the subscript x – the test substance, the subscript st – standard and Φ is the quantum yield.

$$f = 1 - 10^{-A} \quad (2)$$

A is absorbance at the excitation wavelength.

⁵ Würth C., Grabolle M., Pauli J., Spieles M., Resch-Genger U. *Nature Protocols*, **2013**, 8(8), 1535.

Table S1. Optical properties of non-locked compounds **4** and their locked analogues **8** in acetonitrile.

Ar		Abs ^a	Em ^b
Ph	4a	356 (9000)	400
	8a	348 (10500)	480
pOMe-C ₆ H ₄	4b	360 (12000)	413
	8b	352 (13500)	468
pCl-C ₆ H ₄	4c	363 (9500)	385
	8c	353 (10000)	490
pBr-C ₆ H ₄	4d	363 (8500)	387
	8d	353 (9000)	490
pCOOMe-C ₆ H ₄	4e	379 (8000)	410
	8e	365 (7500)	521
Pyridin-4-yl	4f	373 (6500)	400
	8f	362 (6500)	505

a – peak maximum in nm and extinction coefficient in (M cm)⁻¹; b – peak maximum in nm

Table S2. Optical properties of **8a-g** in various solvents.

	Ar		Dioxane	EtOAc	CH ₃ CN	MeOH	H ₂ O
8a	Ph	Abs ^a	351 (10500)	352 (10000)	348 (10500)	341 (9500)	338 (11000)
		Em ^b	460 (9.3)	470 (4.5)	480 (2.8)	472 (1.9)	470 (0.4)
8b	pOMe-C ₆ H ₄	Abs ^a	351 (13000)	353 (12000)	352 (13500)	343 (12000)	343 (14000)
		Em ^b	456 (18)	461 (9.7)	468 (5.1)	460 (3.8)	468 (0.5)
8c	pCl-C ₆ H ₄	Abs ^a	355 (9500)	360 (8500)	353 (10000)	349 (9500)	346 (10500)
		Em ^b	431 (18)	470 (6.2)	490 (2.7)	483 (1.1)	481 (0.3)
8d	pBr-C ₆ H ₄	Abs ^a	361 (9000)	361 (9500)	353 (9000)	350 (8000)	346 (10500)
		Em ^b	431 (18)	470 (6.9)	490 (2.4)	482 (0.9)	481 (0.2)
8e	pCOOMe-C ₆ H ₄	Abs ^a	368 (7000)	372 (7000)	365 (7500)	359 (7000)	349 (8500)
		Em ^b	430 (22)	466 (6.5)	521 (1.7)	517 (0.5)	– ^c
8f	Pyridin-4-yl	Abs ^a	370 (6000)	370 (6500)	362 (6500)	361 (6500)	348 (6500)
		Em ^b	430 (20)	465 (5.8)	505 (1.2)	– ^c	– ^c
8g	pOH-C ₆ H ₄	Abs ^a	352 (8000)	352 (7000)	351 (8500)	350 (8000)	344 (8500)
		Em ^b	448 (10)	458 (7.1)	466 (3.6)	458 (2.2)	461 (0.4)

a – peak maximum in nm and extinction coefficient in (M cm)⁻¹; b – peak maximum in nm and fluorescence quantum yield in %; c – non fluorescent.

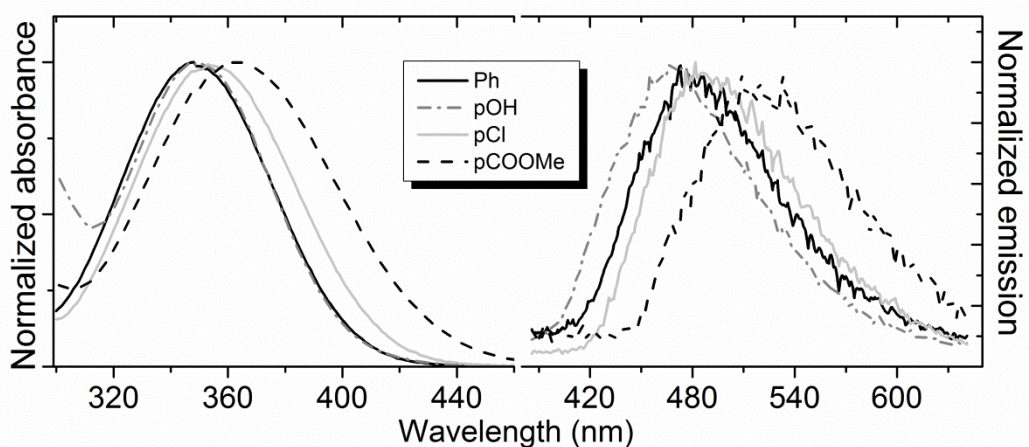


Figure S1 Absorbance (left) and emission (right) spectra of **8a,c,f,g** in acetonitrile. Emission spectra are recorded at an excitation wavelength of 340 nm.

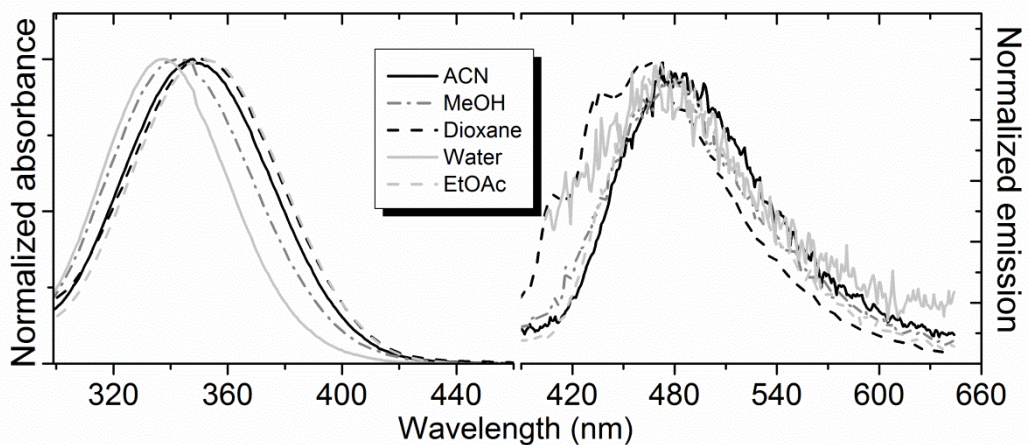


Figure S2 Absorbance (left) and emission (right) spectra of **8a** ($\text{Ar} = \text{Ph}$) in various solvents. Emission spectra are recorded at an excitation wavelength of 340 nm.

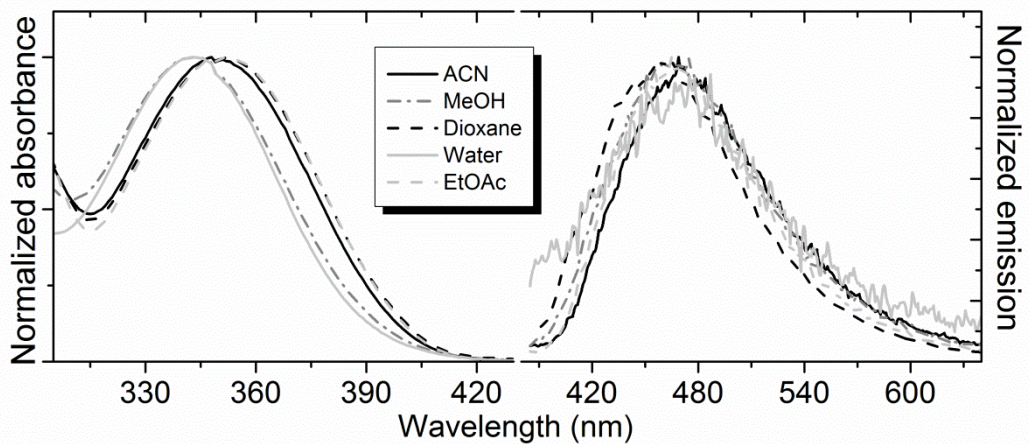


Figure S3 Absorbance (left) and emission (right) spectra of **8b** ($\text{Ar} = \text{pOMe-C}_6\text{H}_4$) in various solvents. Emission spectra are recorded at an excitation wavelength of 340 nm.

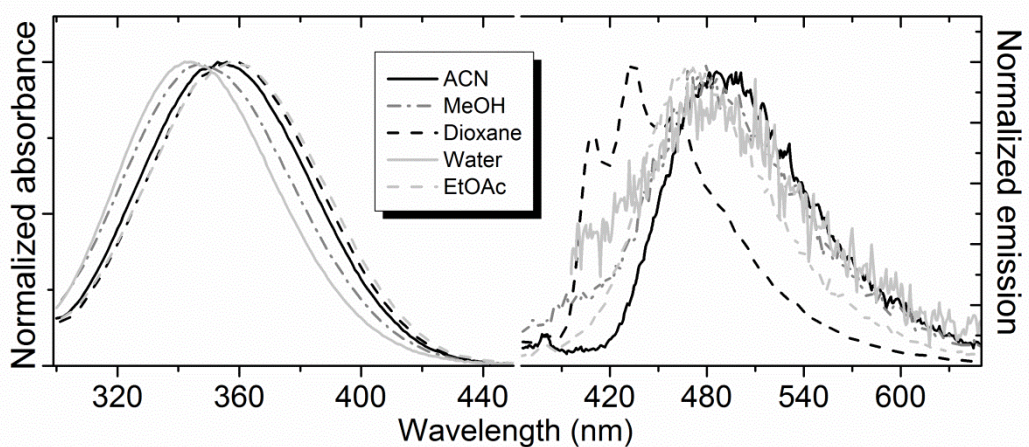


Figure S4 Absorbance (left) and emission (right) spectra of **8c** ($\text{Ar} = \text{pCl-C}_6\text{H}_4$) in various solvents. Emission spectra are recorded at an excitation wavelength of 340 nm.

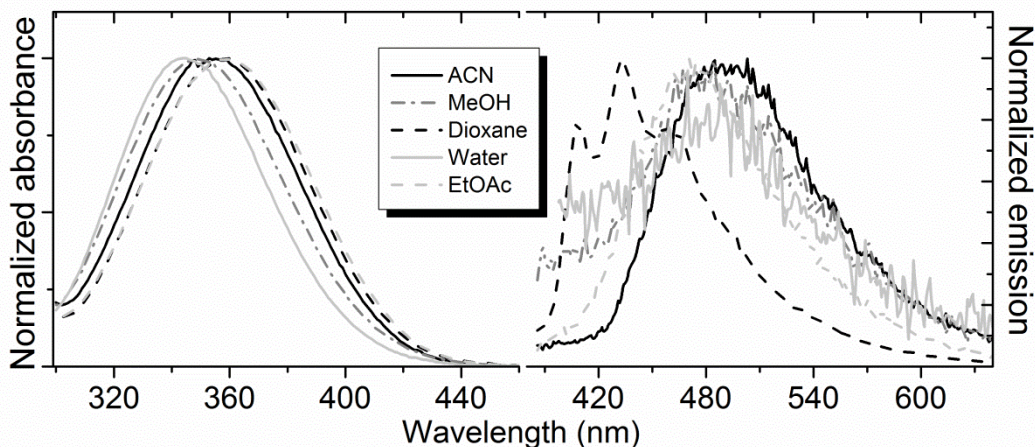


Figure S5 Absorbance (left) and emission (right) spectra of **8d** ($\text{Ar} = \text{pBr-C}_6\text{H}_4$) in various solvents. Emission spectra are recorded at an excitation wavelength of 340 nm.

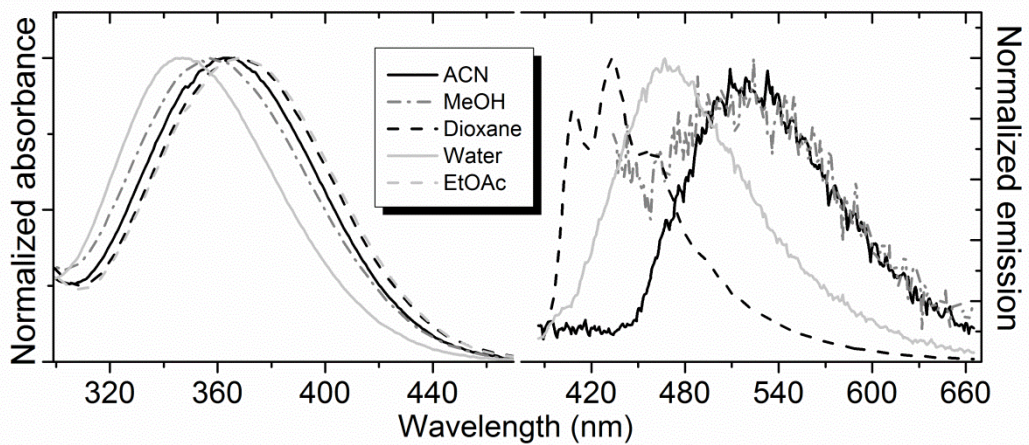


Figure S6 Absorbance (left) and emission (right) spectra of **8e** ($\text{Ar} = \text{pCOOMe-C}_6\text{H}_4$) in various solvents. Emission spectra are recorded at an excitation wavelength of 340 nm.

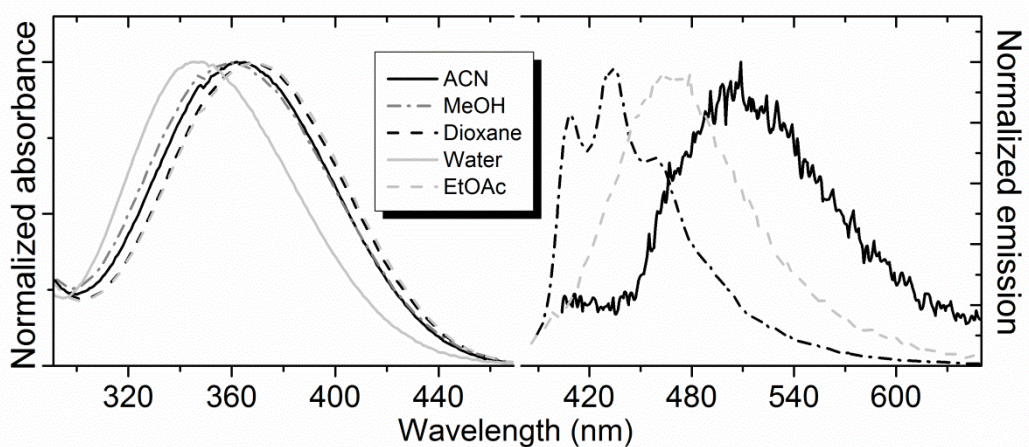


Figure S7 Absorbance (left) and emission (right) spectra of **8f** ($\text{Ar} = \text{Pyridin-4-yl}$) in various solvents. Emission spectra are recorded at an excitation wavelength of 340 nm.

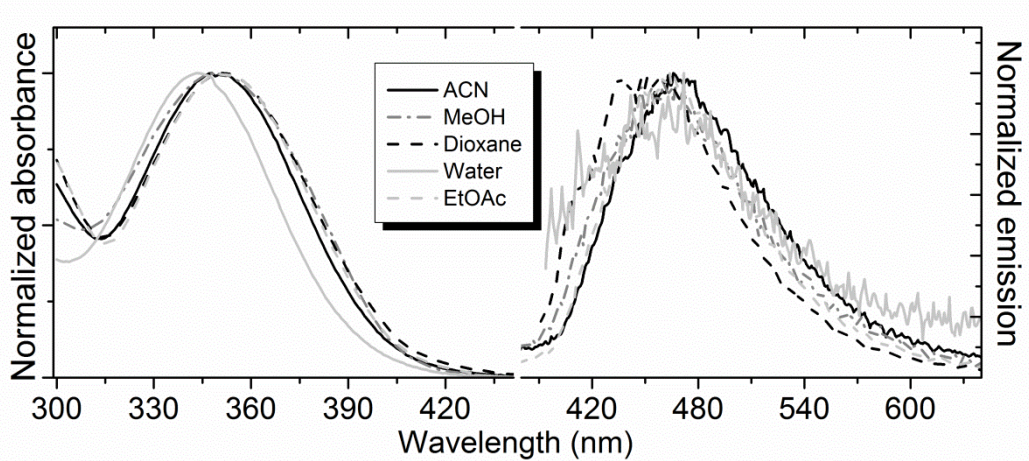


Figure S8 Absorbance (left) and emission (right) spectra of **8g** ($\text{Ar} = \text{pOH-C}_6\text{H}_4$) in various solvents. Emission spectra are recorded at an excitation wavelength of 340 nm.

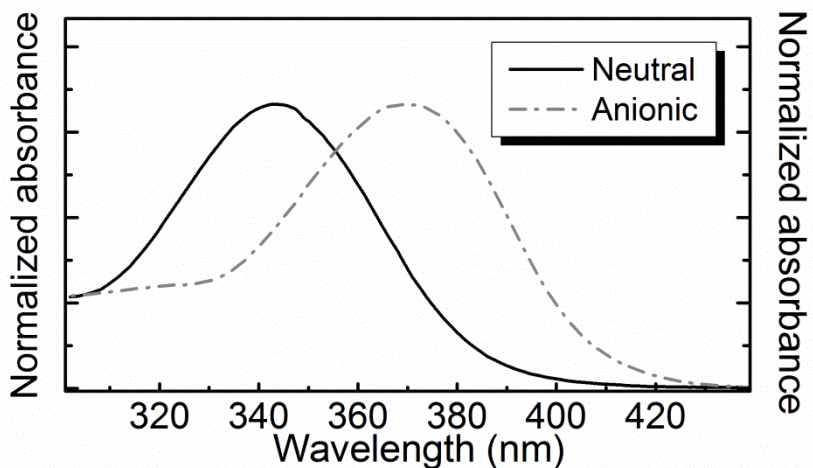


Figure S9 Absorption spectra of **8g** ($\text{Ar} = \text{pOH-C}_6\text{H}_4$) in neutral and anionic forms (in water buffer solutions).

Table S3. Optical properties of non-locked compounds **7** and their locked analogues **9** in acetonitrile.

Ar		Abs ^a	Em ^b
Ph	7a	458 (9500)	515
	9a	419 (7000)	501
pOMe-C ₆ H ₄	7b	461 (10500)	~540
	9b	410 (9000)	533
pCl-C ₆ H ₄	7c	465 (10500)	~540
	9c	422 (7500)	510; 545
pBr-C ₆ H ₄	7d	466 (9000)	~550
	9d	423 (7000)	511; 543
pCOOMe-C ₆ H ₄	7e	476 (9500)	~560
	9e	440 (6000)	~562

a – peak maximum in nm and extinction coefficient in (M cm)⁻¹; b – peak maximum in nm

Table S4. Optical properties of **9a-e** in various solvents

	Ar		Dioxane	EtOAc	CH ₃ CN	MeOH	H ₂ O
9a	Ph	Abs ^a	426 (7000)	426 (8000)	419 (7000)	409 (7000)	402 (7500)
		Em ^b	510 (62)	502 (30)	501 (25)	498 (30)	498 (30)
9b	pOMe-C ₆ H ₄	Abs ^a	402 (9000)	411 (8500)	410 (9000)	416 (7500)	398 (9500)
		Em ^b	530 (43)	532 (34)	533 (23)	528 (23)	495 (13)
9c	pCl-C ₆ H ₄	Abs ^a	425 (8000)	423 (7000)	422 (7500)	414 (6500)	406 (7000)
		Em ^b	518; 550 (16)	512; 547 (15)	510; 545 (12)	510; 542 (11)	535 (4.2)
9d	pBr-C ₆ H ₄	Abs ^a	429 (7500)	427 (7000)	423 (7000)	420 (6500)	408 (7000)
		Em ^b	520; 552 (13)	512; 548 (11)	512; 547 (10)	511; 543 (8.3)	~530 (3.7)
9e	pCOOMe-C ₆ H ₄	Abs ^a	445 (6000)	442 (6000)	440 (6000)	434 (5500)	423 (6000)
		Em ^b	542 (6.0)	538 (6.0)	545 (5.6)	~562 (2.1)	– ^c

a – peak maximum in nm and extinction coefficient in (M cm)⁻¹; b – peak maximum in nm and fluorescence quantum yield in %; c – non fluorescent.

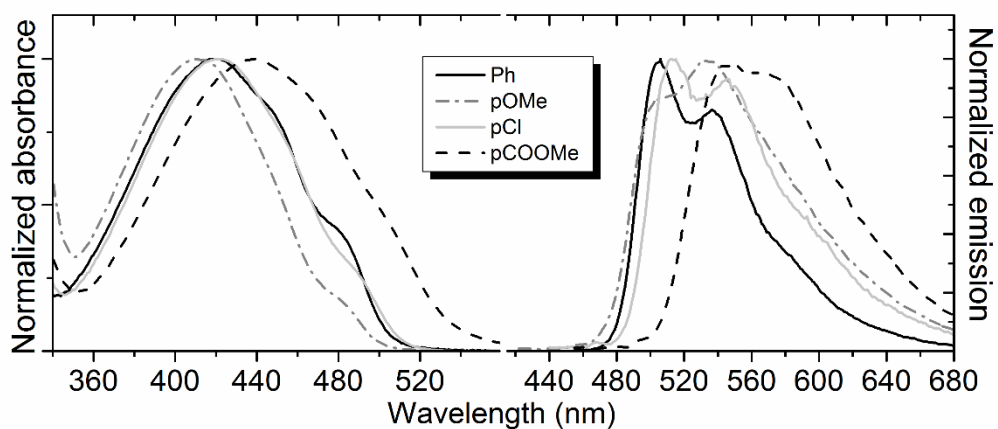


Figure S10 Absorbance (left) and emission (right) spectra of **9a-c,e** in acetonitrile. Emission spectra are recorded at an excitation wavelength of 400 nm.

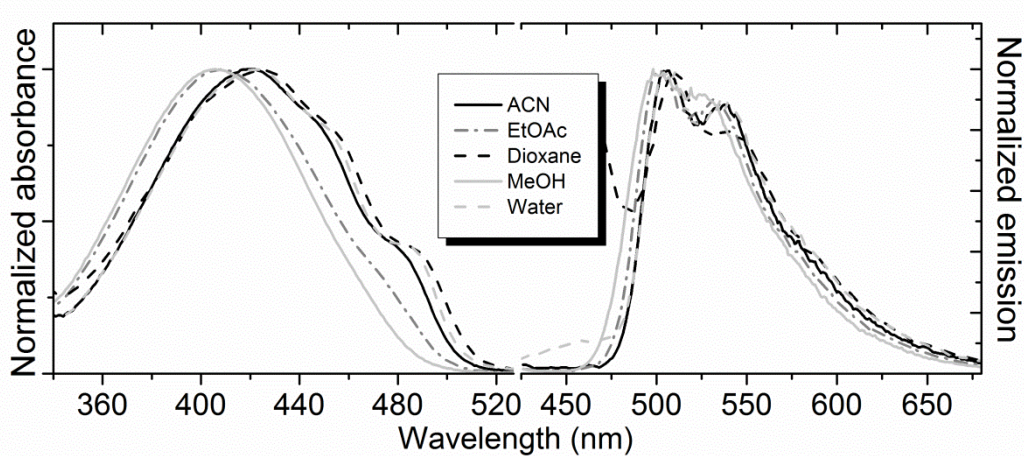


Figure S11 Absorbance (left) and emission (right) spectra of **9a** ($\text{Ar} = \text{Ph}$) in various solvents. Emission spectra are recorded at an excitation wavelength of 400 nm.

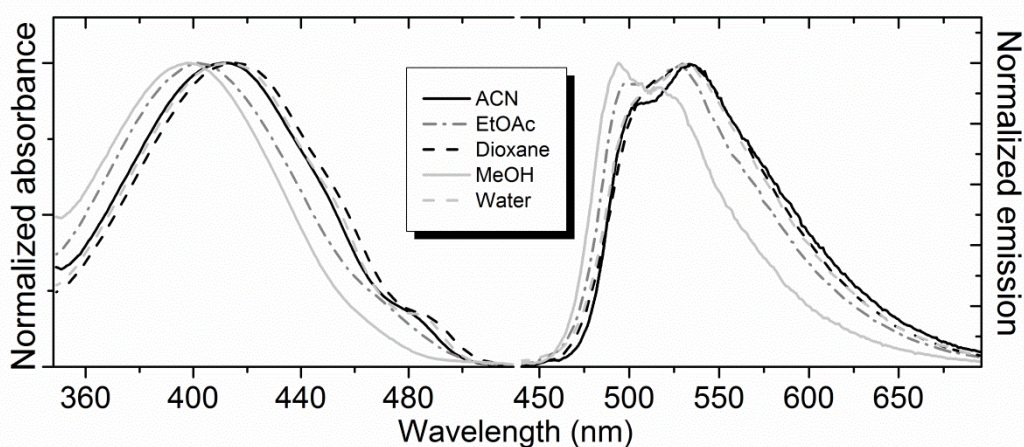


Figure S12 Absorbance (left) and emission (right) spectra of **9b** ($\text{Ar} = \text{pOMe-C}_6\text{H}_4$) in various solvents. Emission spectra are recorded at an excitation wavelength of 400 nm.

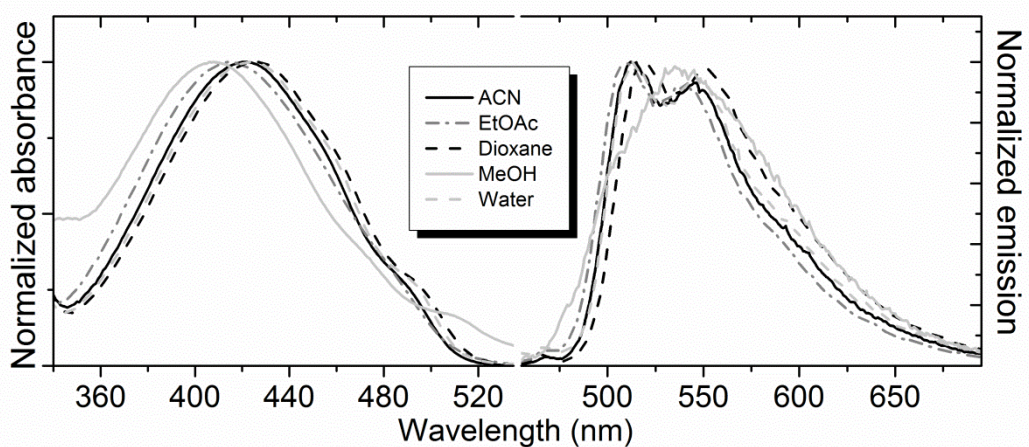


Figure S13 Absorbance (left) and emission (right) spectra of **9c** ($\text{Ar} = \text{pCl-C}_6\text{H}_4$) in various solvents. Emission spectra are recorded at an excitation wavelength of 400 nm.

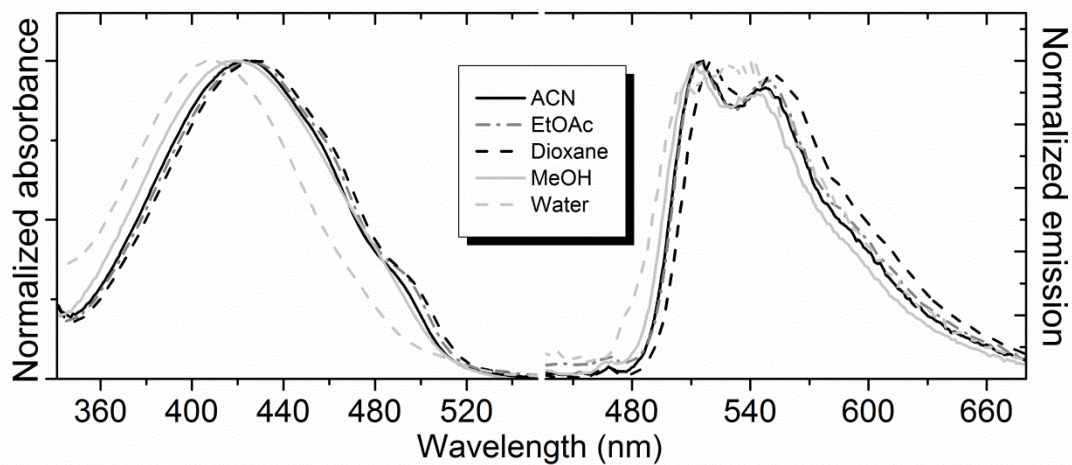


Figure S14 Absorbance (left) and emission (right) spectra of **9d** ($\text{Ar} = \text{pBr-C}_6\text{H}_4$) in various solvents. Emission spectra are recorded at an excitation wavelength of 400 nm.

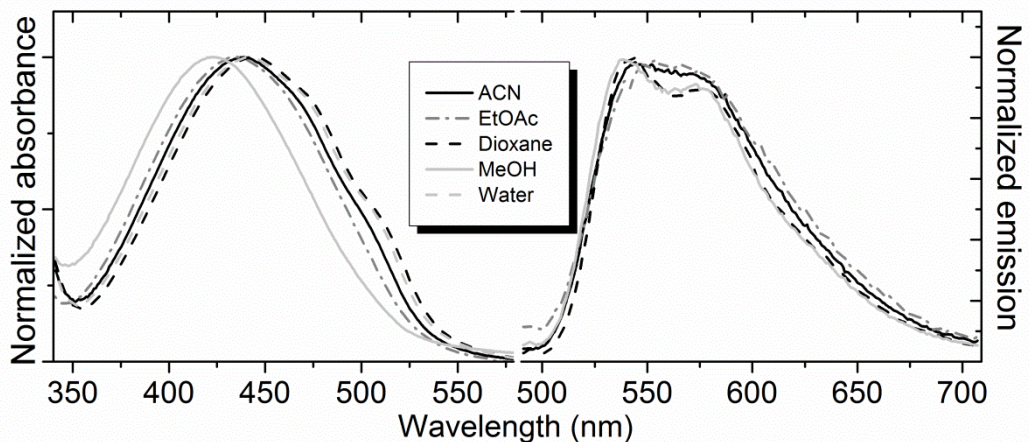
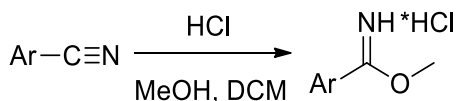


Figure S15 Absorbance (left) and emission (right) spectra of **9e** ($\text{Ar} = \text{pCOOMe-C}_6\text{H}_4$) in various solvents. Emission spectra are recorded at an excitation wavelength of 400 nm.

2. Synthesis

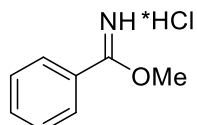
Commercially available reagents were used without additional purification. E. Merck Kieselgel 60 was used for column chromatography. Thin layer chromatography (TLC) was performed on silica gel 60 F₂₅₄ glass-backed plates (MERCK). Visualization was effected by UV light (254 or 312nm) and staining with KMnO₄.

NMR spectra were recorded on a 700 MHz Bruker Avance III NMR at 303 K, 800 MHz Bruker Avance III NMR at 333 K and Bruker Fourier 300. Chemical shifts are reported relative to residue peaks of CDCl₃ (7.27 ppm for ¹H and 77.0 ppm for ¹³C) or DMSO-d₆ (2.51 ppm for ¹H and 39.5 ppm for ¹³C). Melting points were measured on a SMP 30 apparatus. High-resolution mass spectra (HRMS) spectra were recorded on a LTQ Orbitrap Elite (ThermoFisher Scientific, USA) equipped with a dual-nebulizer ESI source.



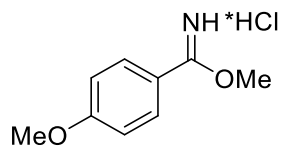
General method for the preparation of methyl arylimidate hydrochlorides (3a-f):

The solution of corresponding nitrile (0.02 mol) in 8 mL of dry dichloromethane and 1 mL (0.025 mol) of methanol was cooled to 0 °C. Dry hydrogen chloride was bubbled through the mixture for 2-3 hours (precipitate formation indicates completion of the reaction) while being intensely stirred; the temperature was maintained within 0-5 °C. Then the reaction mixture was stirred at room temperature for 20 h. Afterwards 20 mL of diethyl ether were added, precipitate was filtered, washed with Et₂O (3x10 mL) and dried under vacuum.



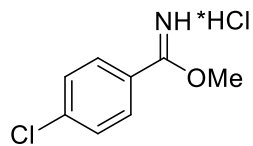
Methyl benzimidate hydrochloride (3a)

White solid (15.41 g, 90%); ¹H NMR (700 MHz, 303 K, CDCl₃) δ ppm 12.84 (s, 1H), 12.11 (s, 1H), 8.43 (d, *J*=7.4 Hz, 2H), 7.74 (t, *J*=7.4 Hz, 1H), 7.60 (t, *J*=7.9 Hz, 2H), 4.60 (s, 3H).⁶



Methyl 4-methoxybenzimidate hydrochloride (3b)

White solid (3.62 g, 87%); ¹H NMR (700 MHz, 303 K, CDCl₃) δ ppm 12.42 (s, 1H), 11.71(s, 1H), 8.42 (d, *J*=9.0 Hz, 2H), 7.03 (d, *J*=9.0 Hz, 2H), 4.53 (s, 3H), 3.89 (s, 3H).⁷



Methyl 4-chlorobenzimidate hydrochloride (3c)

White solid (3.13 g, 76%); ¹H NMR (700 MHz, 303 K, CDCl₃) δ ppm 12.78 (s, 1H), 12.07(s, 1H), 8.35 (d, *J*=8.6 Hz, 2H), 7.53 (d, *J*=8.6 Hz, 2H), 4.55 (s, 3H).⁸

⁶ D. J. Connolly, P. M. Lacey, M. McCarthy, C. P. Saunders, A-M. Carroll, R. Goddard, P. J. Guiry. *J. Org. Chem.* 2004. 69. 20. 6572–6589.

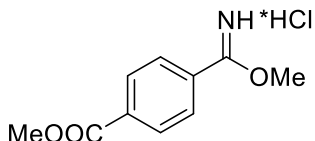
⁷ X-J. Han, M. Yao, C-D. Lu. *Org. Lett.* 2012. 14. 11. 2906-2909.

⁸ M. A. Pérez, C. A. Dorado, J. L. Soto. *Synthesis*. 1983. 6. 483-486.



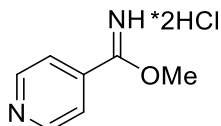
Methyl 4-bromobenzimidate hydrochloride (3d)

White solid (4.17 g, 83%); mp = 186–188 °C; ¹H NMR (700 MHz, 303 K, CDCl₃) δ ppm 12.86 (s, 1H), 12.14 (s, 1H), 8.28 (d, *J*=8.5 Hz, 2H), 7.71 (d, *J*=8.5 Hz, 2H), 4.56 (s, 3H); ¹³C NMR (75 MHz, 303 K, DMSO-d₆) δ ppm 171.2, 132.7, 131.6, 131.0, 123.7, 61.5; HRMS (ESI) m/z: 213.9863 found (calcd for C₈H₉BrNO, [M-Cl]⁺ 213.9862).



Methyl 4-(imino(methoxy)methyl)benzoate hydrochloride (3e)

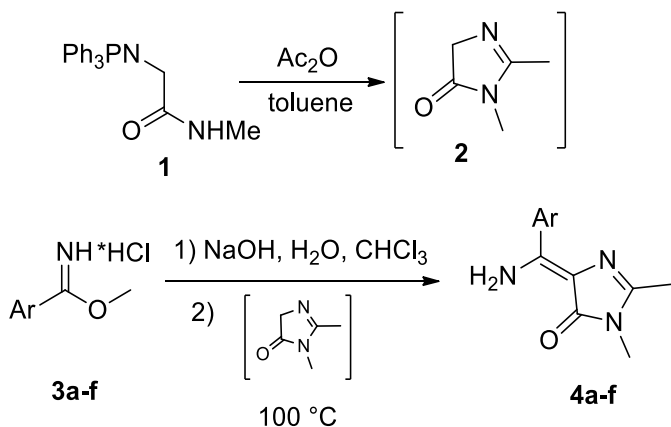
White solid (3.81 g, 83%); mp = 190–193 °C; ¹H NMR (700 MHz, 303 K, CDCl₃) δ ppm 13.05 (s, 1H), 12.33 (s, 1H), 8.47 (d, *J*=8.5 Hz, 2H), 8.21 (d, *J*=8.5 Hz, 2H), 4.60 (s, 3H), 3.96 (s, 3H); ¹³C NMR (75 MHz, 303 K, DMSO-d₆) δ ppm 171.1, 165.4, 136.2, 130.1, 129.7, 128.5, 61.7, 52.7; HRMS (ESI) m/z: 194.0812 found (calcd for C₁₀H₁₂NO₃, [M-Cl]⁺ 194.0812).



Methyl isonicotinimidate hydrochloride (3f)

White solid (3.80 g, 91%); ¹H NMR (700 MHz, 303 K, DMSO-d₆) δ ppm 8.96 (d, *J*=6.4 Hz, 2H), 8.57 (s, 1H), 8.18 (d, *J*=6.4 Hz, 2H), 8.02 (s, 1H), 3.06 (s, 3H).⁹

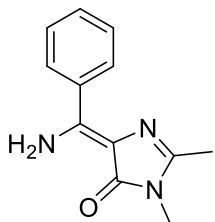
⁹ B. Whelan, I. Iriepa, E. Galvez. Synthesis 1994. 1994. 8. 832-836.



General method for the preparation of (E)-5-(amino(aryl)methylene)-2,3-dimethyl-3,5-dihydro-4*H*-imidazol-4-ones (4a-f):

Solution of 2,3-dimethyl-3,5-dihydro-4*H*-imidazol-4-one **2** in toluene was generated as reported previously¹⁰ - N-methyl-2-((triphenylphosphoranylidene)amino)acetamide **1** (3.50 g, 10.0 mmol) was degassed by three vacuum/argon cycles. Toluene (50 ml) and the acetic anhydride (1.0 g, 10 mmol) were added and the mixture was stirred at room temperature until the complete dissolution (approx. 40 min).

Corresponding imidate hydrochloride **3** (7.0 mmol) was suspended in 50 mL of chloroform, treated with sodium hydroxide solution (1 g in 10 mL of H_2O), dried over Na_2SO_4 and the solvent was removed in vacuum. Afterwards molecular sieves (4\AA , 5 g) and the solution of 2,3-dimethyl-3,5-dihydro-4*H*-imidazol-4-one **2** in toluene (see above) were added to the crude imidate. The mixture was stirred at 100°C for 15-30 minutes. The mixture was cooled to the room temperature, molecular sieves were removed by filtration and washed with dichloromethane (2x50 mL). The solvent was removed in vacuum and the product was purified by silica gel column chromatography (EtOAc-Hex 1:9).

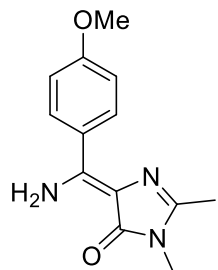


(E)-5-(amino(phenyl)methylene)-2,3-dimethyl-3,5-dihydro-4*H*-imidazol-4-one (4a)

Yellow solid (220 mg, 15%); mp = 210–213 °C; ^1H NMR (700 MHz, 303 K, DMSO-d_6) δ ppm 8.66 (br.s., 1H), 7.89–7.88 (m, 2H), 7.70 (br.s., 1H), 7.51–7.48 (m, 3H), 3.11 (s, 3H), 2.16 (s, 3H); ^{13}C NMR (176 MHz, 303 K, DMSO-d_6) δ ppm 168.1, 153.1, 146.5, 133.7, 130.2, 129.3,

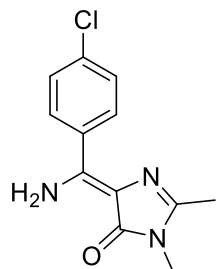
¹⁰ Zaitseva S.O., Golodukhina S.V., Baleeva N.S., Levina E.A., Smirnov A.Yu., Zagudaylova M.B., Baranov M.S. *ChemistrySelect*. 2018, 3, 8593–8596.

127.9, 113.6, 25.8, 14.3; HRMS (ESI) m/z: 216.1132 found (calcd for C₁₂H₁₄N₃O⁺, [M+H]⁺ 216.1132).



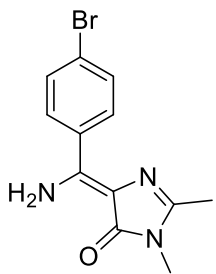
(E)-5-(amino(4-methoxyphenyl)methylene)-2,3-dimethyl-3,5-dihydro-4H-imidazol-4-one (4b)

Yellow solid (240 mg, 14%); mp = 221–224 °C; ¹H NMR (700 MHz, 303 K, DMSO-d₆) δ ppm 8.74 (br.s., 1H), 7.97 (d, J=8.9 Hz, 2H), 7.62 (br.s., 1H), 7.05 (d, J=8.9 Hz, 2H), 3.83 (s, 3H), 3.11 (s, 3H), 2.17 (s, 3H); ¹³C NMR (176 MHz, 303 K, DMSO-d₆) δ ppm 168.0, 160.9, 155.7, 145.8, 131.1, 125.7, 113.4, 113.1, 55.3, 25.8, 14.3; HRMS (ESI) m/z: 246.1237 found (calcd for C₁₃H₁₆N₃O₂⁺, [M+H]⁺ 246.1238).



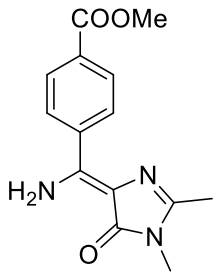
(E)-5-(amino(4-chlorophenyl)methylene)-2,3-dimethyl-3,5-dihydro-4H-imidazol-4-one (4c)

Yellow solid (250 mg, 14%); mp = 168–171 °C; ¹H NMR (700 MHz, 303 K, DMSO-d₆) δ ppm 8.61 (br.s., 1H), 7.93 (d, J=8.5 Hz, 2H), 7.74 (br.s., 1H), 7.57 (d, J=8.5 Hz, 2H), 3.11 (s, 3H), 2.17 (s, 3H); ¹³C NMR (176 MHz, 303 K, DMSO-d₆) δ ppm 168.1, 151.4, 147.0, 134.9, 132.4, 131.2, 128.0, 113.8, 25.8, 14.3; HRMS (ESI) m/z: 250.0739 found (calcd for C₁₂H₁₃ClN₃O⁺, [M+H]⁺ 250.0742).



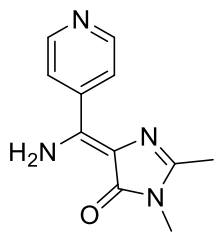
(E)-5-(amino(4-bromophenyl)methylene)-2,3-dimethyl-3,5-dihydro-4H-imidazol-4-one (4d)

Yellow solid (210 mg, 10%); mp = 162–165 °C; ¹H NMR (700 MHz, 303 K, DMSO-d₆) δ ppm 8.59 (br.s., 1H), 7.85 (d, *J*=8.5 Hz, 2H), 7.74 (br.s., 1H), 7.71 (d, *J*=8.5 Hz, 2H), 3.11 (s, 3H), 2.17 (s, 3H); ¹³C NMR (176 MHz, 303 K, DMSO-d₆) δ ppm 168.1, 151.5, 147.0, 132.7, 131.4, 131.0, 123.8, 113.8, 25.8, 14.3; HRMS (ESI) m/z: 294.0235 found (calcd for C₁₂H₁₃BrN₃O⁺, [M+H]⁺ 294.0237).



Methyl (E)-4-(amino(1,2-dimethyl-5-oxo-1,5-dihydro-4H-imidazol-4-ylidene)methyl)benzoate (4e)

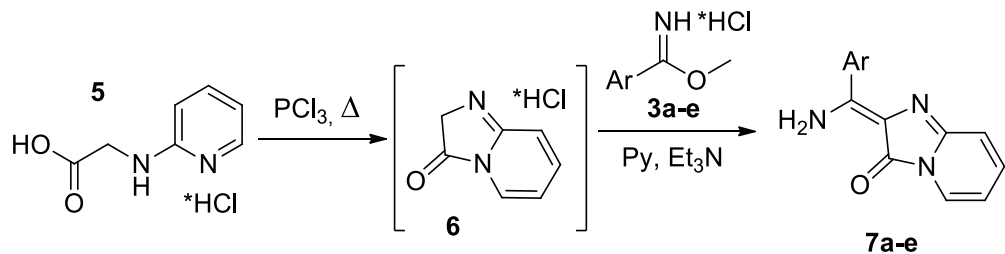
Yellow solid (160 mg, 8%); mp = 181–184 °C; ¹H NMR (700 MHz, 303 K, DMSO-d₆) δ ppm 8.59 (br.s., 1H), 8.05 (d, *J*=8.4 Hz, 2H), 8.00 (d, *J*=8.4 Hz, 2H), 7.80 (br.s., 1H), 3.89 (s, 3H), 3.12 (s, 3H), 2.17 (s, 3H); ¹³C NMR (176 MHz, 303 K, DMSO-d₆) δ ppm 168.2, 165.7, 151.4, 147.4, 138.1, 130.7, 129.7, 128.6, 114.2, 52.3, 25.8, 14.3; HRMS (ESI) m/z: 274.1182 found (calcd for C₁₄H₁₆N₃O₃⁺, [M+H]⁺ 274.1186).



(E)-5-(amino(pyridin-4-yl)methylene)-2,3-dimethyl-3,5-dihydro-4H-imidazol-4-one

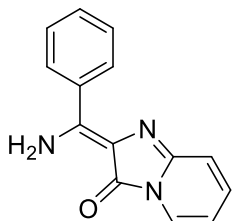
(4f)

Yellow solid (120 mg, 8%); mp = 159–162 °C; ¹H NMR (700 MHz, 303 K, DMSO-d₆) δ ppm 8.72 (dd, *J*=6.1, 1.6 Hz, 2H), 7.83 (dd, *J*=6.1 Hz, 1.6 Hz, 2H), 3.12 (s, 3H), 2.18 (s, 3H); ¹³C NMR (176 MHz, 303 K, DMSO-d₆) δ ppm 168.2, 149.58, 149.56, 148.1, 140.9, 123.4, 114.6, 25.9, 14.3; HRMS (ESI) m/z: 217.1082 found (calcd for C₁₁H₁₃N₄O⁺, [M+H]⁺ 217.1084).



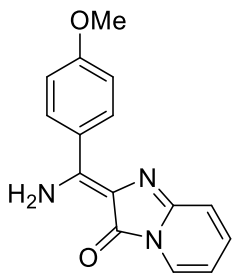
General method for the preparation of (E)-2-(amino(aryl)methylene)imidazo[1,2-a]pyridin-3(2H)-ones (7a-e):

Pyridin-2-yl-glycine hydrochloride **5** (1 g, 5 mmol) was dissolved in PCl_3 (10mL) under argon. The mixture was refluxed for 3 h and phosphorus trichloride was removed under vacuum. Afterwards pyridine (8 mL), triethylamine (1 mL) and corresponding imidate hydrochloride **3** (4 mmol) were added and the mixture was stirred for 18 h at room temperature. The solvent was removed under vacuum, the residue was dissolved in 200 mL of chloroform and washed with saturated NaHCO_3 solution (1x100 mL) and brine (1x50 mL). The solution was dried over Na_2SO_4 and the solvent was removed under vacuum. The product was purified by column chromatography (CHCl_3).



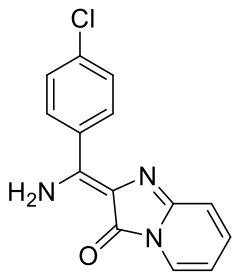
(E)-2-(amino(phenyl)methylene)imidazo[1,2-a]pyridin-3(2H)-one (7a)

Red solid (237 mg, 25%); mp \sim 145 °C with decomposition; ^1H NMR (700 MHz, 303 K, DMSO-d_6) δ ppm 9.64 (s, 1H), 8.82 (s, 1H), 8.23 (d, $J=8.8$ Hz, 2H), 7.88 (d, $J=7.0$ Hz, 1H), 7.20 (d, $J=8.8$ Hz, 2H), 7.10-7.03 (m, 3H), 6.46 (t, $J=6.6$ Hz, 1H); ^{13}C NMR (176 MHz, 303 K, DMSO-d_6) δ ppm 161.8, 158.8, 142.0, 132.9, 131.0, 129.9, 128.9, 128.1, 124.0, 118.7, 114.1, 108.8; HRMS (ESI) m/z: 238.0973 found (calcd for $\text{C}_{14}\text{H}_{12}\text{N}_3\text{O}^+$, $[\text{M}+\text{H}]^+$ 238.0980).



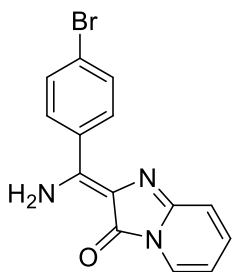
(E)-2-(amino(4-methoxyphenyl)methylene)imidazo[1,2-a]pyridin-3(2H)-one (7b)

Light green solid (120 mg, 11%); mp = 164–166 °C; ¹H NMR (700 MHz, 303 K, DMSO-d₆) δ ppm 9.57 (br.s., 1H), 8.75 (br.s., 1H), 8.16 (d, J=8.9 Hz, 2H), 7.80 (d, J=7.0 Hz), 7.12 (d, J=8.9 Hz, 2H), 7.04–6.96 (m, 2H), 6.39 (td, J=6.6, 1.0 Hz, 1H), 3.86 (s, 3H); ¹³C NMR (176 MHz, 303 K, DMSO-d₆) δ ppm 161.7, 161.6, 158.3, 141.5, 132.0, 128.5, 124.8, 124.0, 118.6, 113.7, 113.6, 108.7, 55.4; HRMS (ESI) m/z: 268.1076 found (calcd for C₁₅H₁₄N₃O₂⁺, [M+H]⁺ 268.1081).



(E)-2-(amino(4-chlorophenyl)methylene)imidazo[1,2-a]pyridin-3(2H)-one (7c)

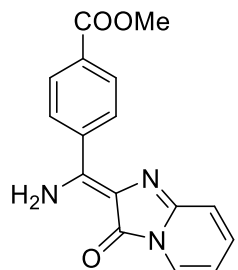
Orange solid (366 mg, 34%); mp ~ 235 °C with decomposition; ¹H NMR (700 MHz, 303 K, DMSO-d₆) δ ppm 9.42 (br.s., 1H), 8.87 (br.s., 1H), 8.08 (d, J=8.6 Hz, 2H), 7.81 (d, J=7.0 Hz, 1H), 7.64 (d, J=8.6 Hz, 2H), 7.01–6.98 (m, 2H), 6.39 (ddd, J=7.1, 4.0, 3.2 Hz, 1H); ¹³C NMR (176 MHz, 303 K, DMSO-d₆) δ ppm 161.9, 157.1, 142.3, 135.9, 131.8, 131.6, 129.2, 128.2, 124.1, 118.6, 114.2, 108.8; HRMS (ESI) m/z: 272.0581 found (calcd for C₁₄H₁₁ClN₃O⁺, [M+H]⁺ 272.0585).



(E)-2-(amino(4-bromophenyl)methylene)imidazo[1,2-a]pyridin-3(2H)-one (7d)

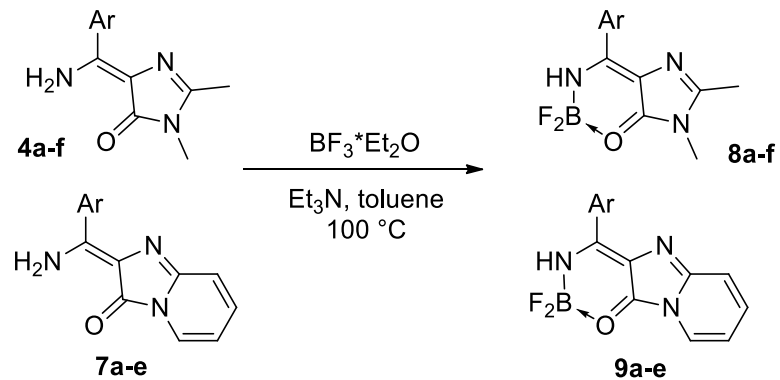
Orange solid (142 mg, 11%); mp = 243–245 °C; ¹H NMR (700 MHz, 303 K, DMSO-d₆) δ ppm 9.41 (br.s., 1H), 8.86 (br.s., 1H), 8.00 (d, J=8.5 Hz, 2H), 7.80 (d, J=7.0 Hz, 1H), 7.78 (d,

J=8.5 Hz, 2H), 7.01-6.97 (m, 2H), 6.39 (ddd, *J*=7.0, 3.7, 3.6 Hz, 1H); ^{13}C NMR (176 MHz, 303 K, DMSO-*d*₆) δ ppm 161.9, 157.2, 142.4, 132.0, 132.0, 131.2, 129.2, 124.8, 124.1, 118.6, 114.2, 108.9; HRMS (ESI) m/z: 316.0078 found (calcd for C₁₄H₁₁BrN₃O⁺, [M+H]⁺ 316.0080).



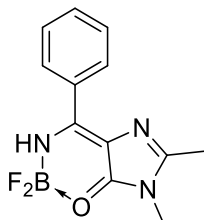
Methyl (E)-4-(amino(3-oxoimidazo[1,2-a]pyridin-2(3H)-ylidene)methyl)benzoate (7e)

Red solid (280mg, 24%); mp = 242–245 °C; ^1H NMR (700 MHz, 303 K, DMSO-d₆) δ ppm 9.39 (br.s., 1H), 8.92 (br.s., 1H), 8.14 (d, *J*=8.3 Hz, 2H), 8.11 (d, *J*=8.3 Hz, 2H), 7.81 (d, *J*=7.0 Hz, 1H), 7.02-6.97 (m, 2H), 6.40 (ddd, *J*=7.0, 5.2, 2.0 Hz, 1H), 3.91 (s, 3H); ^{13}C NMR (176 MHz, 303 K, DMSO-d₆) δ ppm 165.7, 162.1, 157.1, 142.7, 137.3, 131.3, 130.3, 129.4, 128.7, 124.1, 118.7, 114.6, 108.9, 52.4; HRMS (ESI) m/z: 296.1026 found (calcd for C₁₆H₁₄N₃O₃⁺, [M+H]⁺ 296.1030).



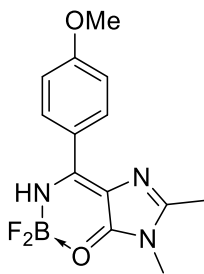
General method for the preparation of locked derivatives:

Corresponding chromophore **4** or **7** (0.3 mmol) and triethylamine (0.42 mL, 3 mmol) were dissolved in toluene (5 mL). Boron trifluoride diethyl etherate (0.22 mL, 1.8 mmol) was added and the reaction mixture was heated up to 100 °C for 2-2.5 hours. After that 20 mL of ethylacetate were added and organic layer was washed with water (3x10 mL), brine (1x10 mL) and dried over Na₂SO₄ and the solvent was removed in vacuum. The product was purified by column chromatography (CHCl₃).



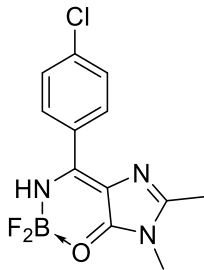
(E)-5-(((difluoroboranyl)amino)(phenyl)methylene)-2,3-dimethyl-3,5-dihydro-4*H*-imidazol-4-one (8a**)**

Yellow solid (54 mg, 69%); mp = 230–233 °C; ¹H NMR (700 MHz, 303 K, DMSO-d₆) δ ppm 9.51 (s, 1H), 8.21 (d, *J*=7.2 Hz, 2H), 7.67 (t, *J*=7.3 Hz, 1H), 7.59 (t, *J*=7.5 Hz, 2H), 3.43 (s, 3H), 2.33 (s, 3H); ¹³C NMR (176 MHz, 303 K, DMSO-d₆) δ ppm 161.7, 157.9, 144.1, 132.6, 130.7, 129.7, 128.5, 112.2, 27.9, 13.4; HRMS (ESI) m/z: 264.1111 found (calcd for C₁₂H₁₃BF₂N₃O⁺, [M+H]⁺ 264.1115).



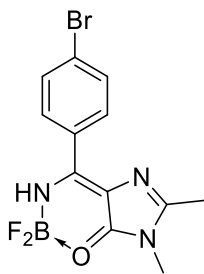
(E)-5-((difluoroboranyl)amino)(4-methoxyphenyl)methylene-2,3-dimethyl-3,5-dihydro-4H-imidazol-4-one (8b)

Yellow solid (31 mg, 35%); mp = 208–211 °C; ¹H NMR (700 MHz, 303 K, DMSO-d₆) δ ppm 9.29 (s, 1H), 8.39 (d, *J*=8.9 Hz, 2H), 7.15 (d, *J*=8.9 Hz, 2H), 3.87 (s, 3H), 3.42 (s, 3H), 2.33 (s, 3H); ¹³C NMR (176 MHz, 303 K, DMSO-d₆) δ ppm 162.9, 160.4, 157.4, 143.5, 132.0, 122.7, 114.0, 111.9, 55.5, 27.9, 13.3; HRMS (ESI) m/z: 294.1223 found (calcd for C₁₃H₁₅BF₂N₃O₂⁺, [M+H]⁺ 294.1220).



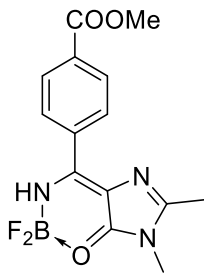
(E)-5-((4-chlorophenyl)((difluoroboranyl)amino)methylene)-2,3-dimethyl-3,5-dihydro-4H-imidazol-4-one (8c)

Yellow solid (30 mg, 34%); mp ~ 218 °C with decomposition; ¹H NMR (700 MHz, 303 K, DMSO-d₆) δ ppm 9.56 (br.s., 1H), 8.26 (d, *J*=8.6 Hz, 2H), 7.69 (d, *J*=8.6 Hz, 2H), 3.43 (s, 3H), 2.33 (s, 3H); ¹³C NMR (176 MHz, 303 K, DMSO-d₆) δ ppm 160.2, 158.1, 144.4, 137.6, 131.6, 129.4, 128.7, 112.2, 27.9, 13.4; HRMS (ESI) m/z: 298.0723 found (calcd for C₁₂H₁₂BClF₂N₃O⁺, [M+H]⁺ 298.0725).



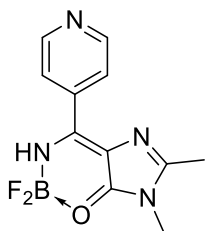
(E)-5-((4-bromophenyl)((difluoroboranyl)amino)methylene)-2,3-dimethyl-3,5-dihydro-4H-imidazol-4-one (8d)

Yellow solid (50 mg, 48%); mp = 228–230 °C; ^1H NMR (700 MHz, 303 K, DMSO- d_6) δ ppm 9.57 (br.s., 1H), 8.17 (d, $J=8.5$ Hz, 2H), 7.83 (d, $J=8.5$ Hz, 2H), 3.43 (s, 3H), 2.33 (s, 3H); ^{13}C NMR (176 MHz, 303 K, DMSO- d_6) δ ppm 160.3, 158.1, 144.4, 131.7, 131.6, 129.7, 126.7, 112.2, 28.0, 13.4; HRMS (ESI) m/z: 342.0217 found (calcd for $\text{C}_{12}\text{H}_{12}\text{BBrF}_2\text{N}_3\text{O}^+$, $[\text{M}+\text{H}]^+$ 342.0219).



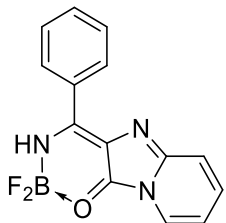
Methyl (E)-4-(((difluoroboranyl)amino)(1,2-dimethyl-5-oxo-1,5-dihydro-4H-imidazol-4-ylidene)methyl)benzoate (8e)

Yellow solid (61 mg, 63%); mp ~ 260 °C with decomposition; ^1H NMR (700 MHz, 303 K, DMSO- d_6) δ ppm 9.68 (br.s., 1H), 8.27 (d, $J=8.6$ Hz, 2H), 8.13 (d, $J=8.6$ Hz, 2H), 3.91 (s, 3H), 3.44 (s, 3H), 2.33 (s, 3H); ^{13}C NMR (176 MHz, 303 K, DMSO- d_6) δ ppm 165.5, 160.6, 158.3, 1448, 134.8, 132.7, 130.0, 129.1, 112.4, 52.5, 28.0, 13.4; HRMS (ESI) m/z: 322.1167 found (calcd for $\text{C}_{14}\text{H}_{15}\text{BF}_2\text{N}_3\text{O}_3^+$, $[\text{M}+\text{H}]^+$ 322.1169).



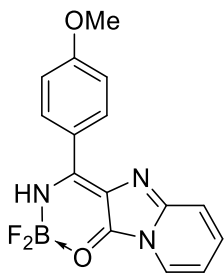
(E)-5-(((difluoroboranyl)amino)(pyridin-4-yl)methylene)-2,3-dimethyl-3,5-dihydro-4*H*-imidazol-4-one (8f)

Yellow solid (19 mg, 24%); mp = 178–181 °C; ^1H NMR (700 MHz, 303 K, DMSO- d_6) δ ppm 9.78 (br.s., 1H), 8.84 (d, $J=4.5$, 1.6 Hz, 2H), 8.07 (dd, $J=4.5$, 1.6 Hz, 2H), 3.44 (s, 3H), 2.34 (s, 3H); ^{13}C NMR (176 MHz, 303 K, DMSO- d_6) δ ppm 159.5, 158.6, 150.2, 145.2, 137.8, 123.1, 112.6, 28.0, 13.4; HRMS (ESI) m/z: 265.1066 found (calcd for $\text{C}_{11}\text{H}_{12}\text{BF}_2\text{N}_4\text{O}^+$, $[\text{M}+\text{H}]^+$ 265.1067).



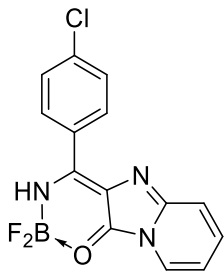
(E)-2-(((difluoroboranyl)amino)(phenyl)methylene)imidazo[1,2-a]pyridin-3(2*H*)-one (9a)

Orange solid (44 mg, 52%); mp ~ 230 °C with decomposition; ^1H NMR (700 MHz, 303 K, DMSO- d_6) δ ppm 10.68 (s, 1H), 8.38 (d, $J=7.8$, 2H), 8.26 (d, $J=7.0$, 1H), 7.76 (t, $J=7.4$, 1H), 7.67 (t, $J=7.8$, 2H) 7.50 (d, $J=9.4$, 2H), 7.28-7.25 (m, 1H), 6.91 (t, $J=6.8$, 1H); ^{13}C NMR (176 MHz, 303 K, DMSO- d_6) δ ppm 165.8, 148.8, 140.2, 133.4, 130.4, 130.2, 128.7, 127.2, 122.8, 118.4, 115.6, 113.0; HRMS (ESI) m/z: 286.0955 found (calcd for $\text{C}_{14}\text{H}_{11}\text{BF}_2\text{N}_3\text{O}^+$, $[\text{M}+\text{H}]^+$ 286.0958).



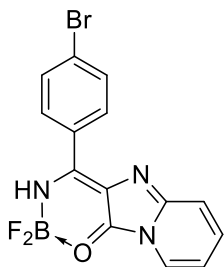
(E)-2-((difluoroboranyl)amino)(4-methoxyphenyl)methyleneimidazo[1,2-a]pyridin-3(2H)-one (9b)

Orange solid (44 mg, 47%); mp = 240–243 °C; ¹H NMR (700 MHz, 303 K, DMSO-d₆) δ ppm 10.37 (br.s., 1H), 8.59 (d, J=8.9 Hz, 2H) 8.24 (d, J=6.9 Hz, 1H), 7.51 (d, J=9.4 Hz, 1H), 7.28-7.24 (m, 1H), 7.22 (d, J=8.9 Hz, 2H), 6.90 (t, J=6.9 Hz, 1H), 3.91 (s, 3H); ¹³C NMR (176 MHz, 303 K, DMSO-d₆) δ ppm 164.1, 163.7, 148.4, 139.8, 132.9, 127.0, 122.7, 122.2, 118.3, 115.5, 114.3, 112.9, 55.7; HRMS (ESI) m/z: 316.1061 found (calcd for C₁₅H₁₃BF₂N₃O₂⁺, [M+H]⁺ 316.1063).



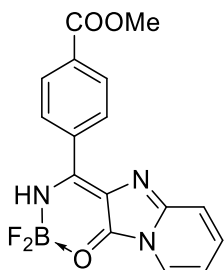
(E)-2-((4-chlorophenyl)((difluoroboranyl)amino)methyleneimidazo[1,2-a]pyridin-3(2H)-one (9c)

Orange solid (62 mg, 65%); mp = 250–252 °C; ¹H NMR (700 MHz, 303 K, DMSO-d₆) δ ppm 10.73 (br.s., 1H), 8.43 (d, J=8.6 Hz, 2H), 8.26 (d, J=7.0 Hz, 1H), 7.77 (d, J=8.6 Hz, 2H), 7.50 (d, J=9.4 Hz, 1H), 7.27 (ddd, J=9.4, 6.7, 0.8 Hz, 1H), 6.91 (t, J=6.7 Hz, 1H); ¹³C NMR (176 MHz, 303 K, DMSO-d₆) δ ppm 164.4, 148.9, 140.3, 138.6, 132.3, 130.5, 128.9, 127.4, 122.8, 118.4, 115.5, 113.1; HRMS (ESI) m/z: 320.0567 found (calcd for C₁₄H₁₀BClF₂N₃O⁺, [M+H]⁺ 320.0568).



(E)-2-((4-bromophenyl)((difluoroboranyl)amino)methylene)imidazo[1,2-a]pyridin-3(2H)-one (9d)

Orange solid (65 mg, 60%); mp = 248–250 °C; ^1H NMR (700 MHz, 303 K, DMSO-d₆) δ ppm 10.74 (br.s., 1H), 8.34 (d, J =8.6 Hz, 2H), 8.26 (d, J =7.1 Hz, 1H), 7.91 (d, J =8.6 Hz, 2H), 7.49 (d, J =9.4 Hz, 1H), 7.25 - 7.29 (ddd, J =9.4, 6.6, 0.9 Hz, 1H), 6.91 (t, J =6.5 Hz, 1H); ^{13}C NMR (176 MHz, 303 K, DMSO-d₆) δ ppm 164.6, 148.9, 140.3, 132.3, 131.8, 129.2, 127.7, 127.4, 122.9, 118.4, 115.5, 113.1; HRMS (ESI) m/z: 364.0066 found (calcd for C₁₄H₁₁BF₂N₃O, [M+H]⁺ 364.0063).

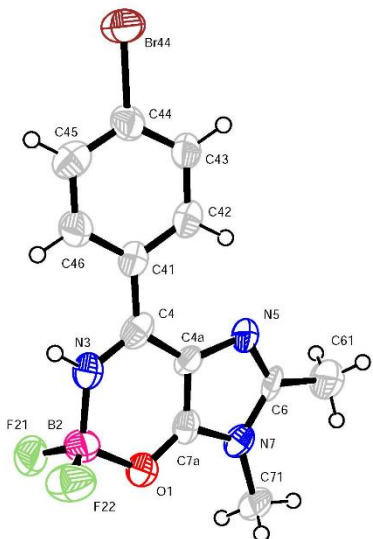


Methyl (E)-4-(((difluoroboranyl)amino)(3-oxoimido[1,2-a]pyridin-2(3H)-ylidene)methyl) benzoate (9e)

Dark red solid (52 mg, 50%); mp ~ 245 °C with decomposition; ^1H NMR (700 MHz, 303 K, DMSO-d₆) δ ppm 10.87 (br.s., 1H), 8.44 (d, J =8.5 Hz, 2H), 8.27 (d, J =7.2 Hz, 1H), 8.20 (d, J =8.5 Hz, 2H) 7.49 (d, J =9.5 Hz, 1H), 7.27 (ddd, J =9.4, 6.6, 1.0 Hz, 1H), 6.91 (dd, J =6.7, 0.7 Hz, 1H), 3.93 (s, 3H); ^{13}C NMR (176 MHz, 303 K, DMSO-d₆) δ ppm 165.4, 149.1, 140.5, 134.2, 133.3, 130.7, 130.2, 129.1, 128.8, 127.5, 122.9, 118.4, 113.1, 52.5; HRMS (ESI) m/z: 344.1010 found (calcd for C₁₆H₁₃BF₂N₃O₃⁺, [M+H]⁺ 344.1013).

3. X-Ray data

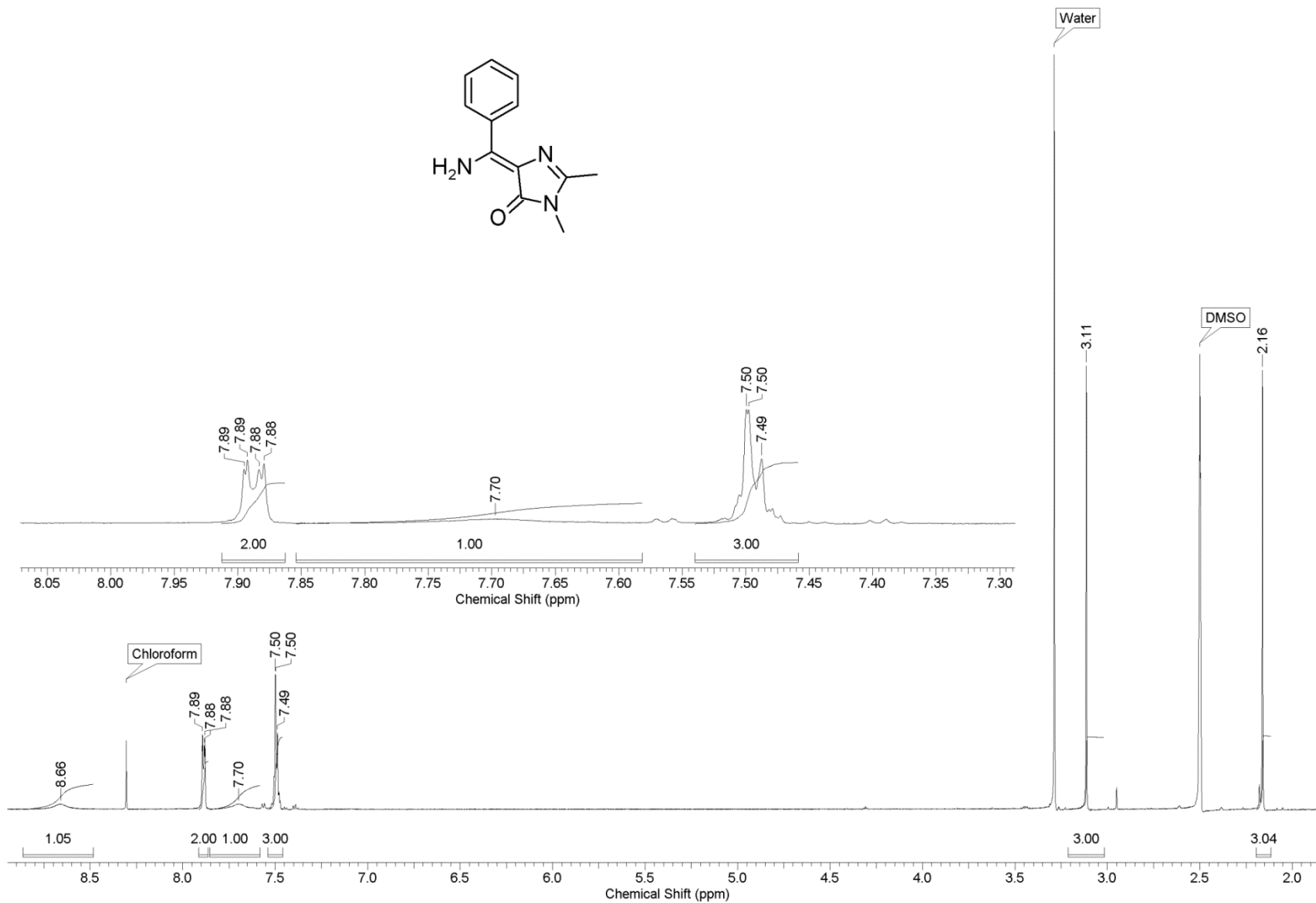
Crystals of compound **8d** ($C_{12}H_{11}BBrF_2N_3O$, $M = 341.96$) were grown from acetonitrile were light yellow, triclinic, space group $P-1$. X-ray diffraction data were collected using a STADI-VARI Pilatus-100K four cycle diffractometer ($\lambda(Mo\ K\alpha) = 0.71073\ \text{\AA}$, plane graphite monochromator) at 295 K: $a = 4.8377(6)$, $b = 9.7590(13)$, $c = 14.1241(19)\ \text{\AA}$, $\alpha = 82.194(11)$, $\beta = 85.642(10)$, $\gamma = 84.183(10)^\circ$, $V = 655.92(15)\ \text{\AA}^3$, $Z = 2$. Intensities of 29448 reflections were measured and 3318 independent reflections [$R_{\text{int}} = 0.0513$] were used in further refinement. Initially spherical atom refinements were undertaken with using SHELXS-97 [11], then non-hydrogen atoms were refined anisotropically with using SHELXL-2015 [12]. The refinement converged to $wR_2 = 0.2383$, $GOF = 0.756$ for all independent reflections ($R_1 = 0.0615$ was calculated against F^2 for 871 observed reflections with $I > 2\sigma(I)$). Atomic coordinates, bond lengths, angles, and displacement atom parameters have been deposited at the Cambridge Crystallographic Data Center (CCDC) with number 1919301.

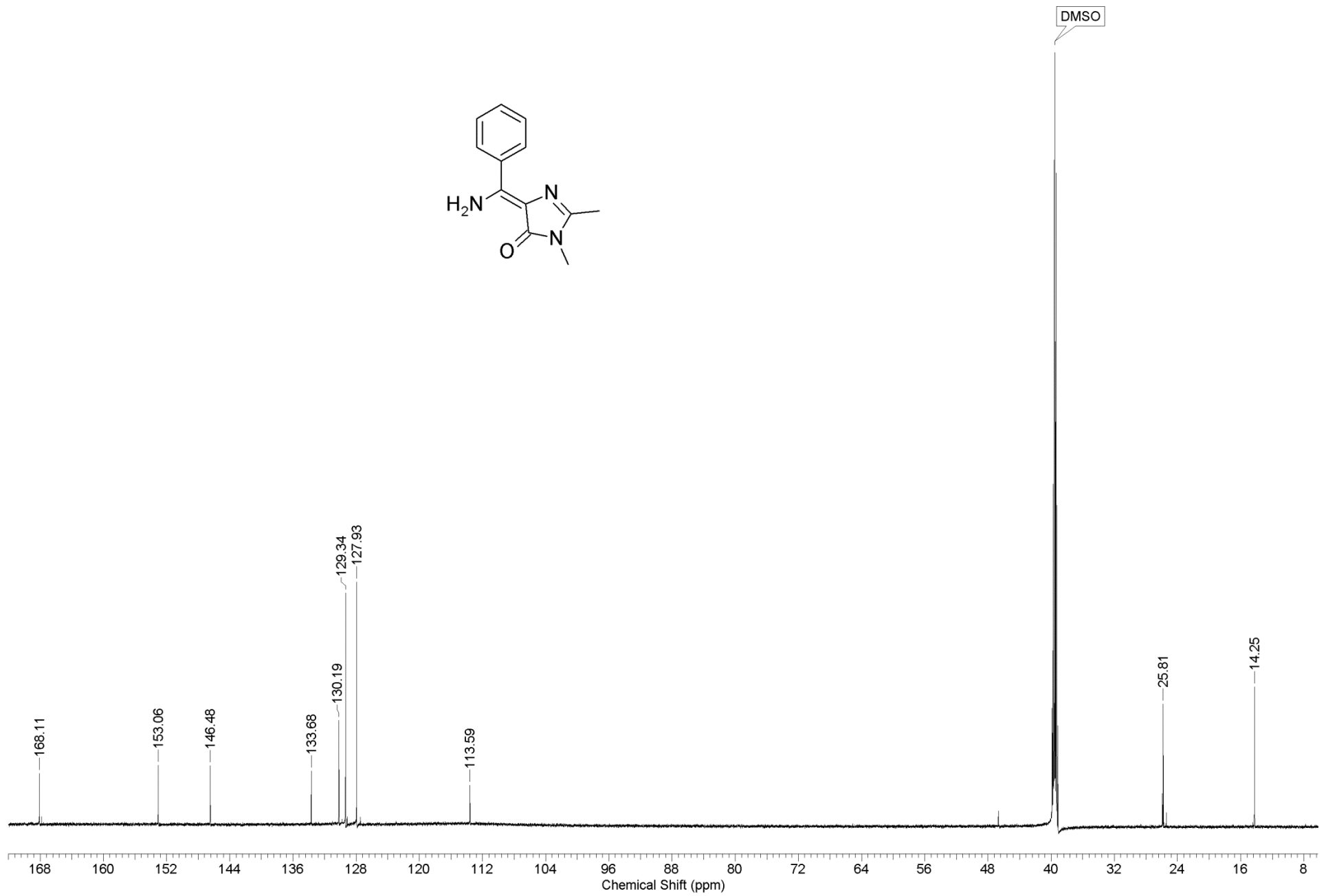


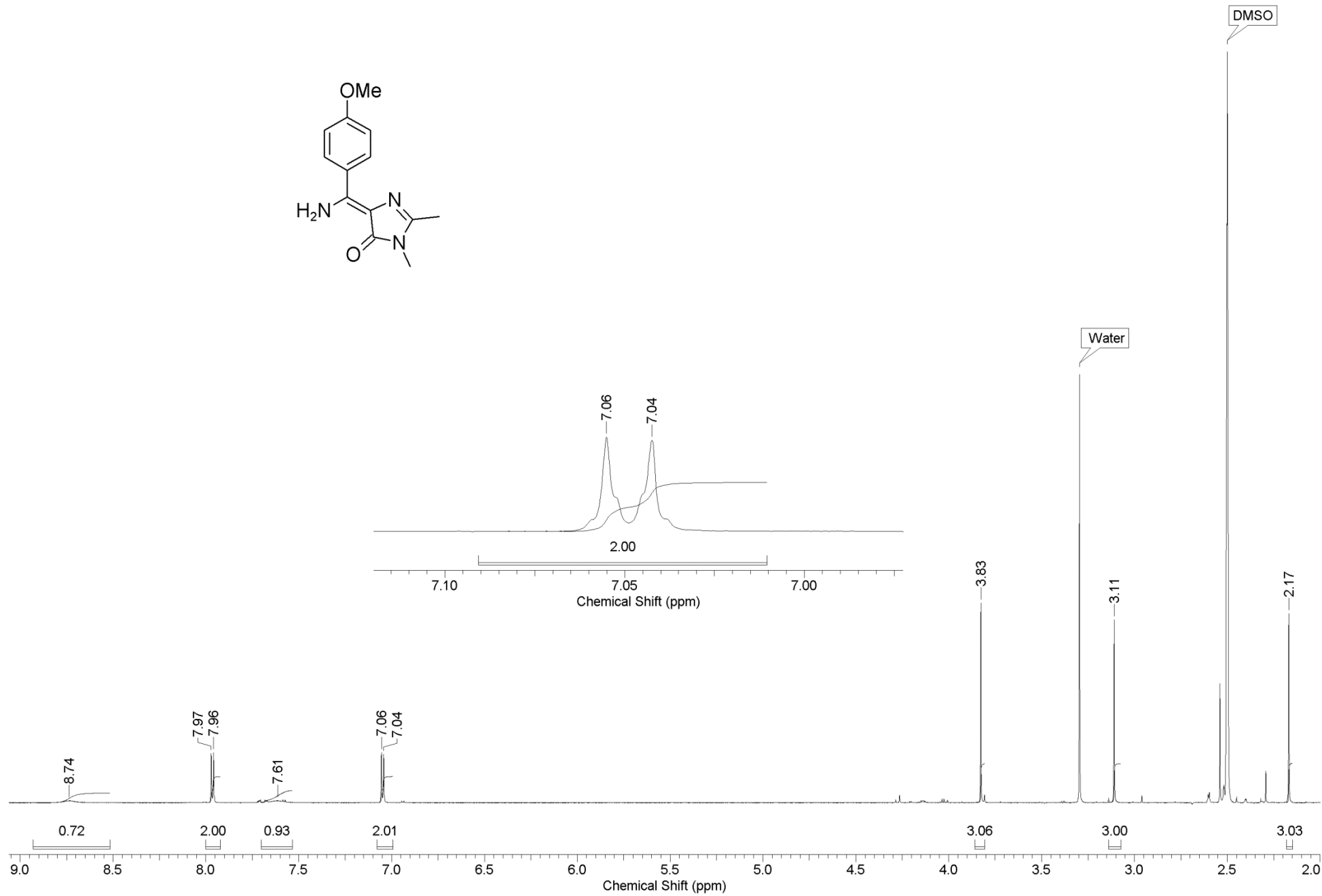
¹¹ Sheldrick G.M. Acta Cryst. 2008, A64, 112-122.

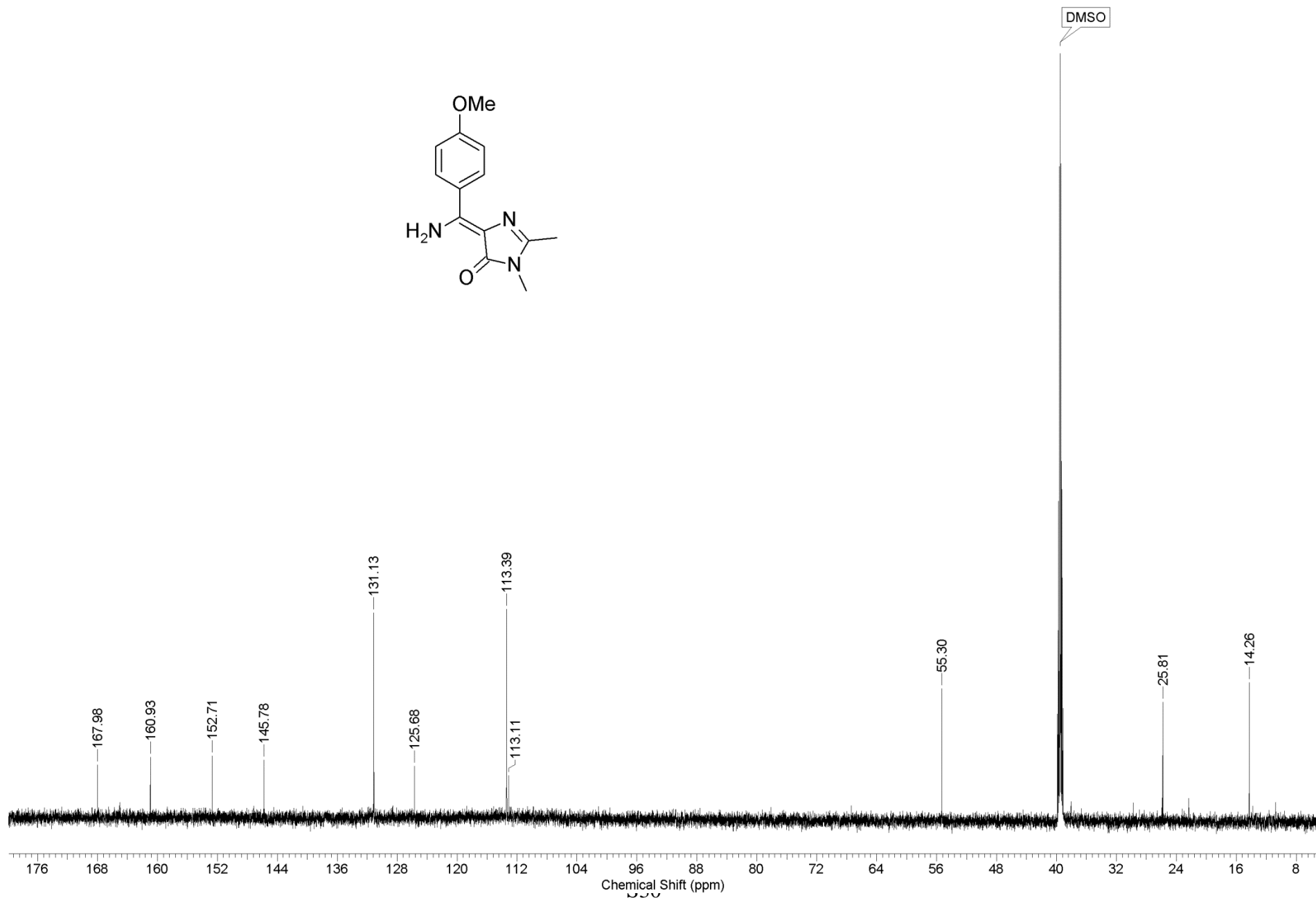
¹² Sheldrick G.M. Acta Cryst. 2015, C71, 3-8.

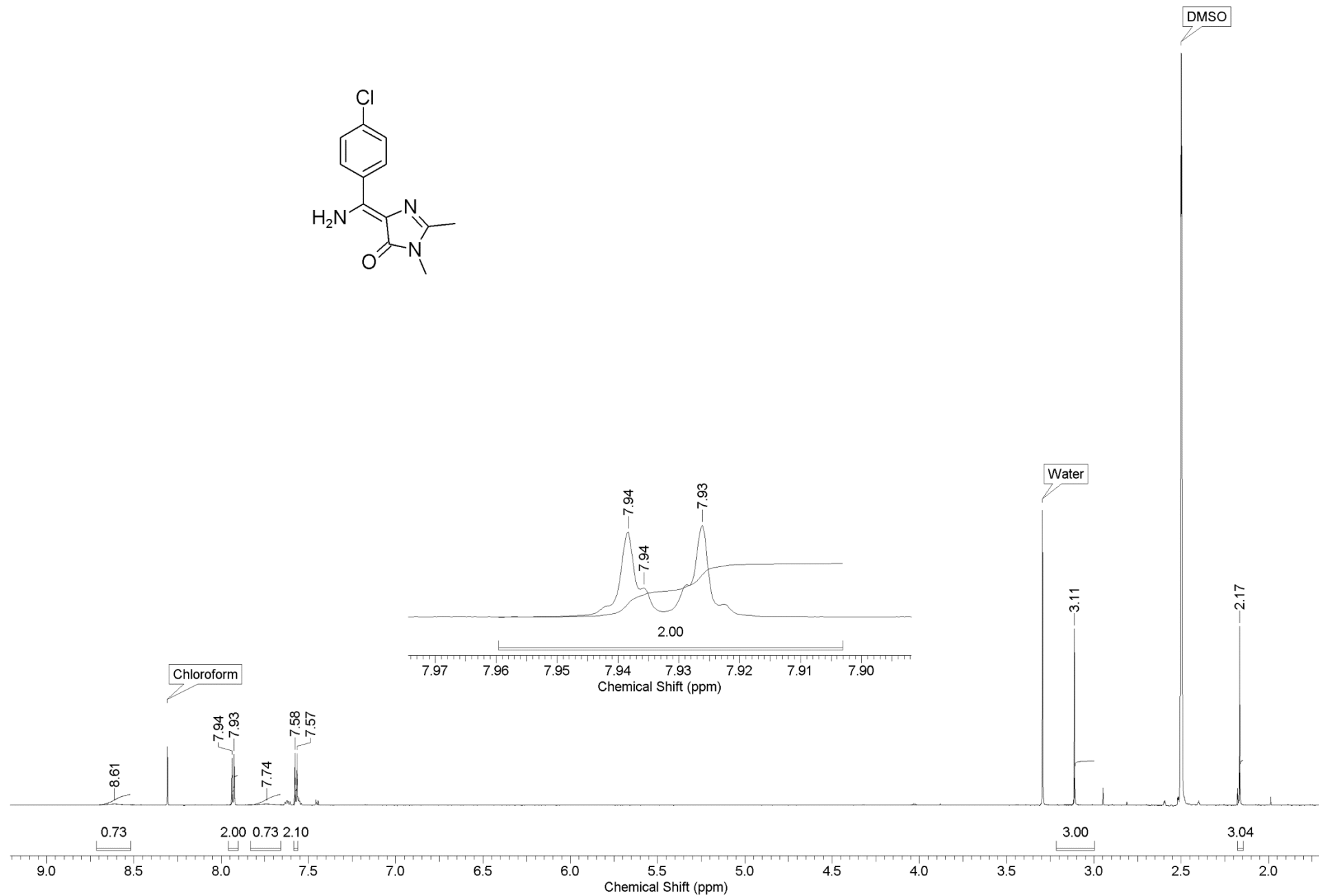
4. Copies of ^1H and ^{13}C NMR spectra

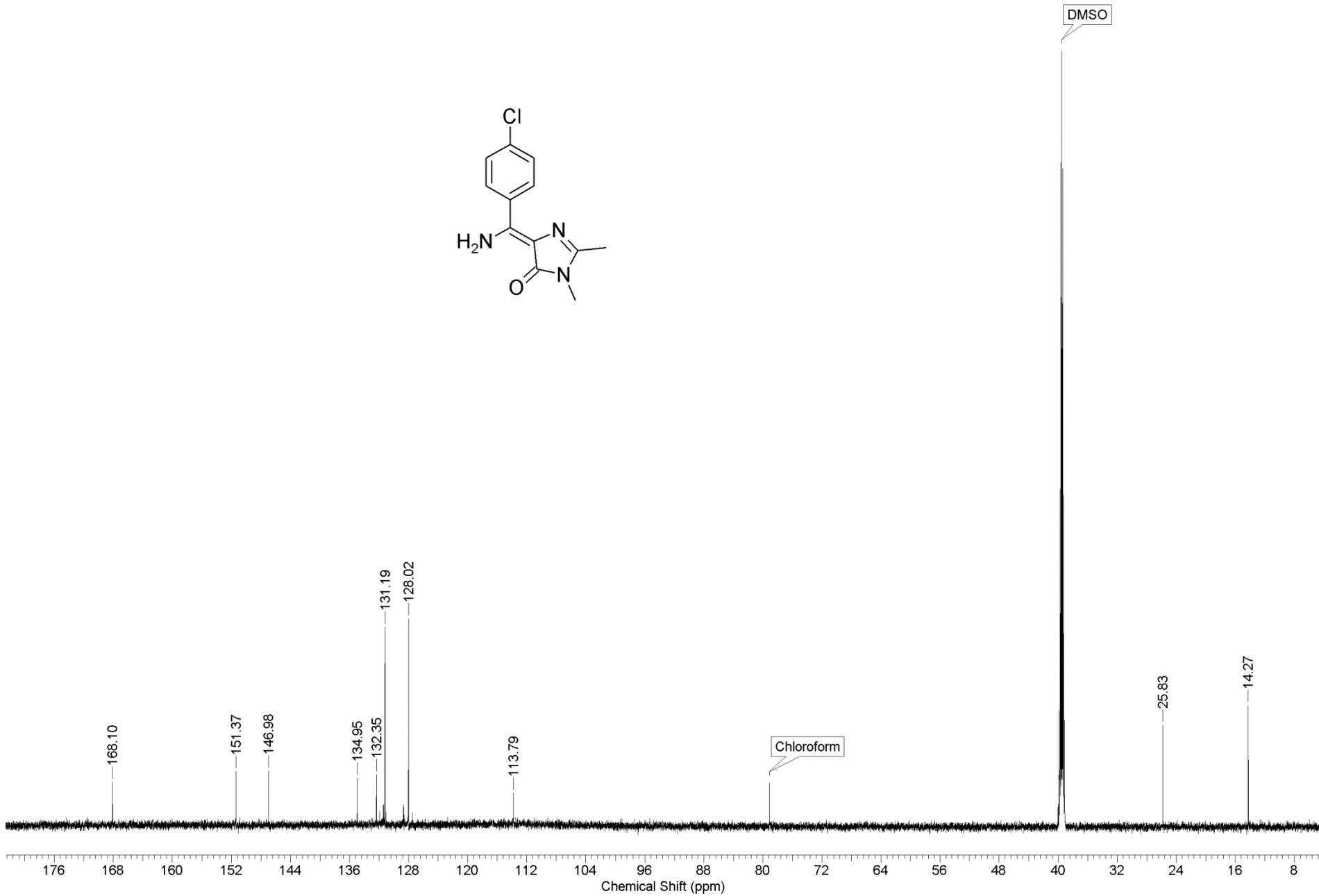


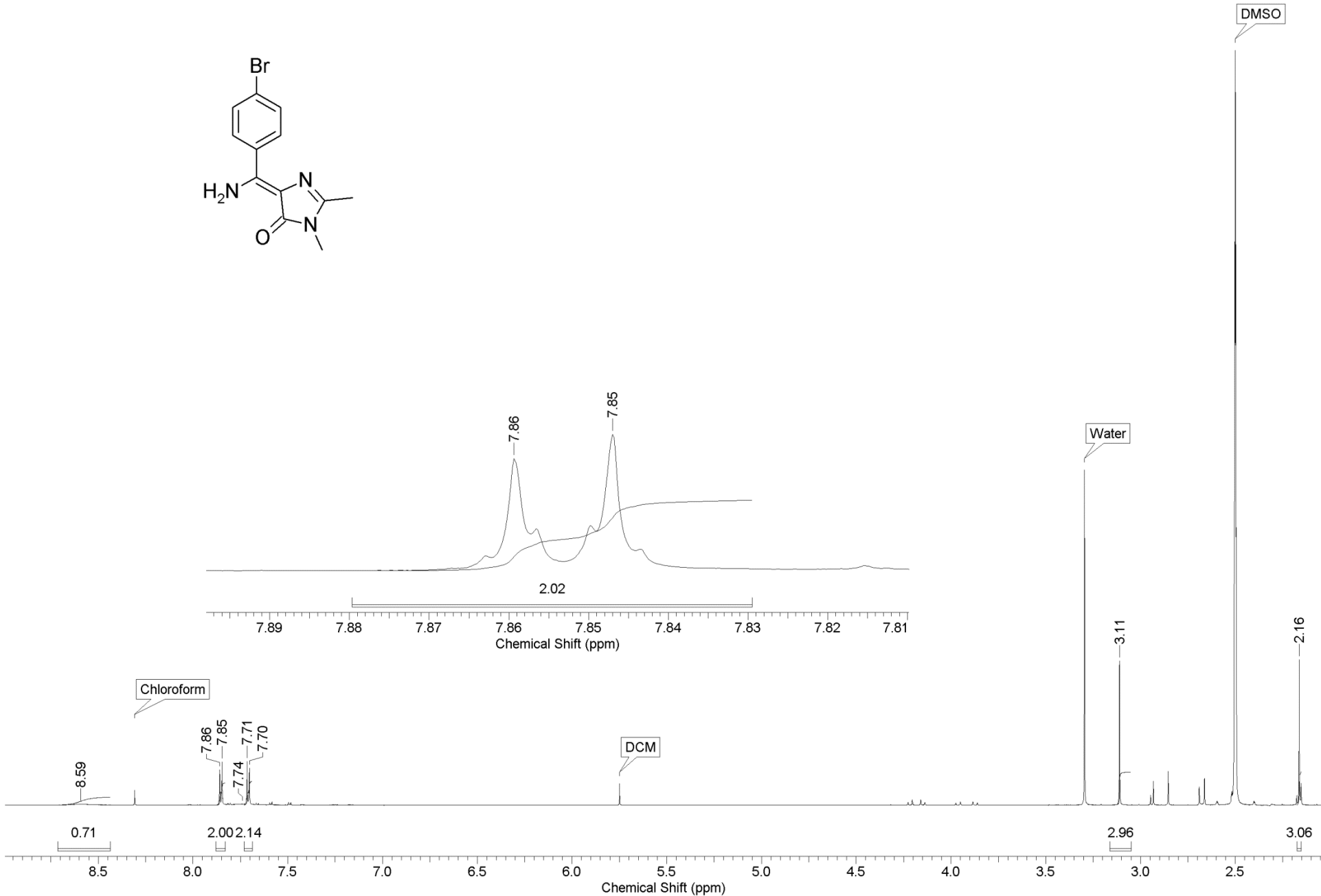


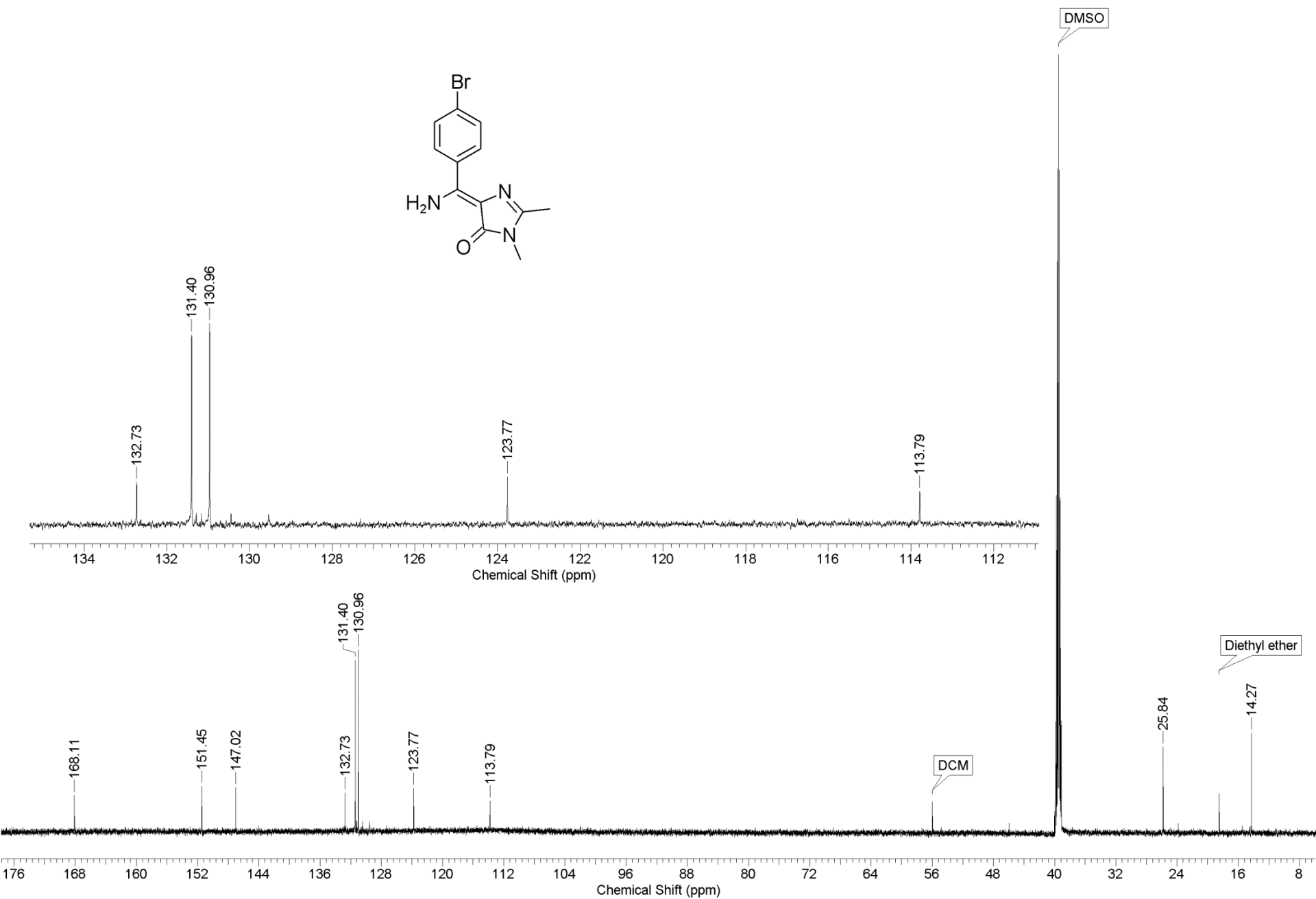
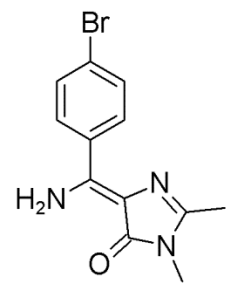


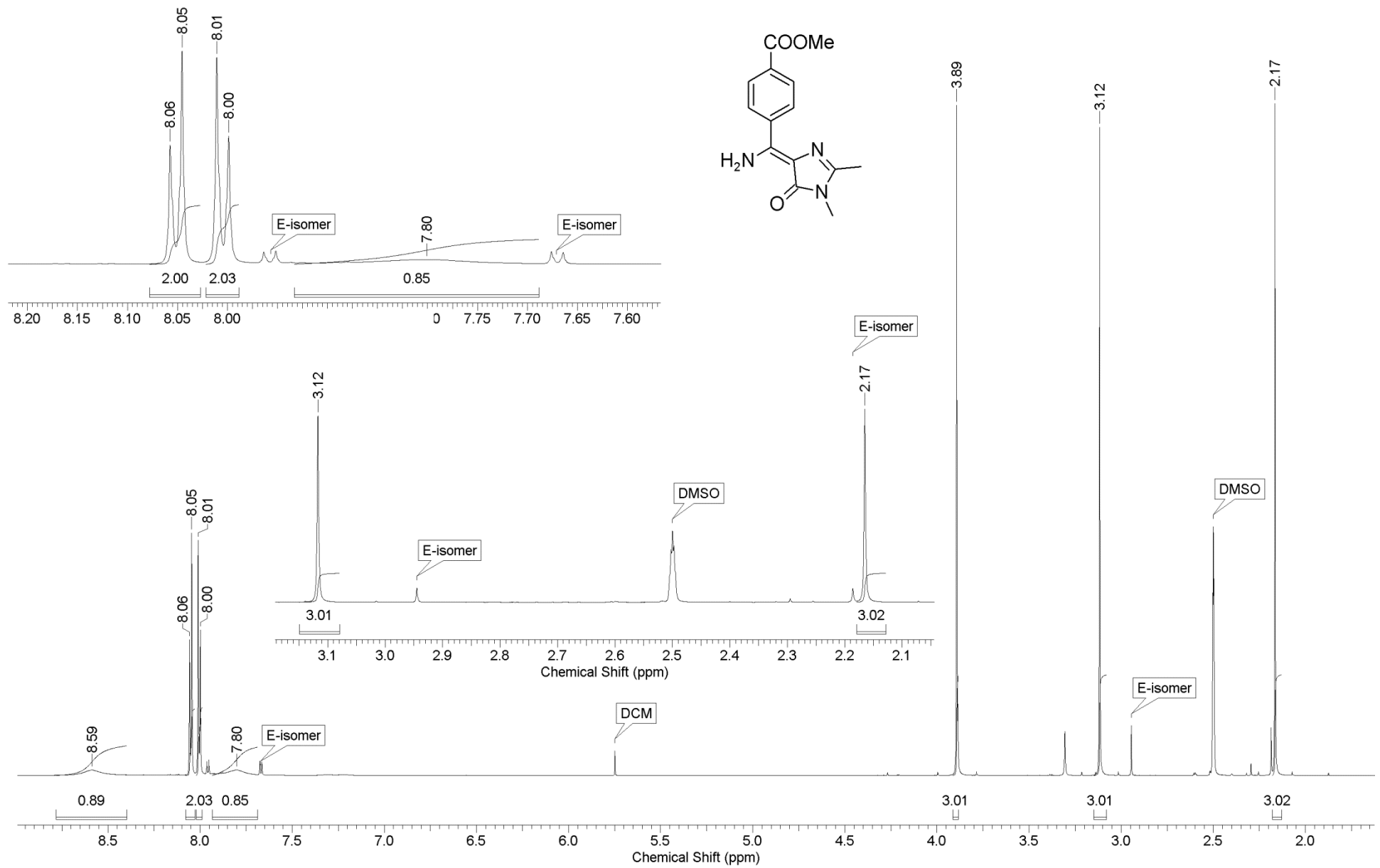


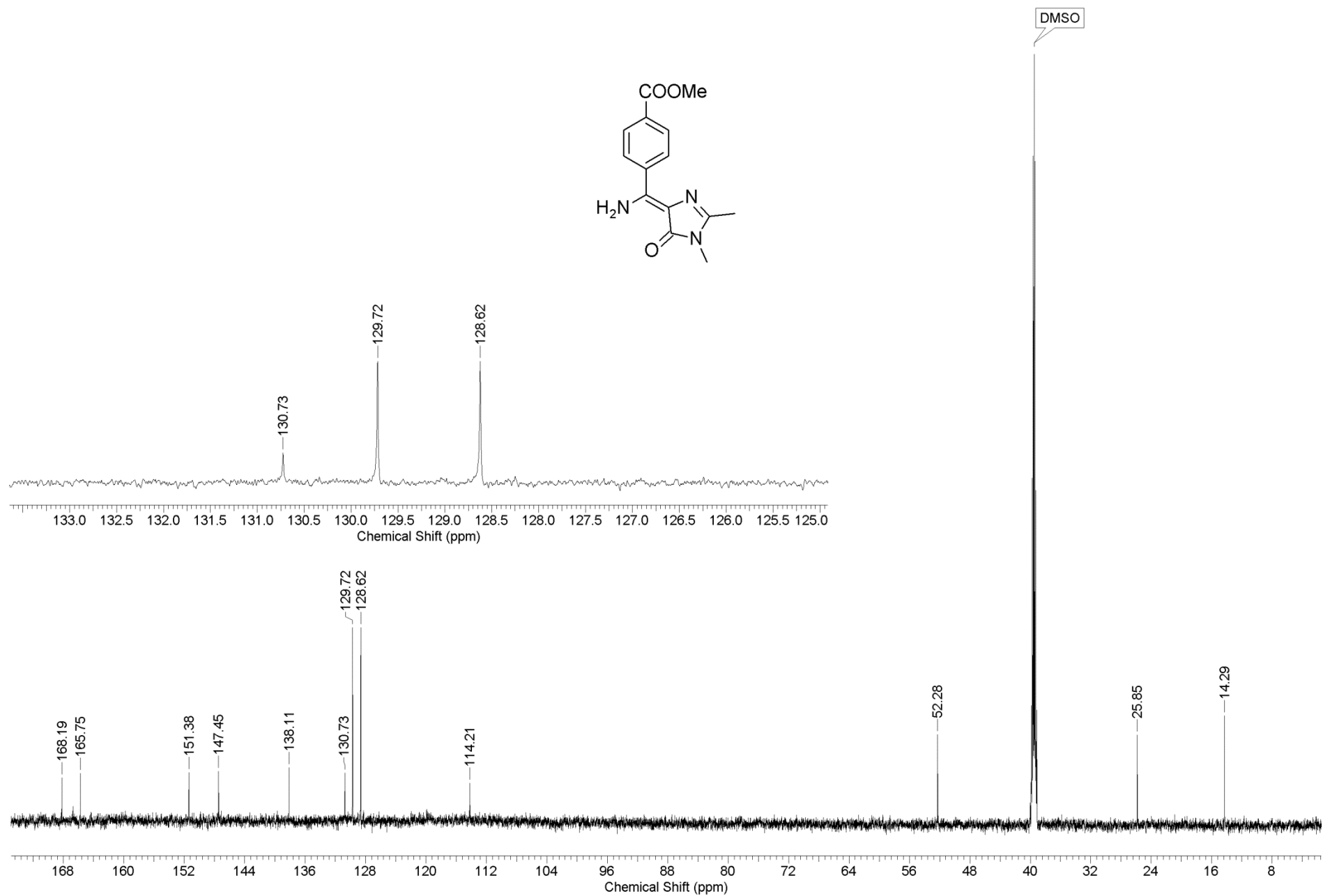


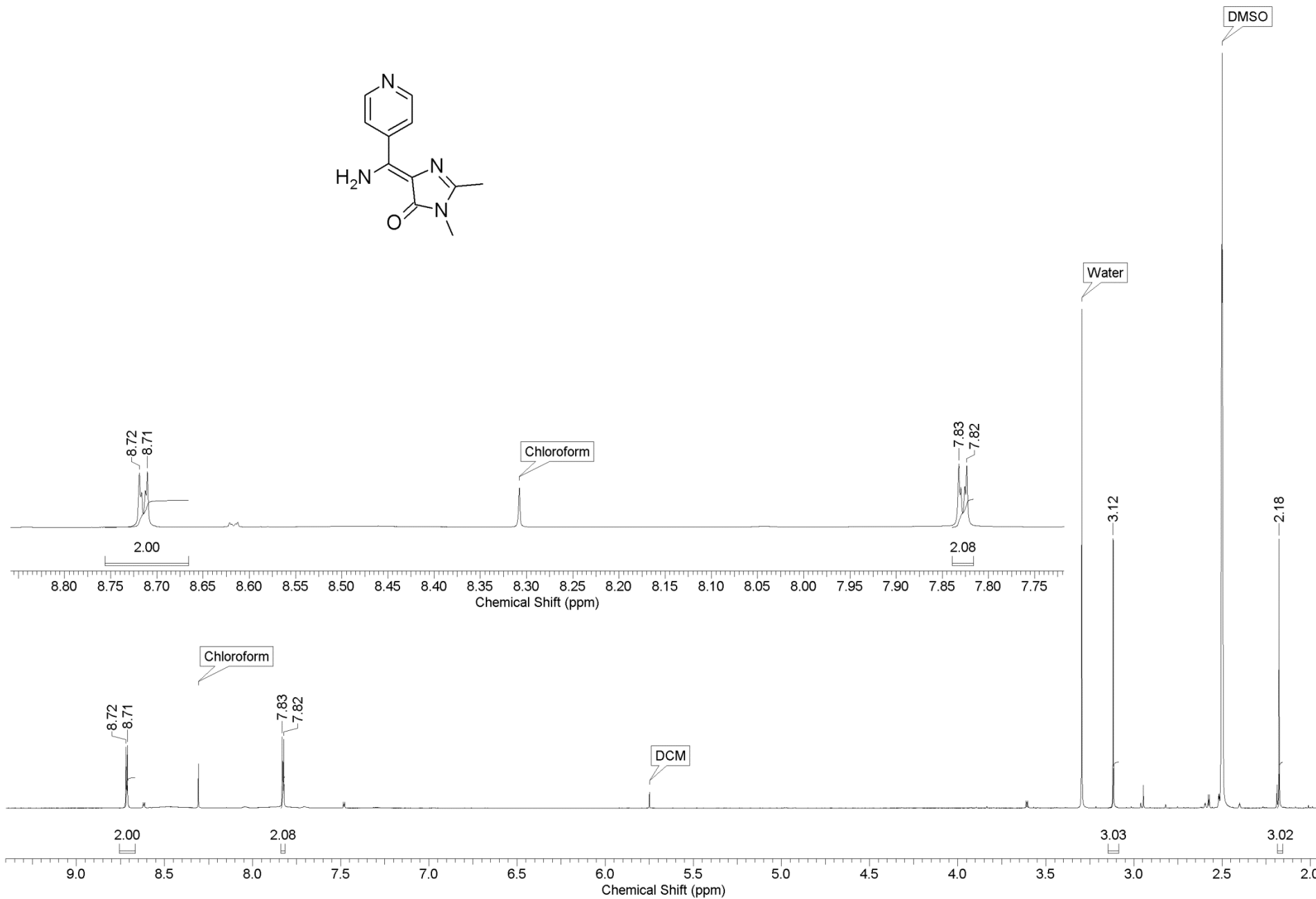


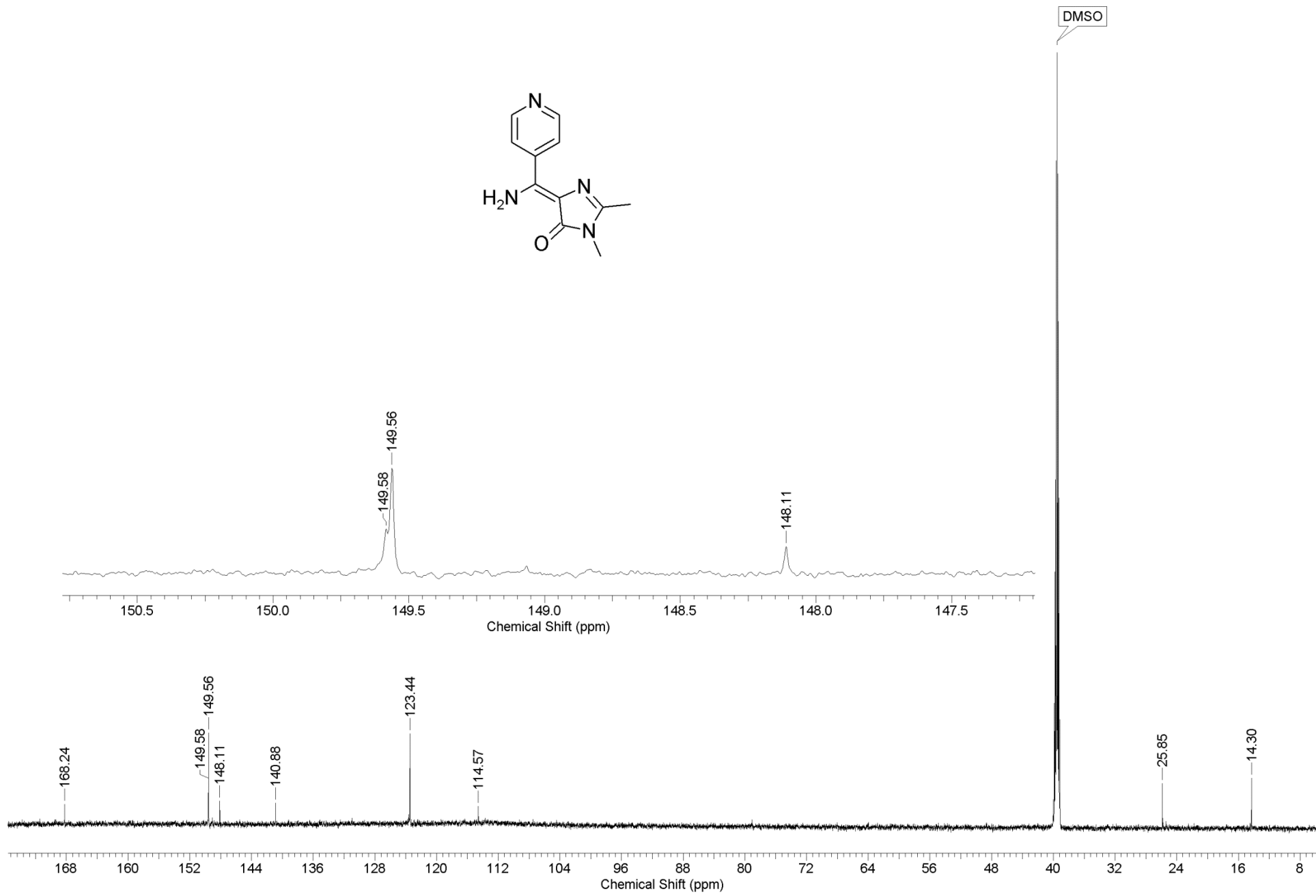


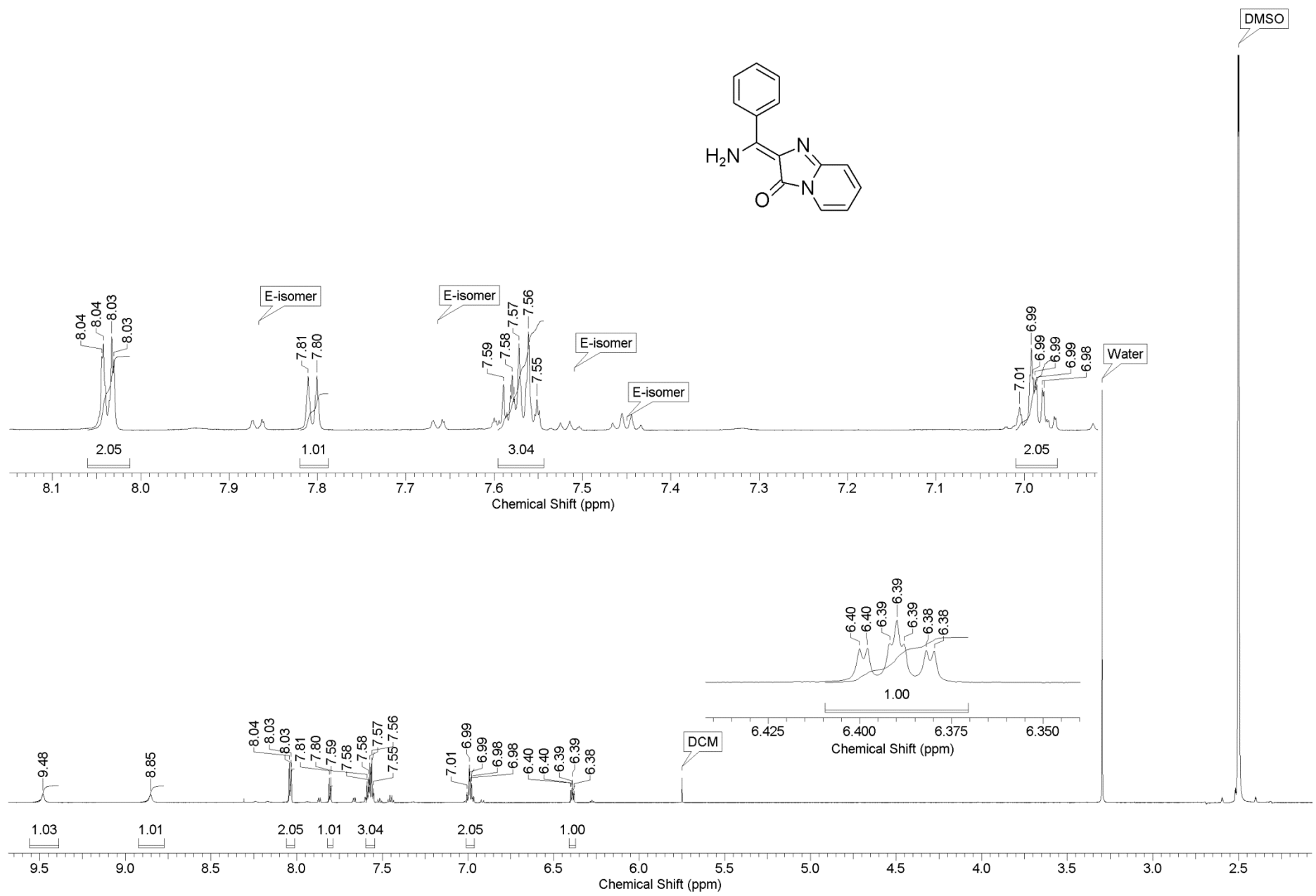


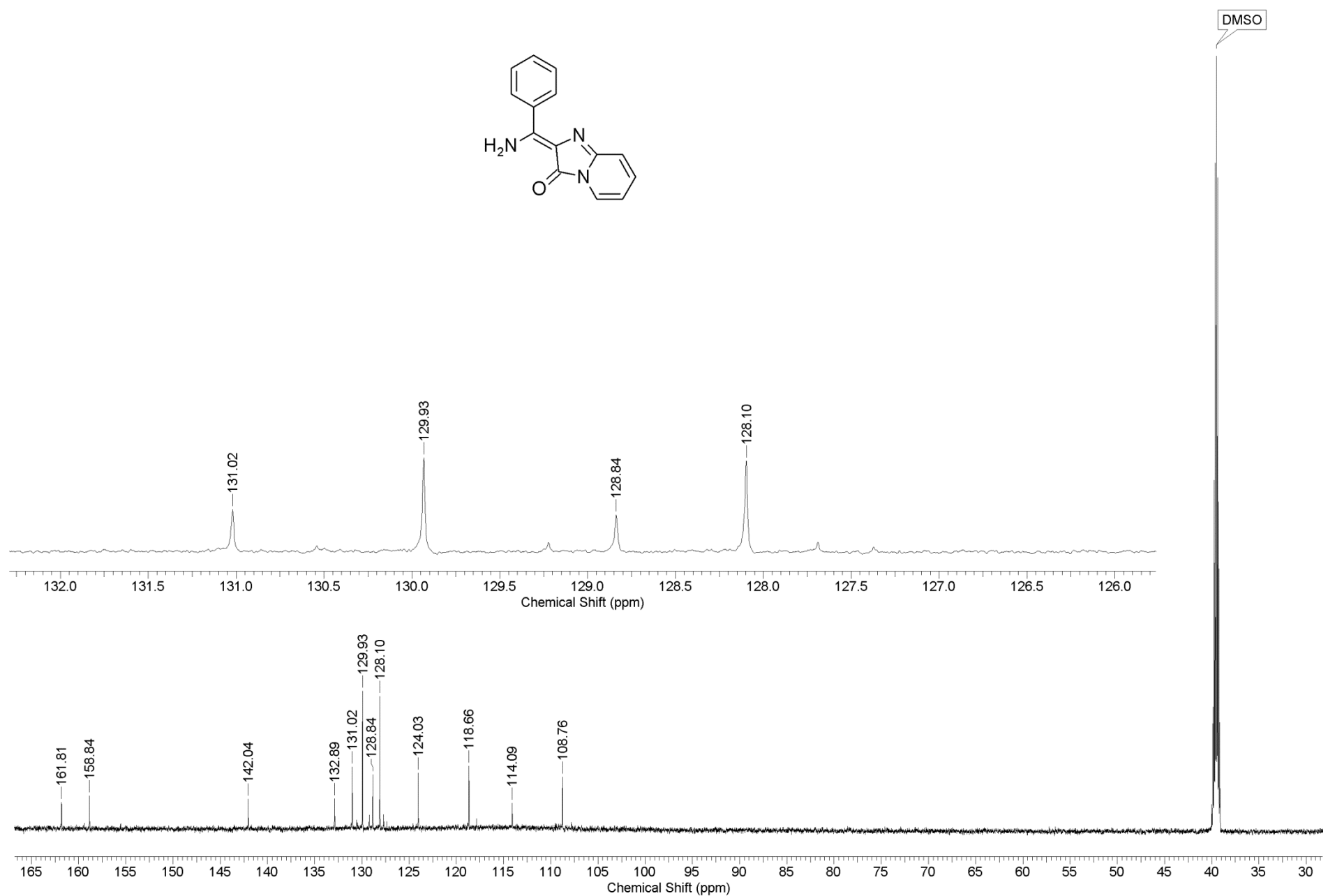


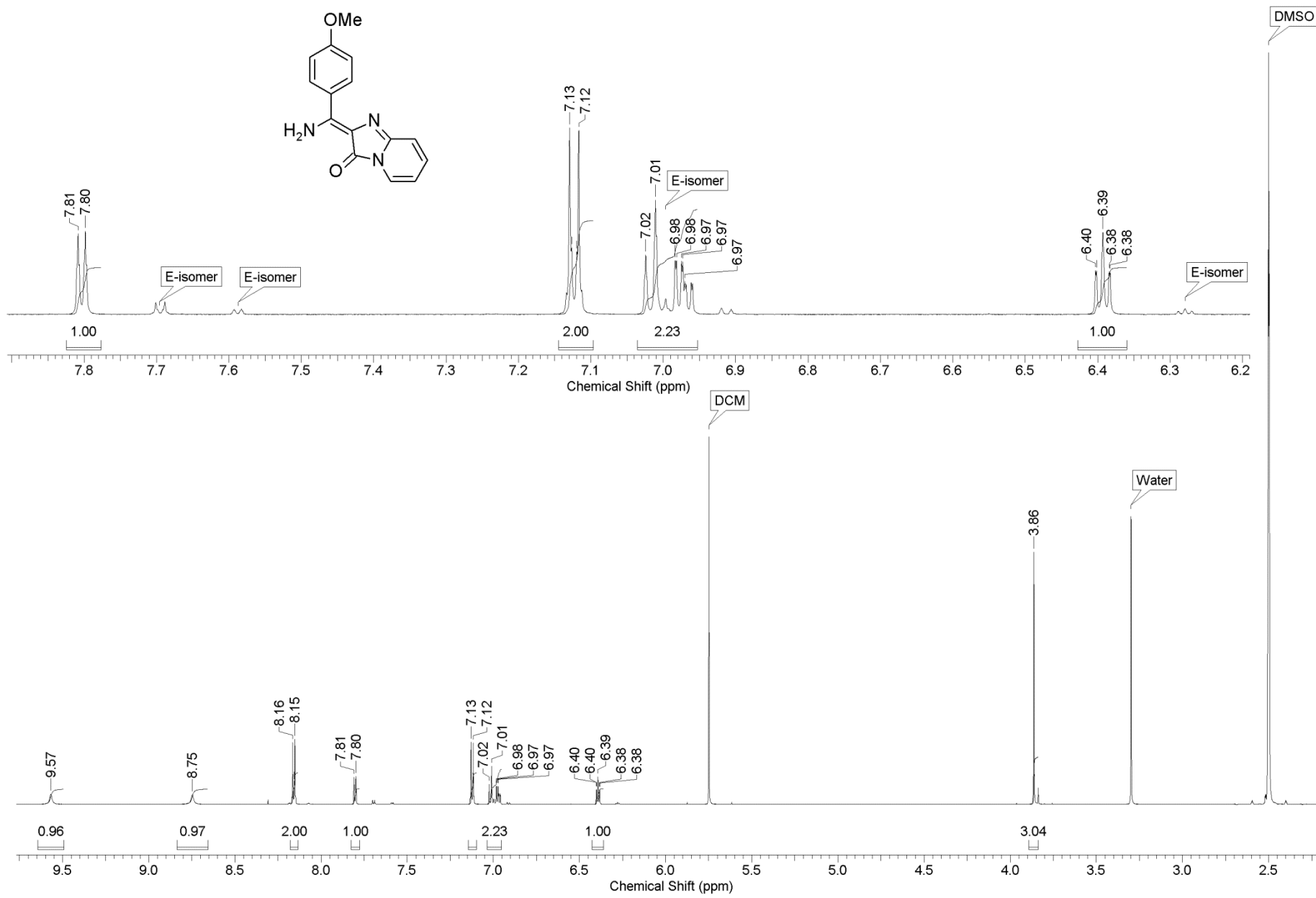




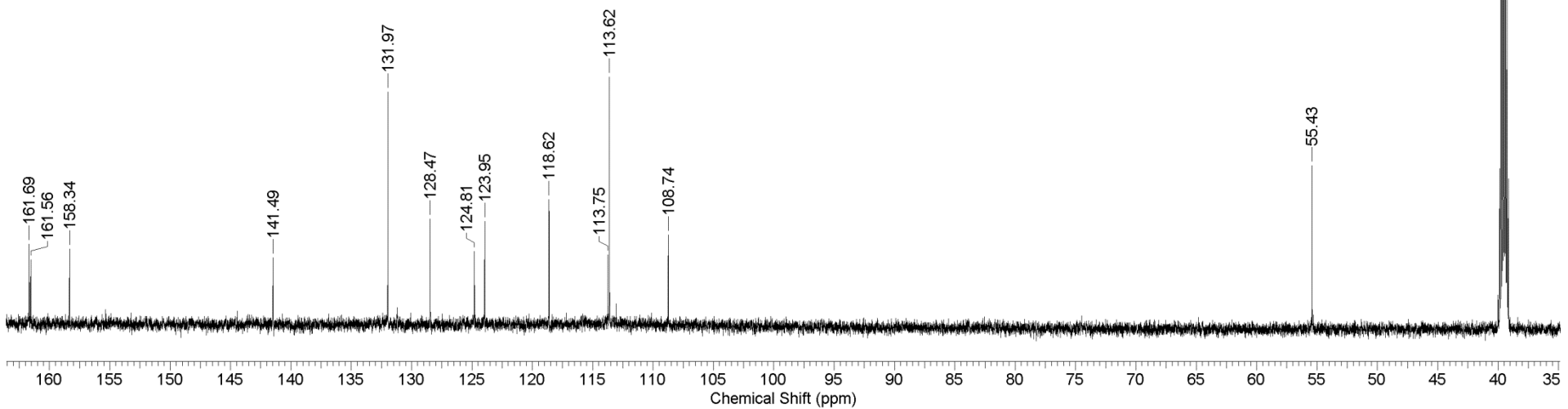
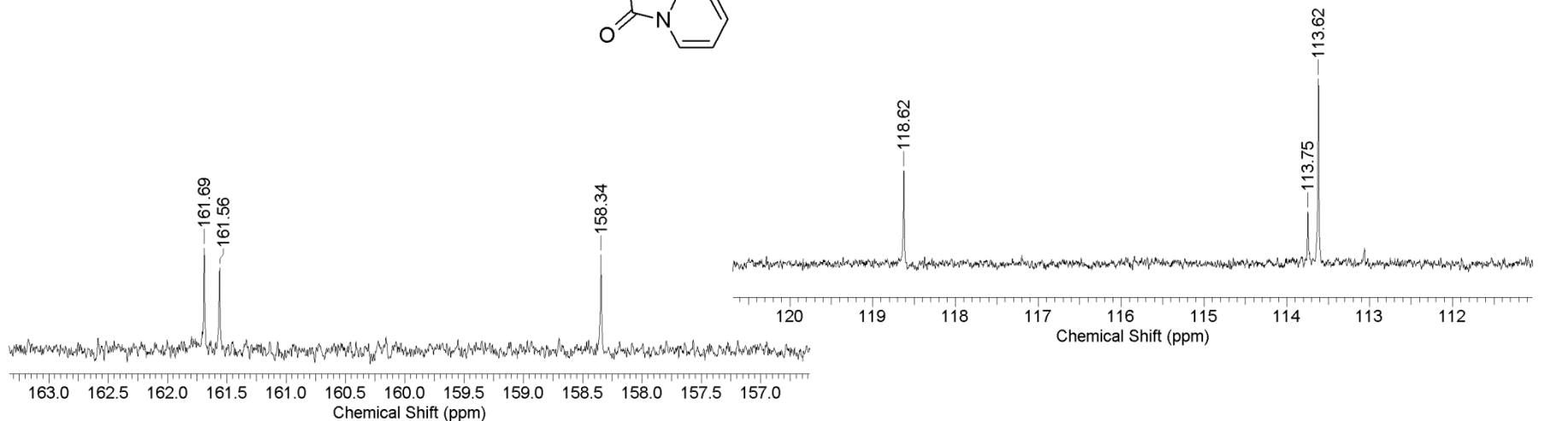
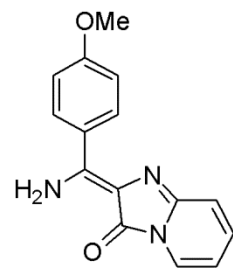


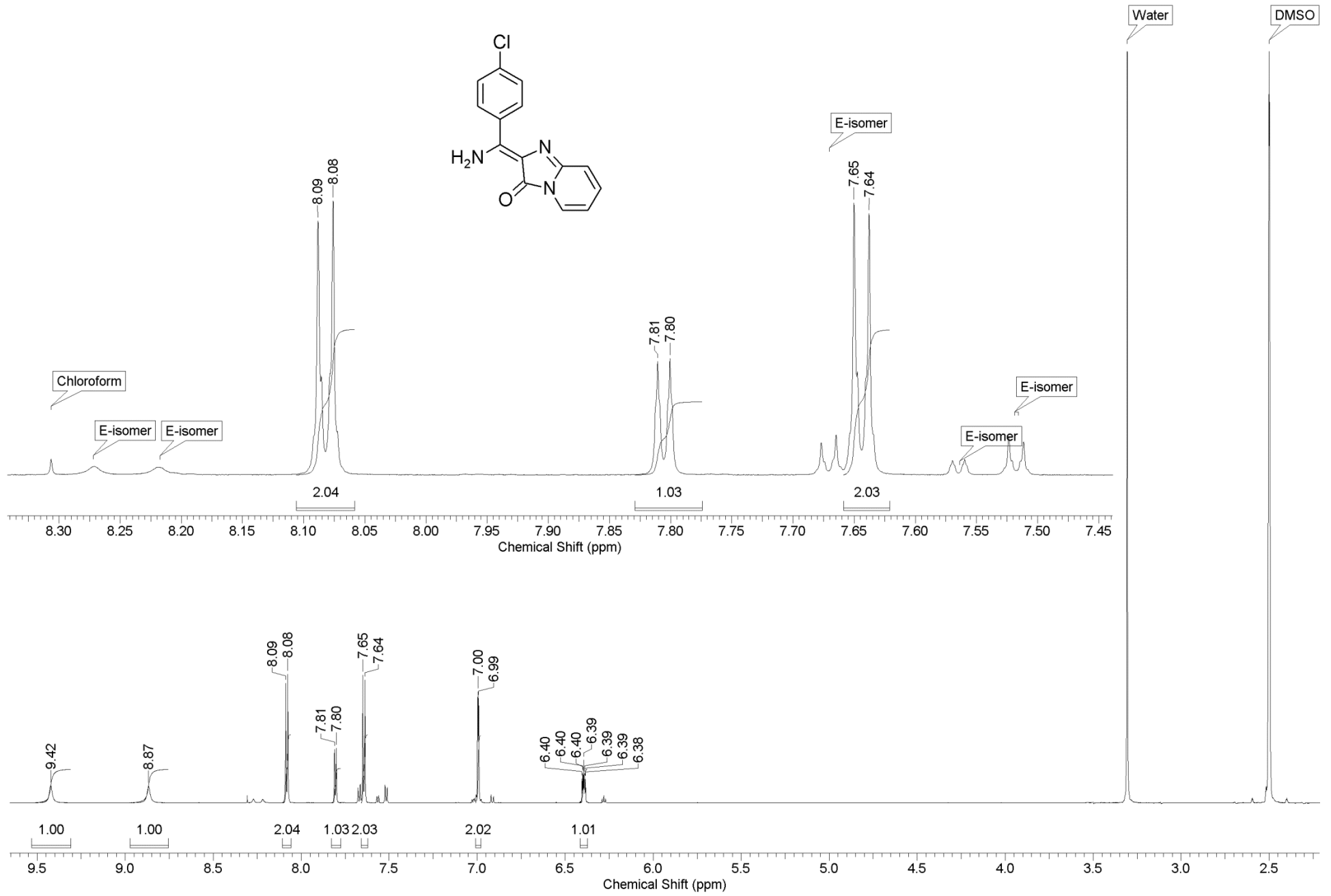




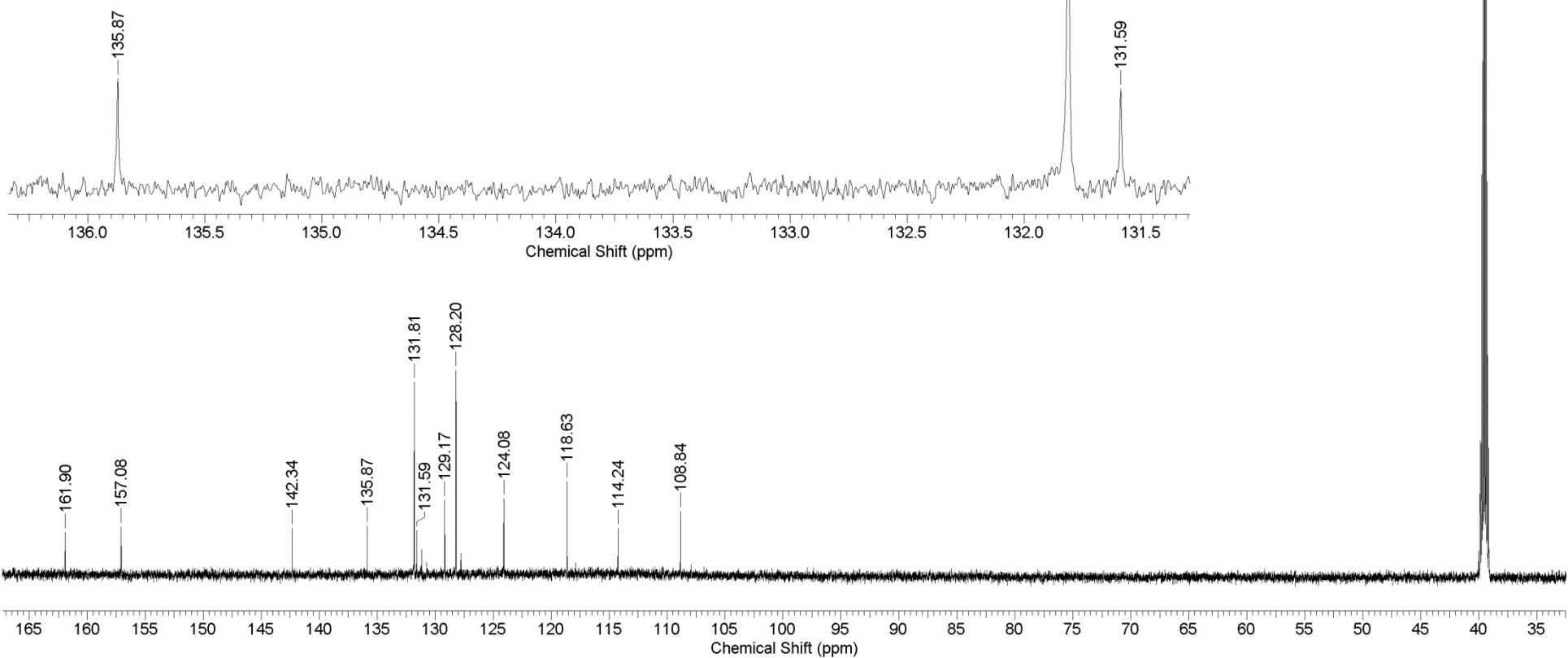
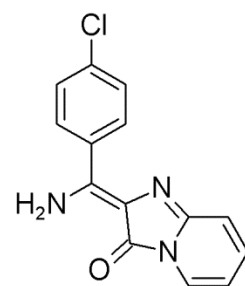


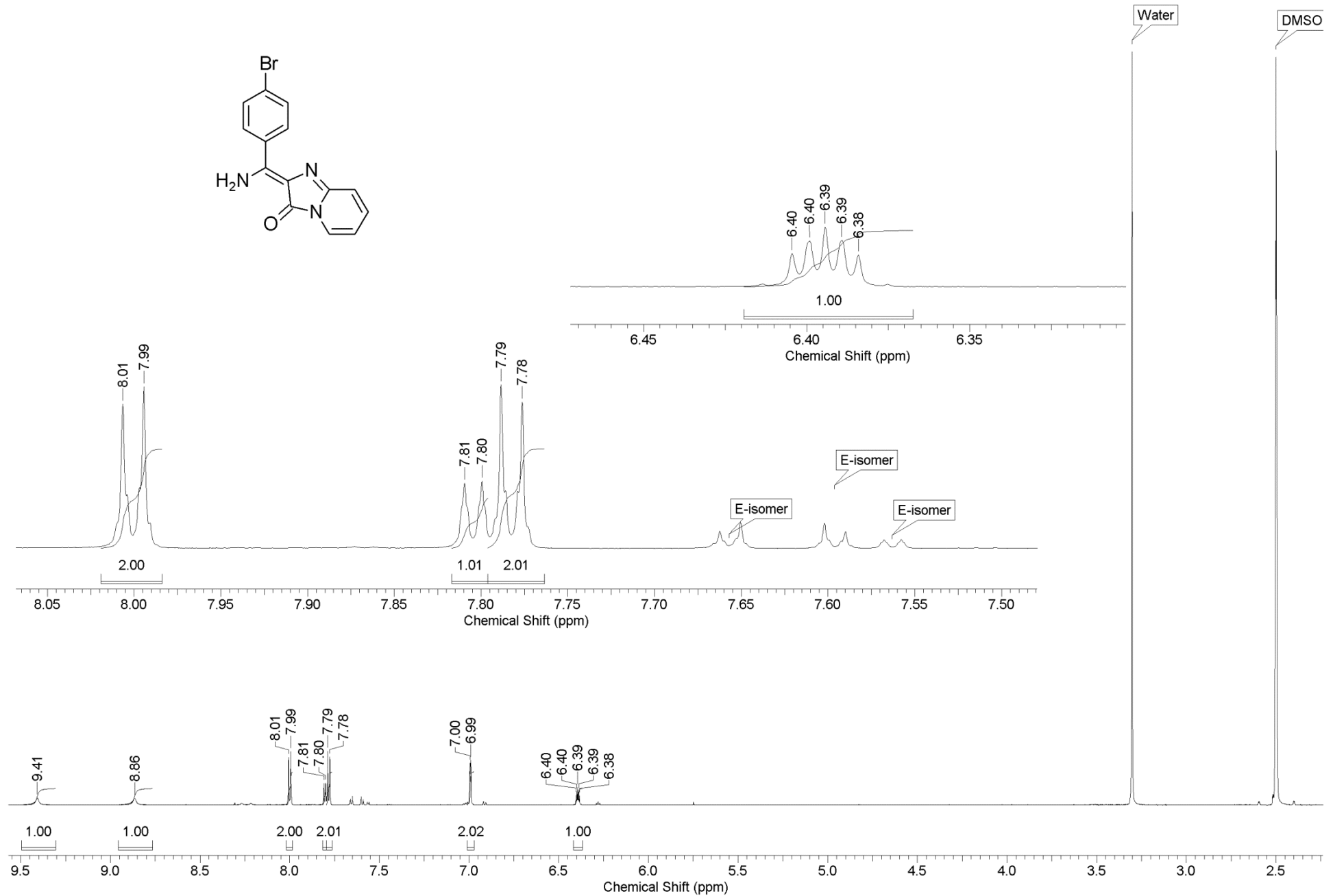
DMSO

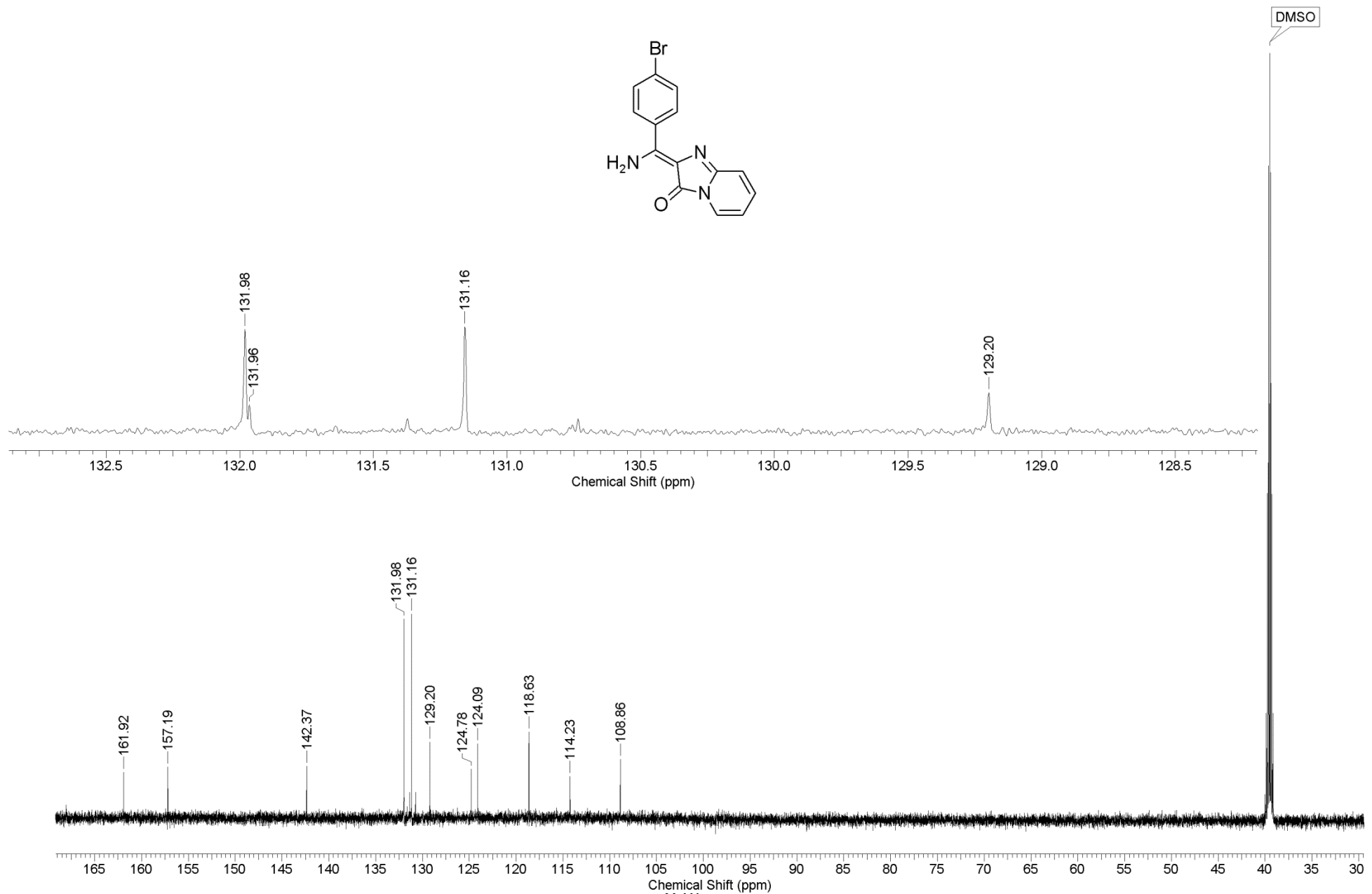


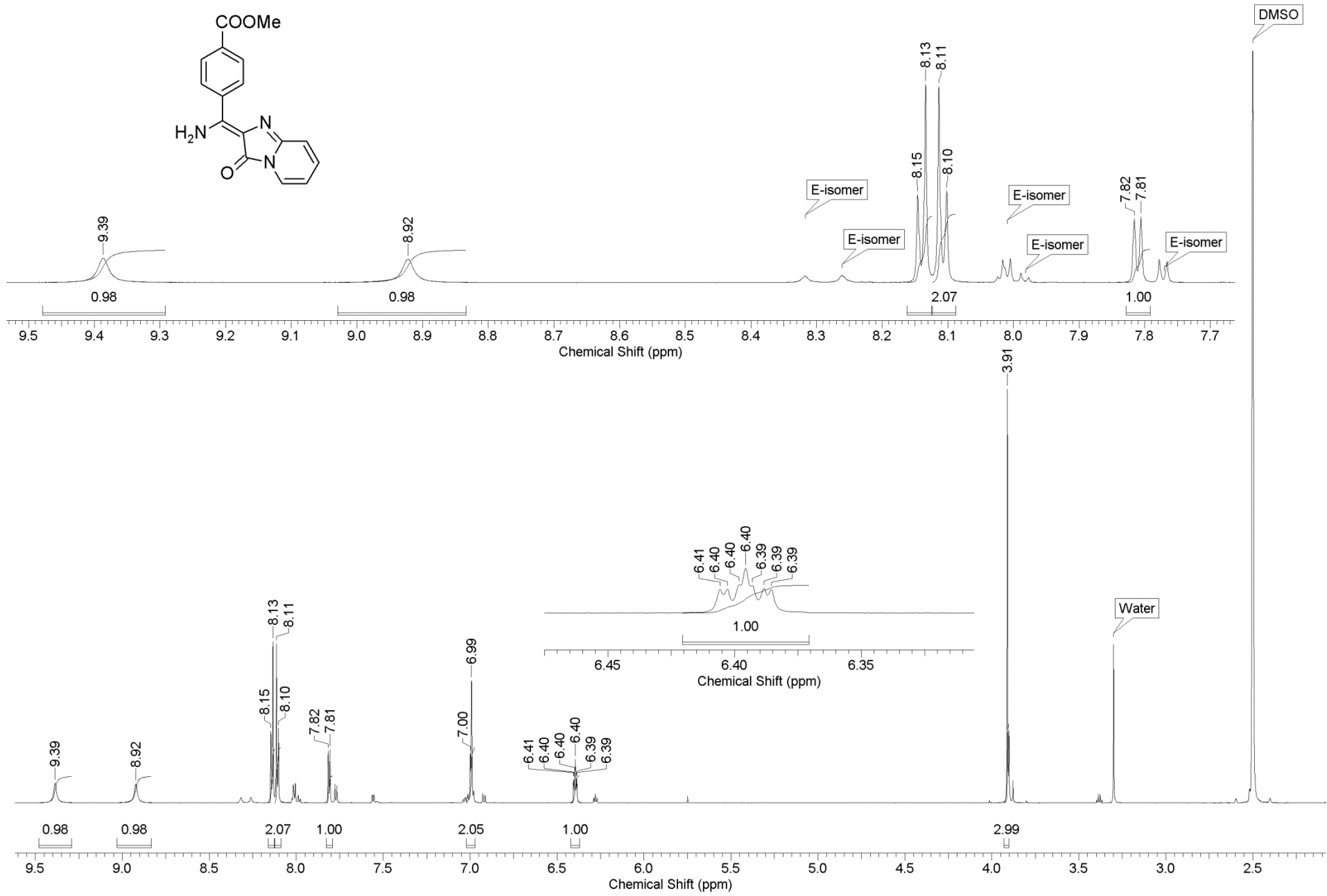


DMSO

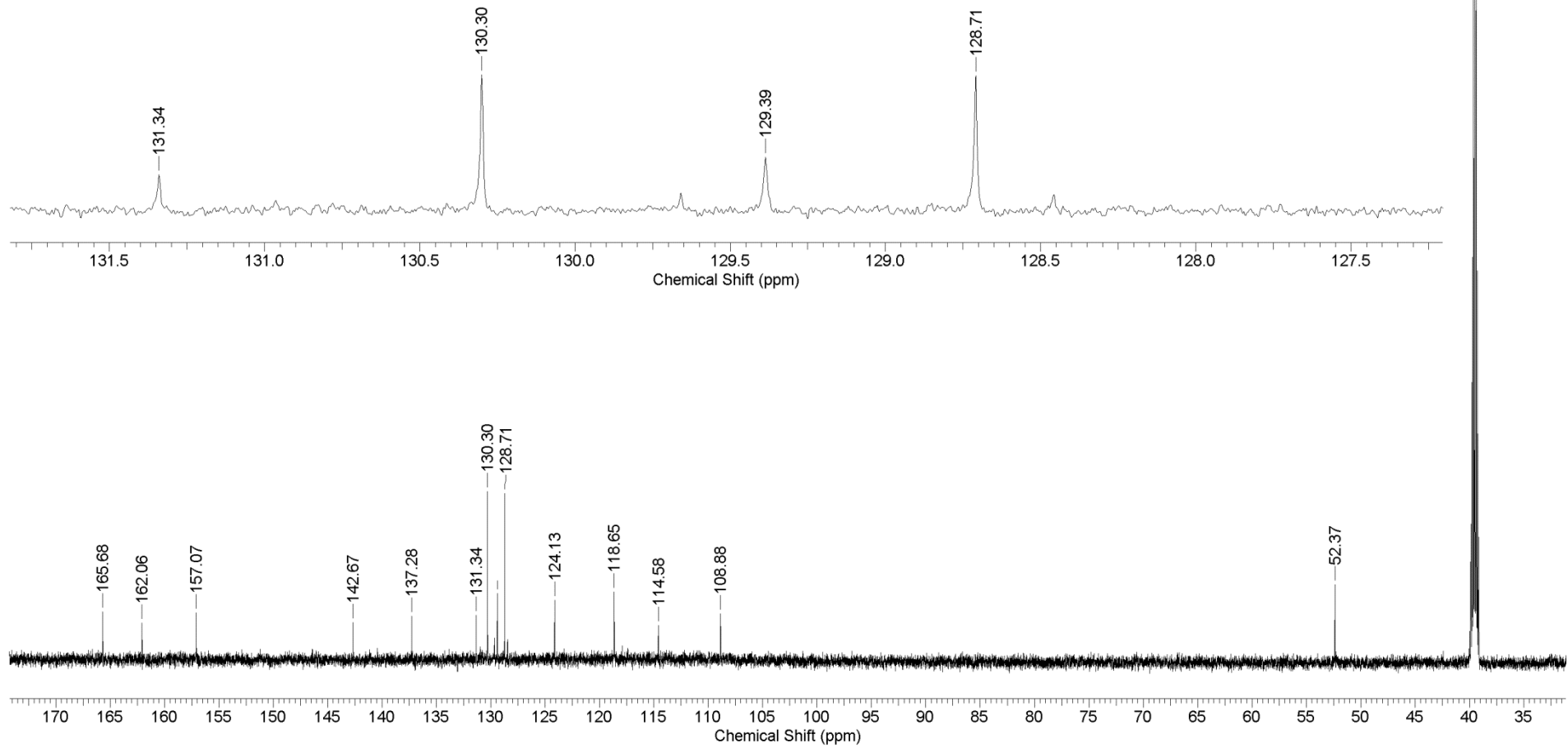
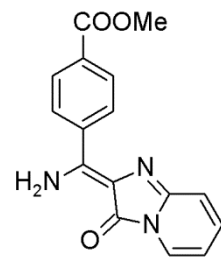


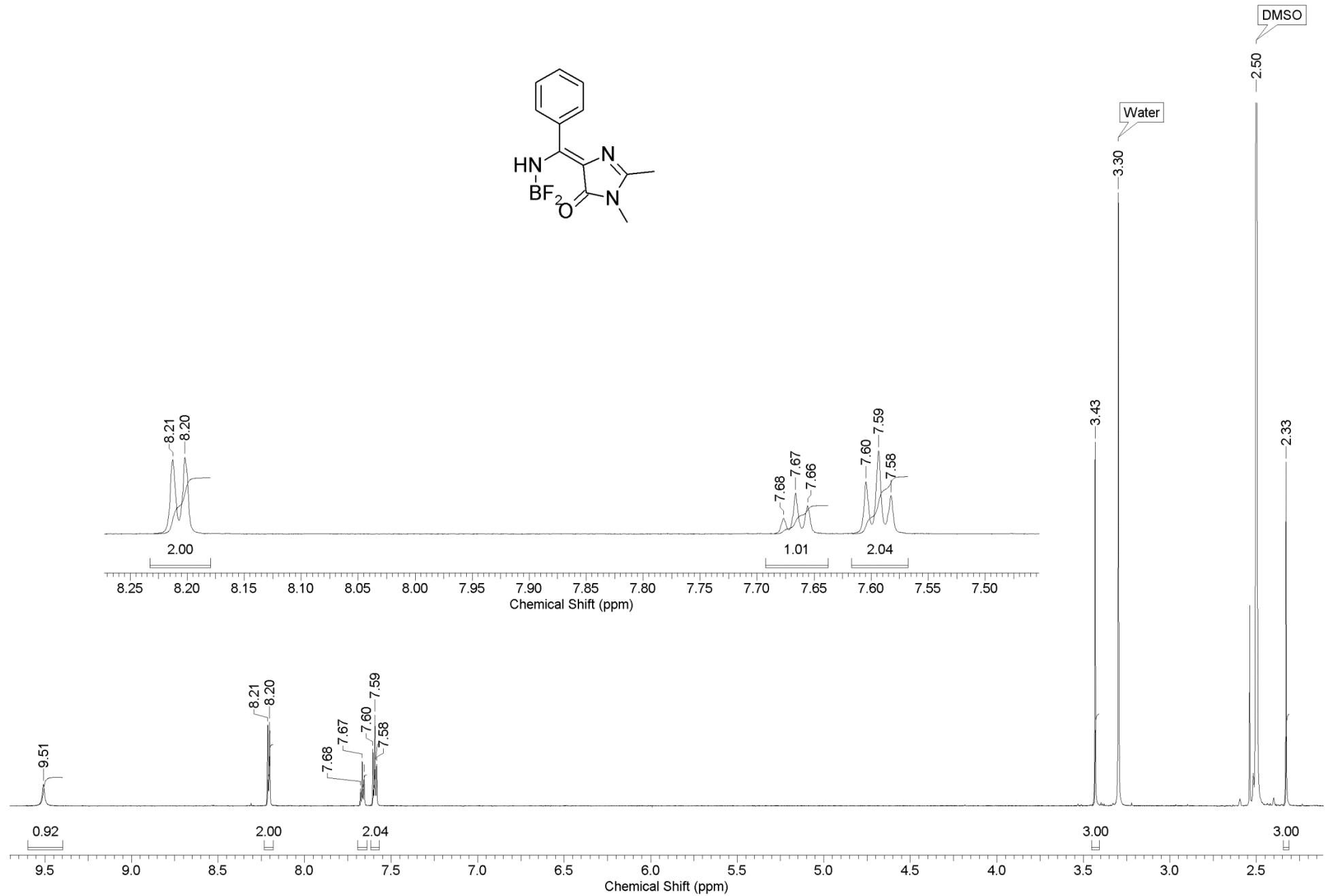


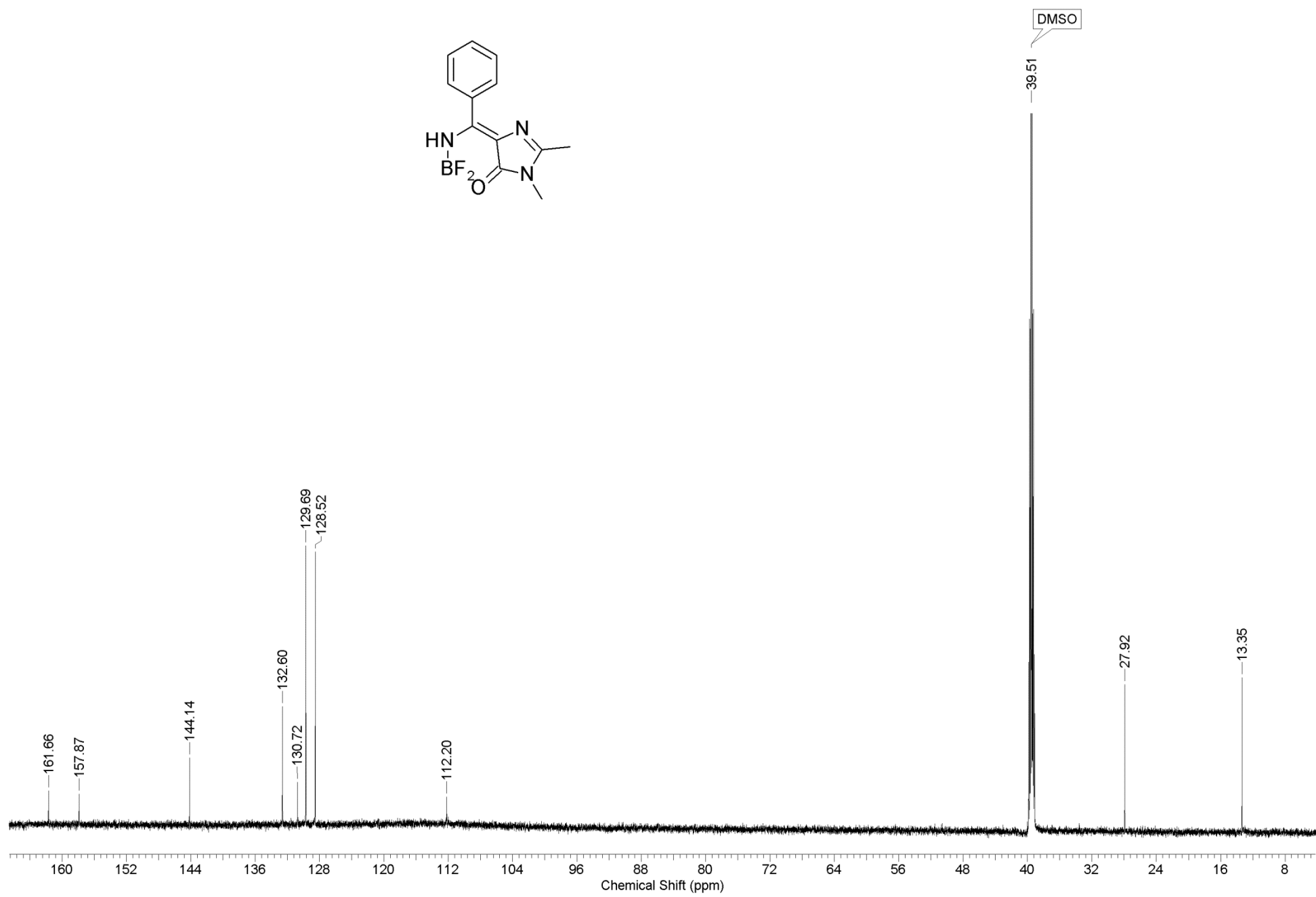


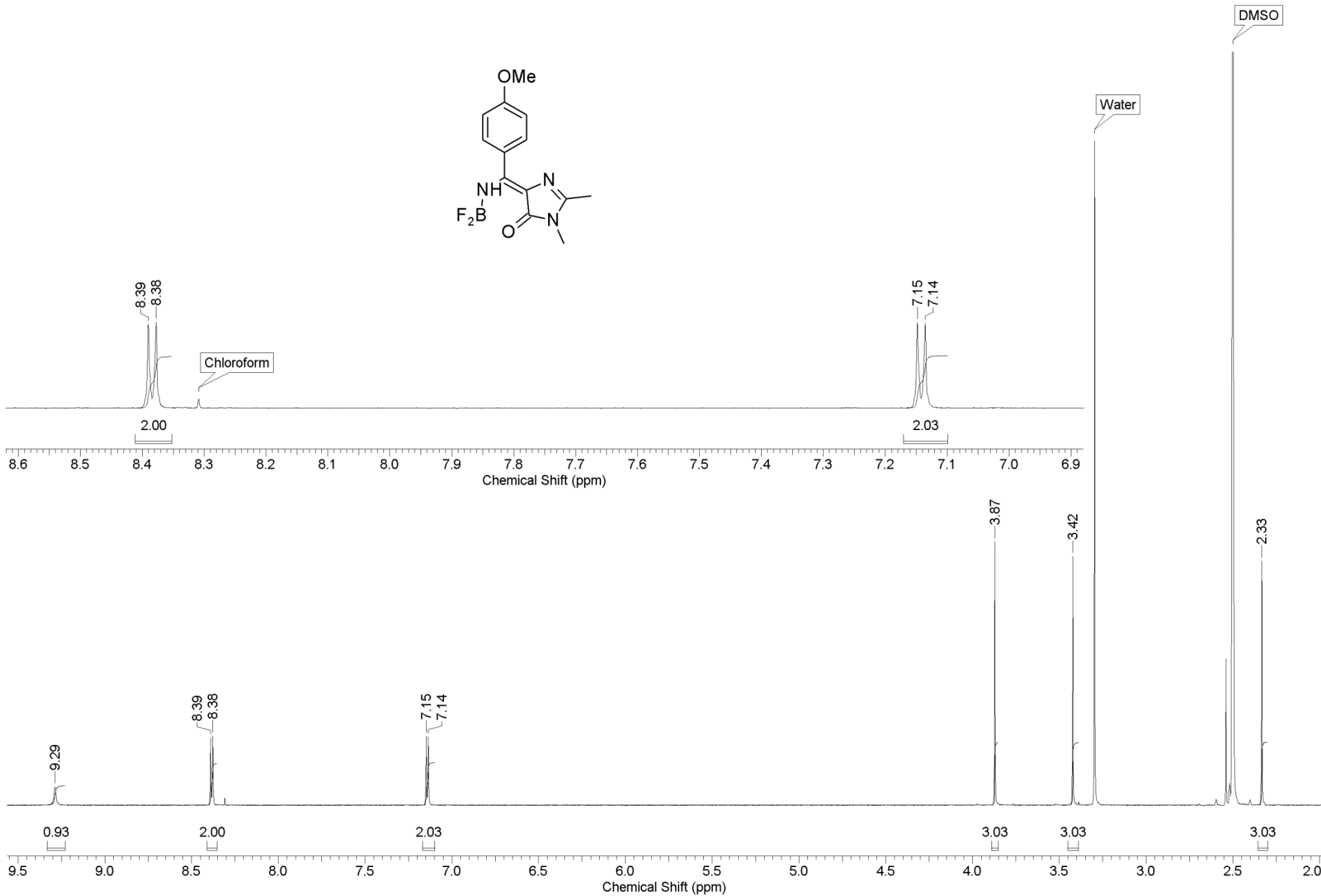


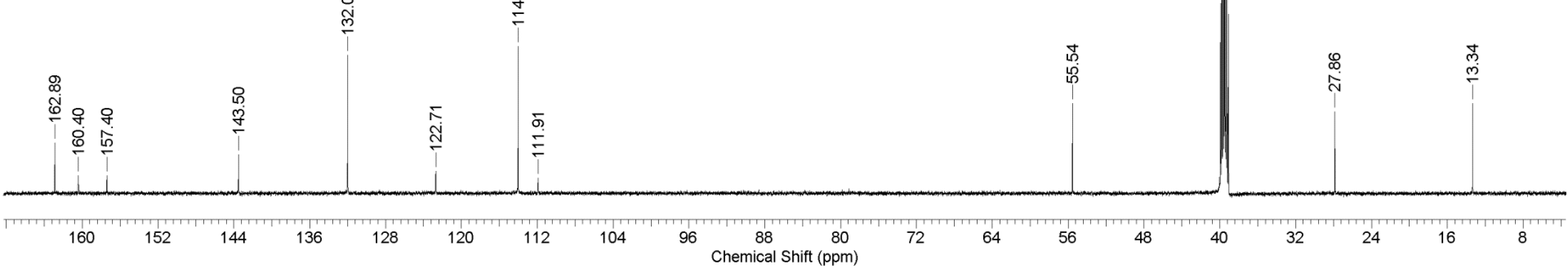
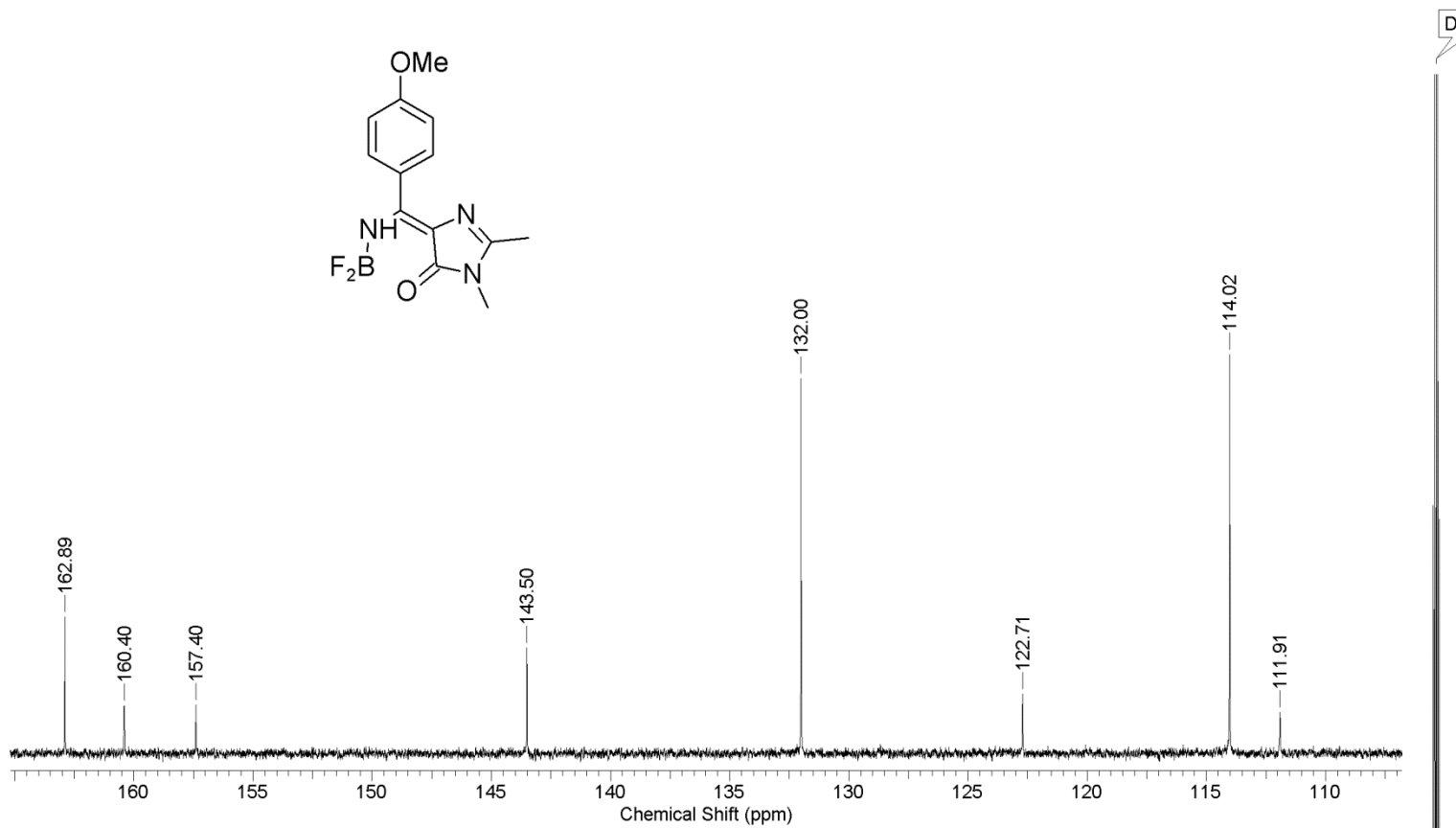
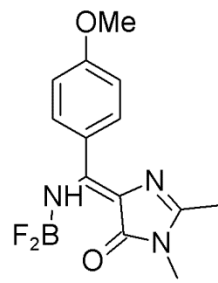
DMSO

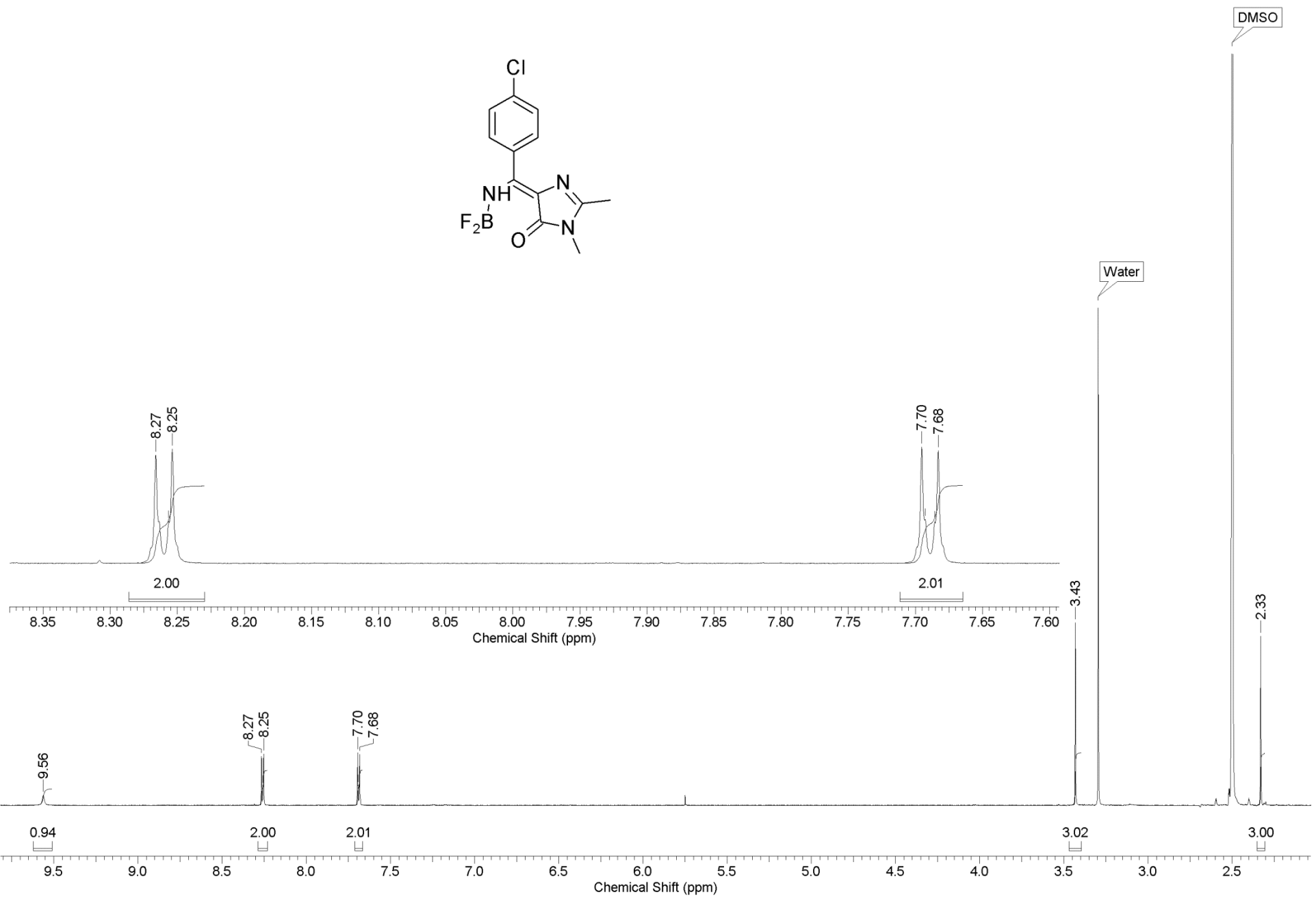


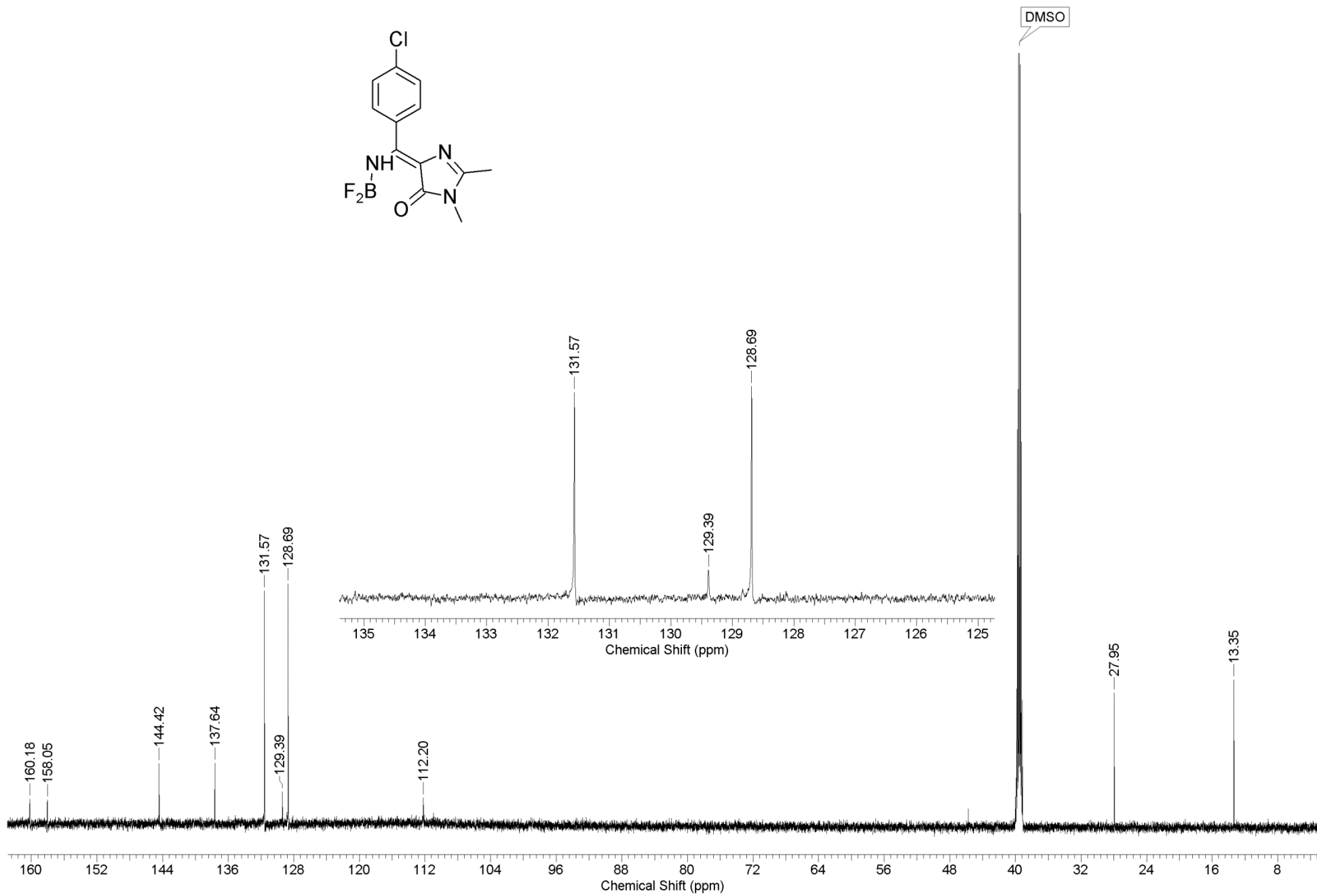
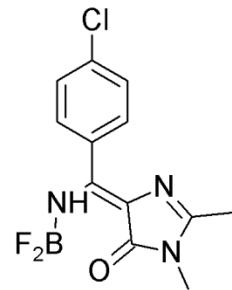




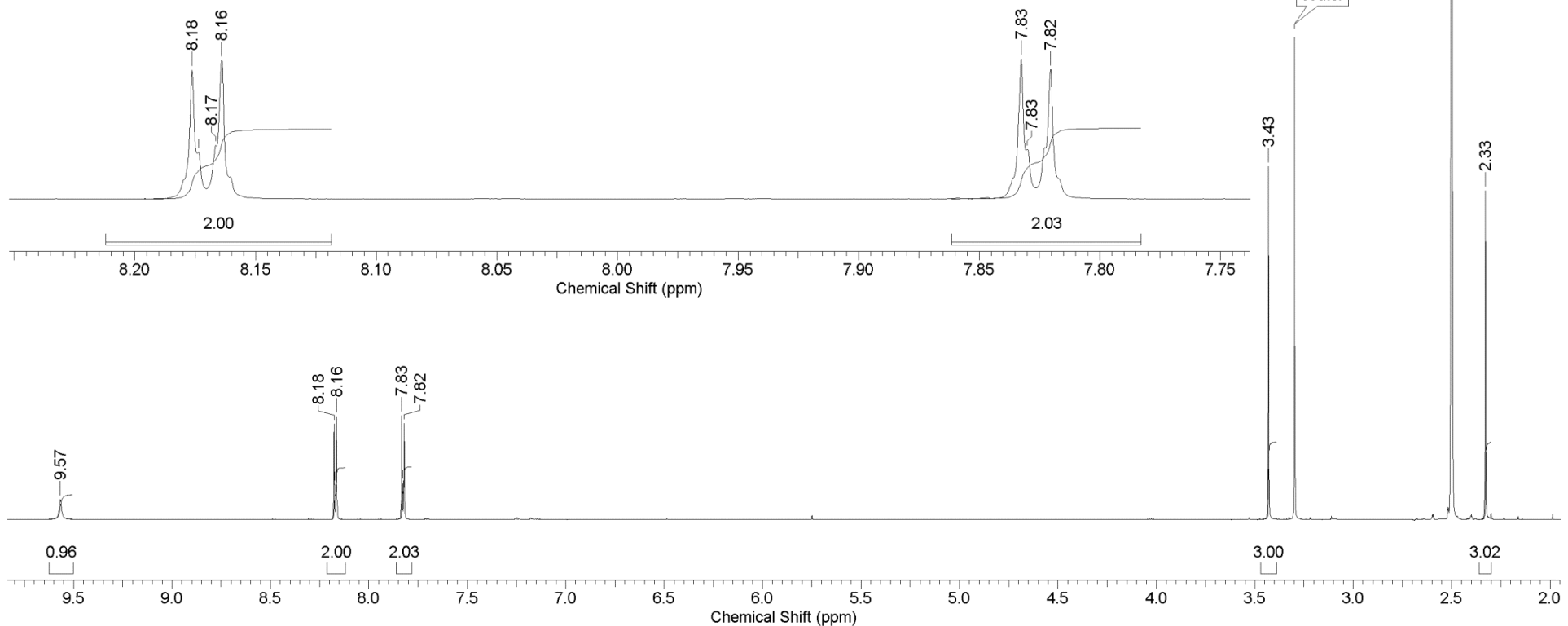
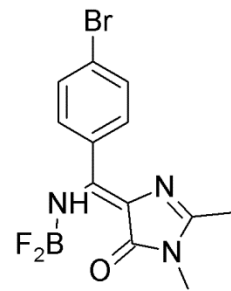


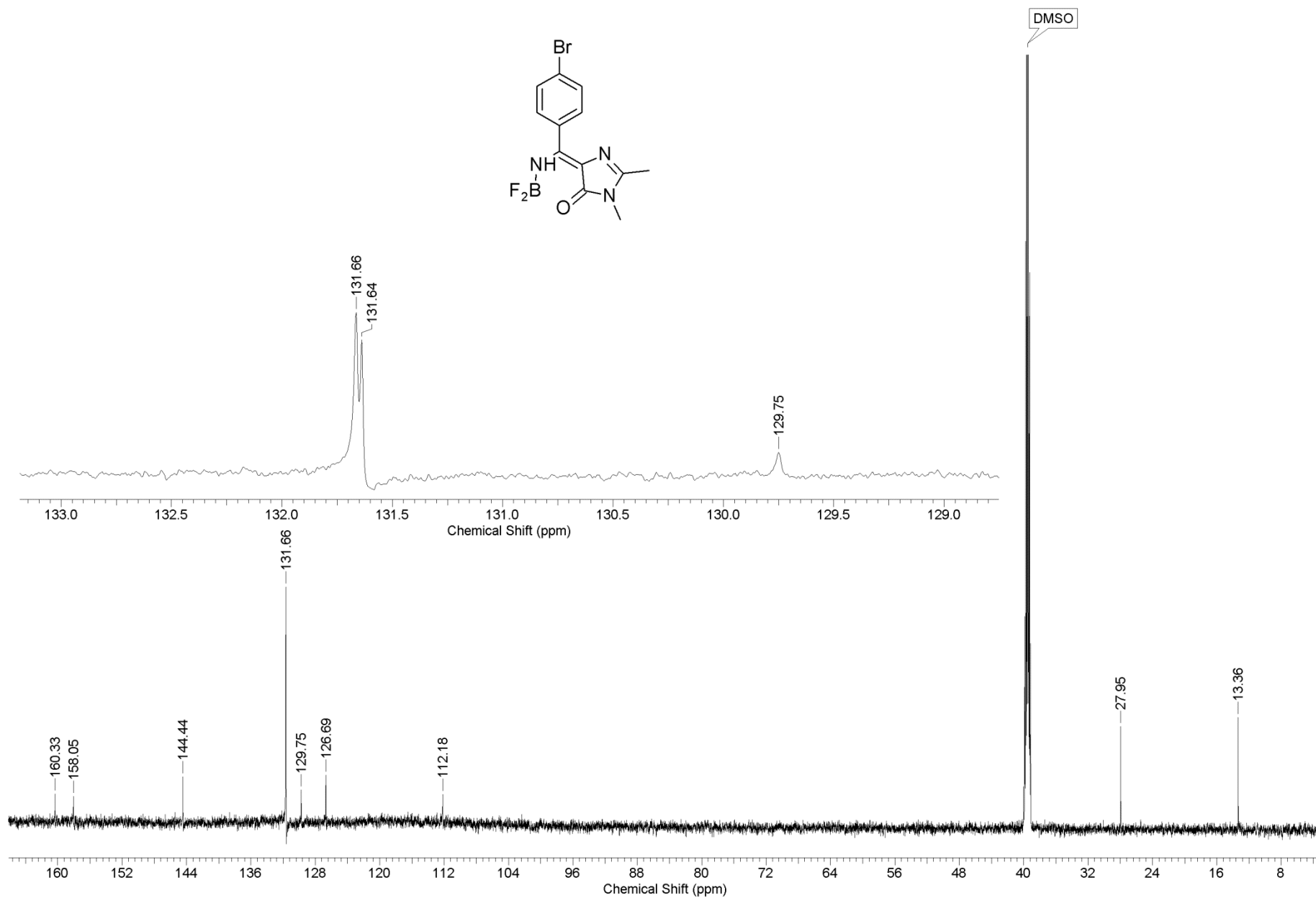


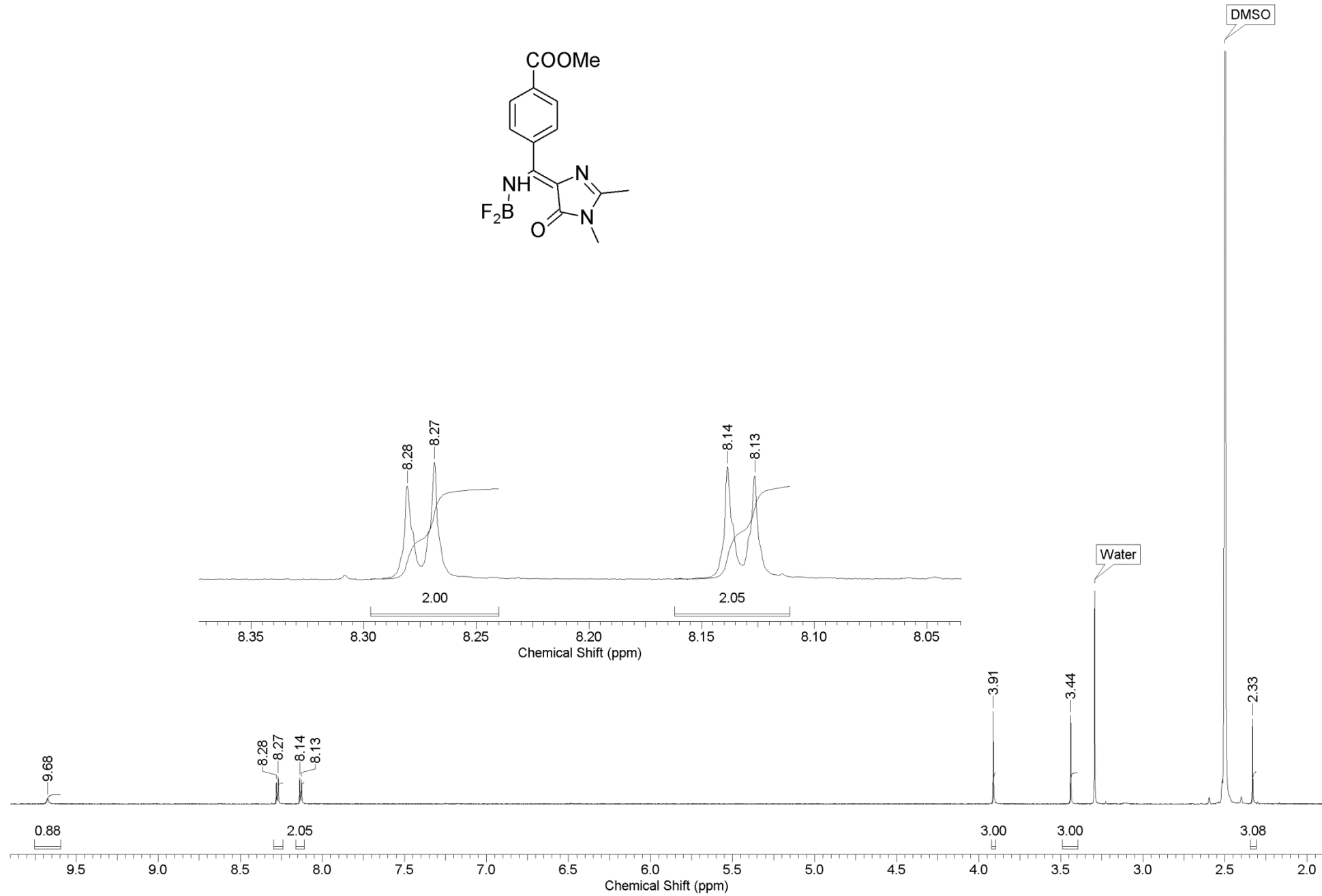


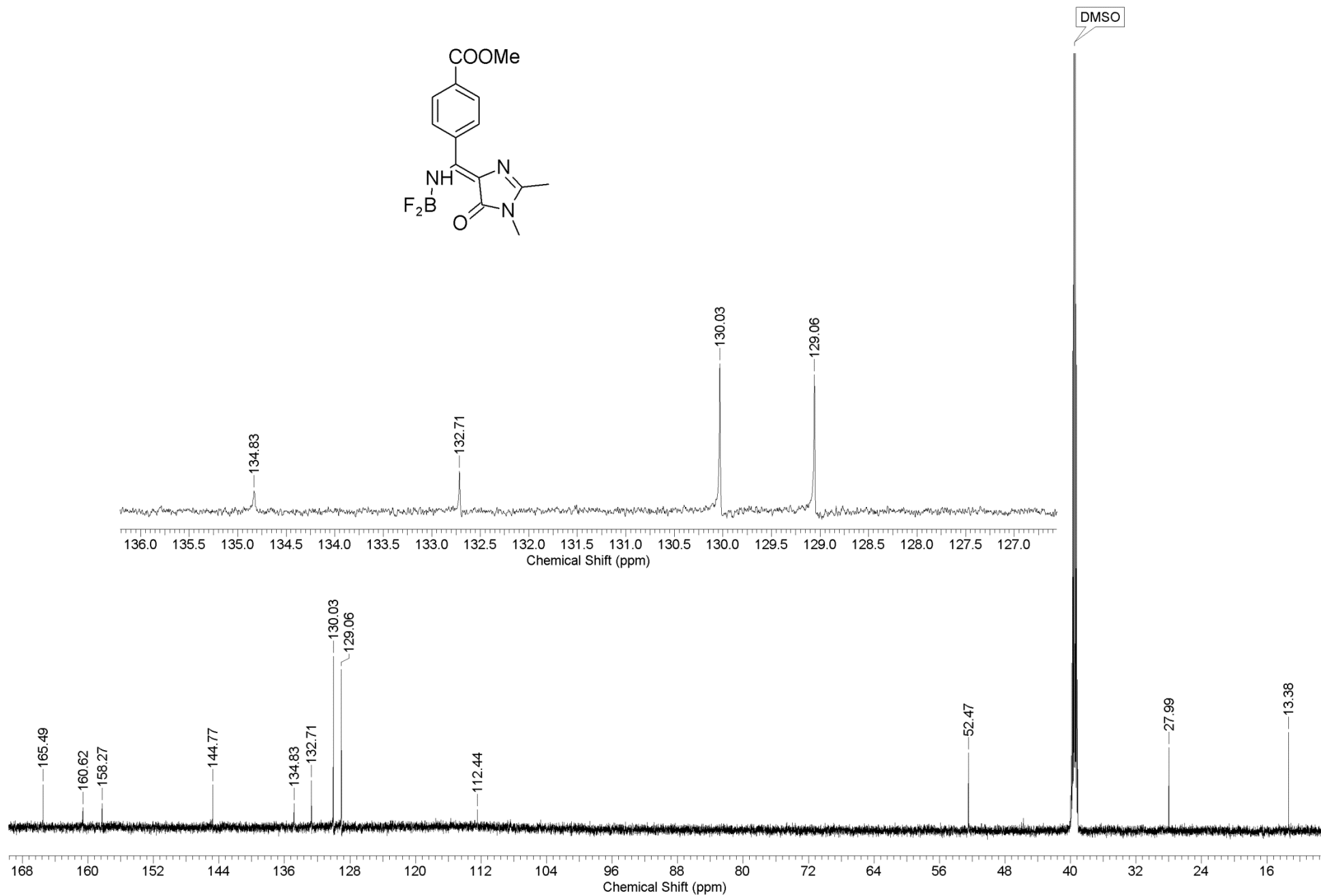


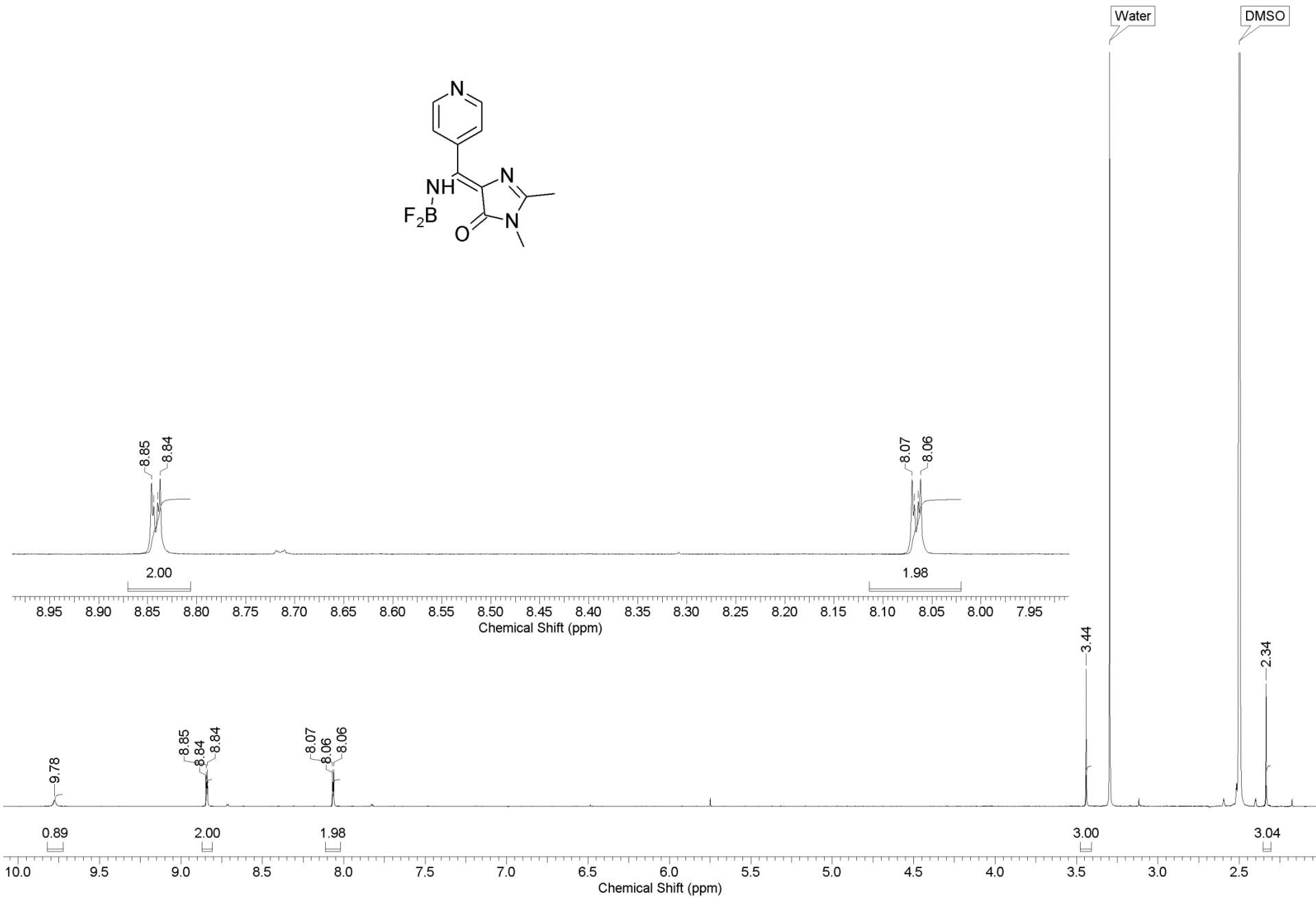
DMSO

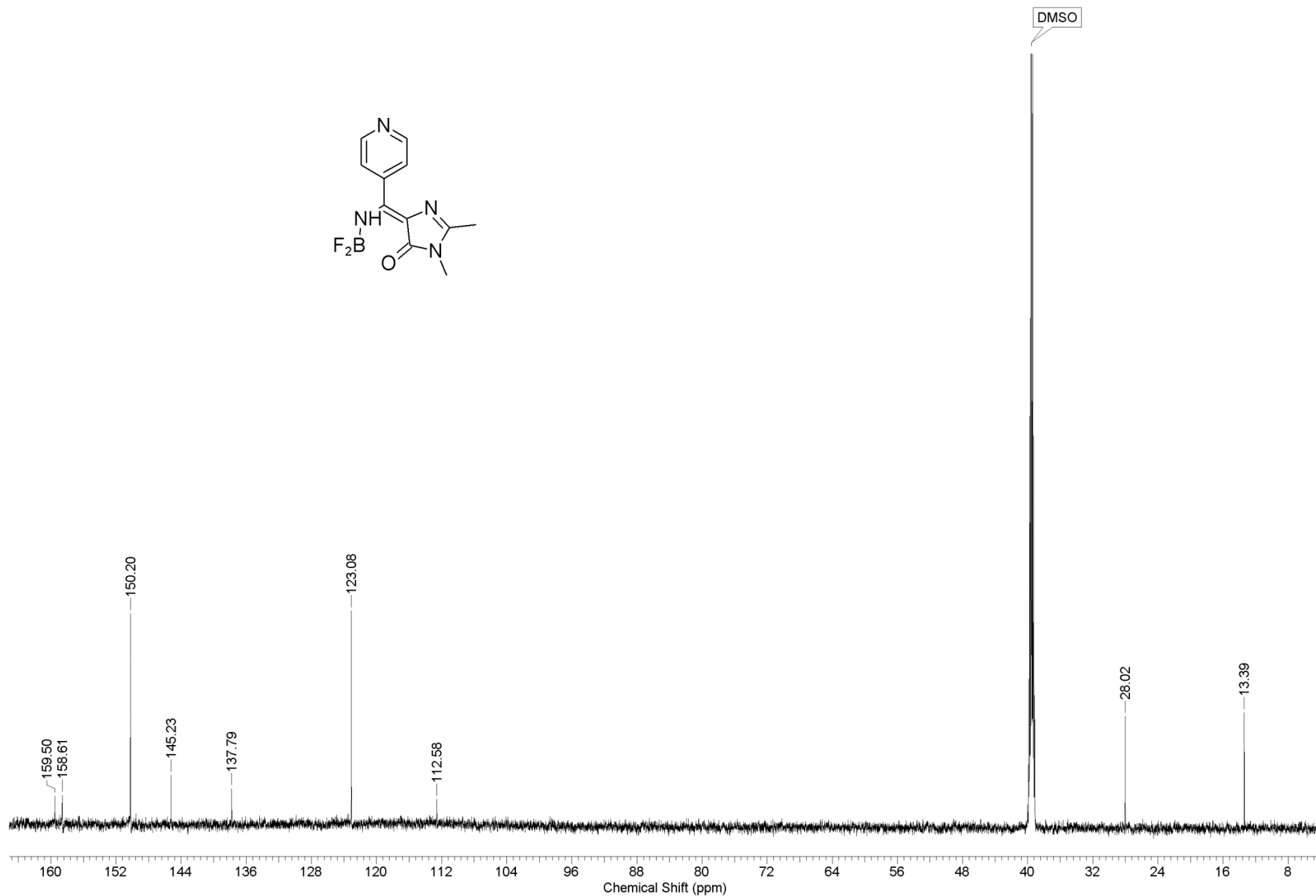


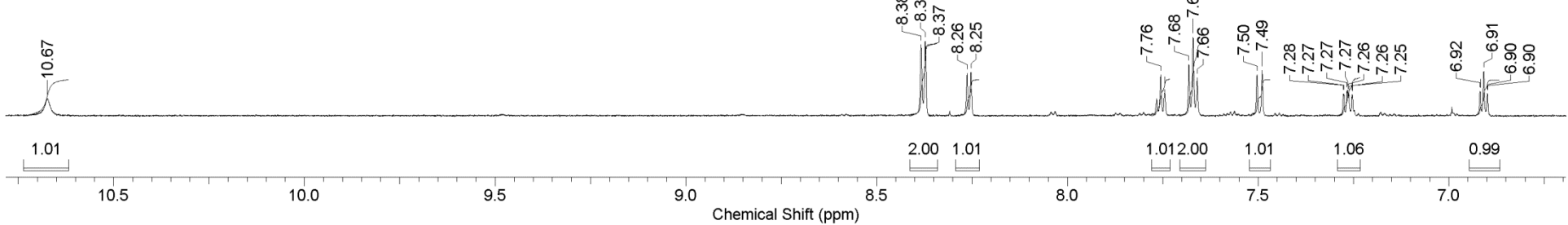
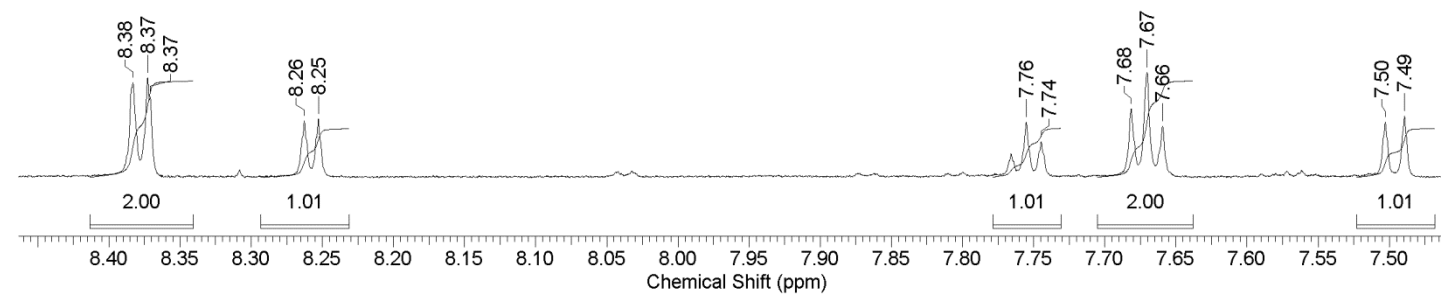
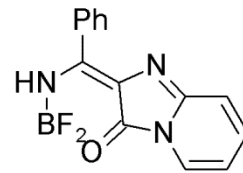




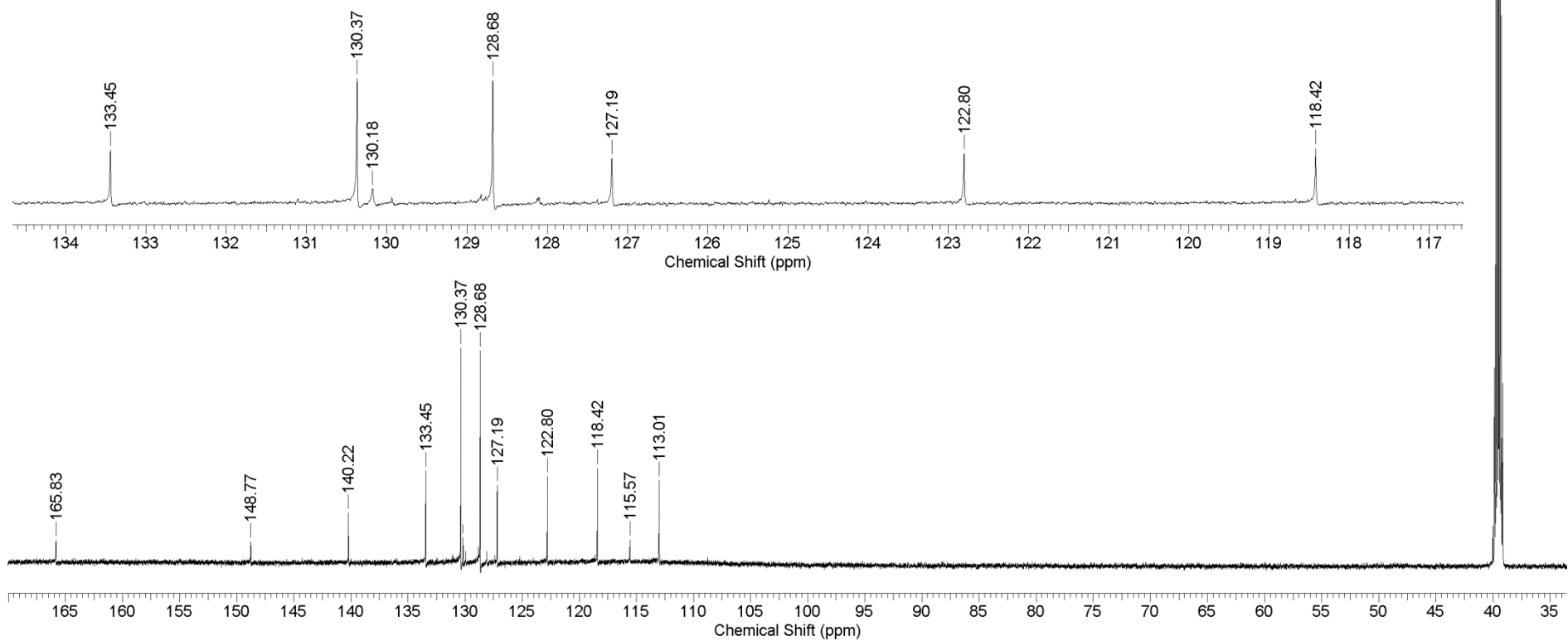
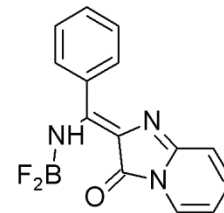


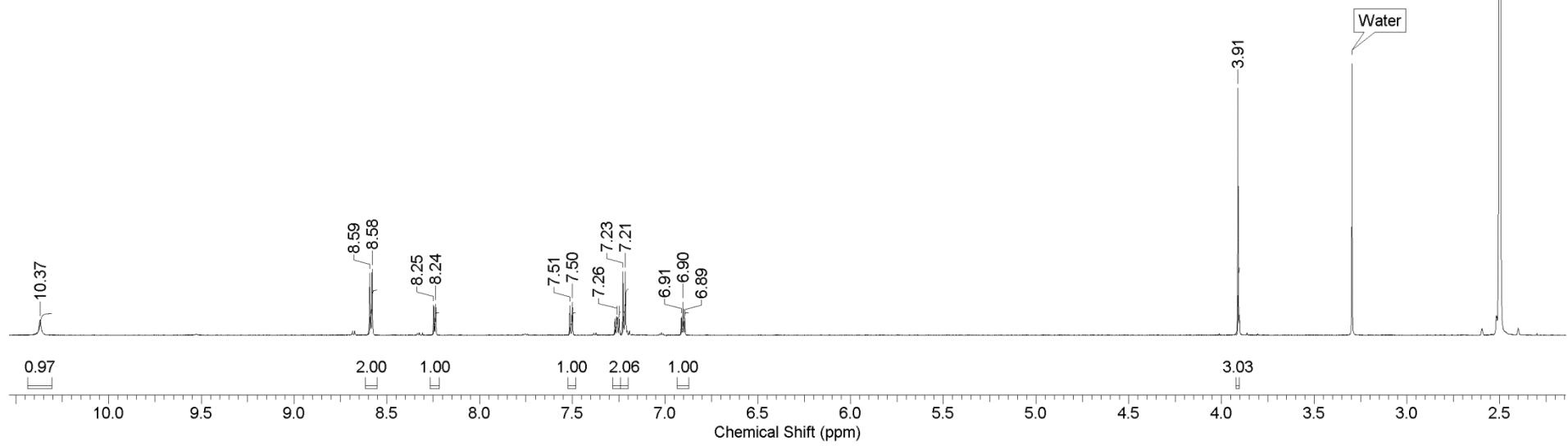
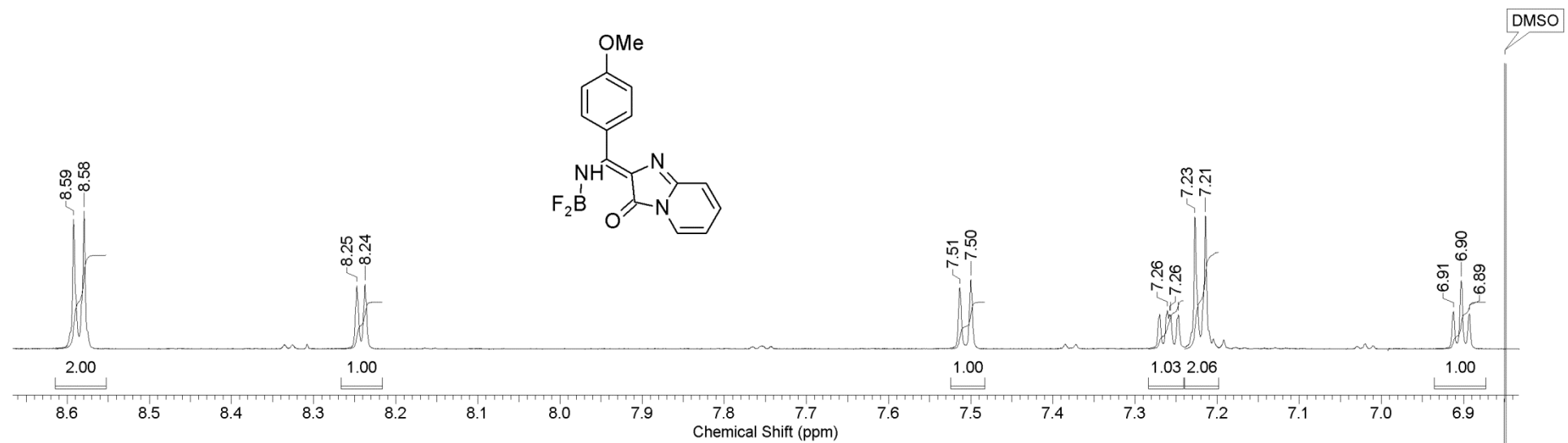


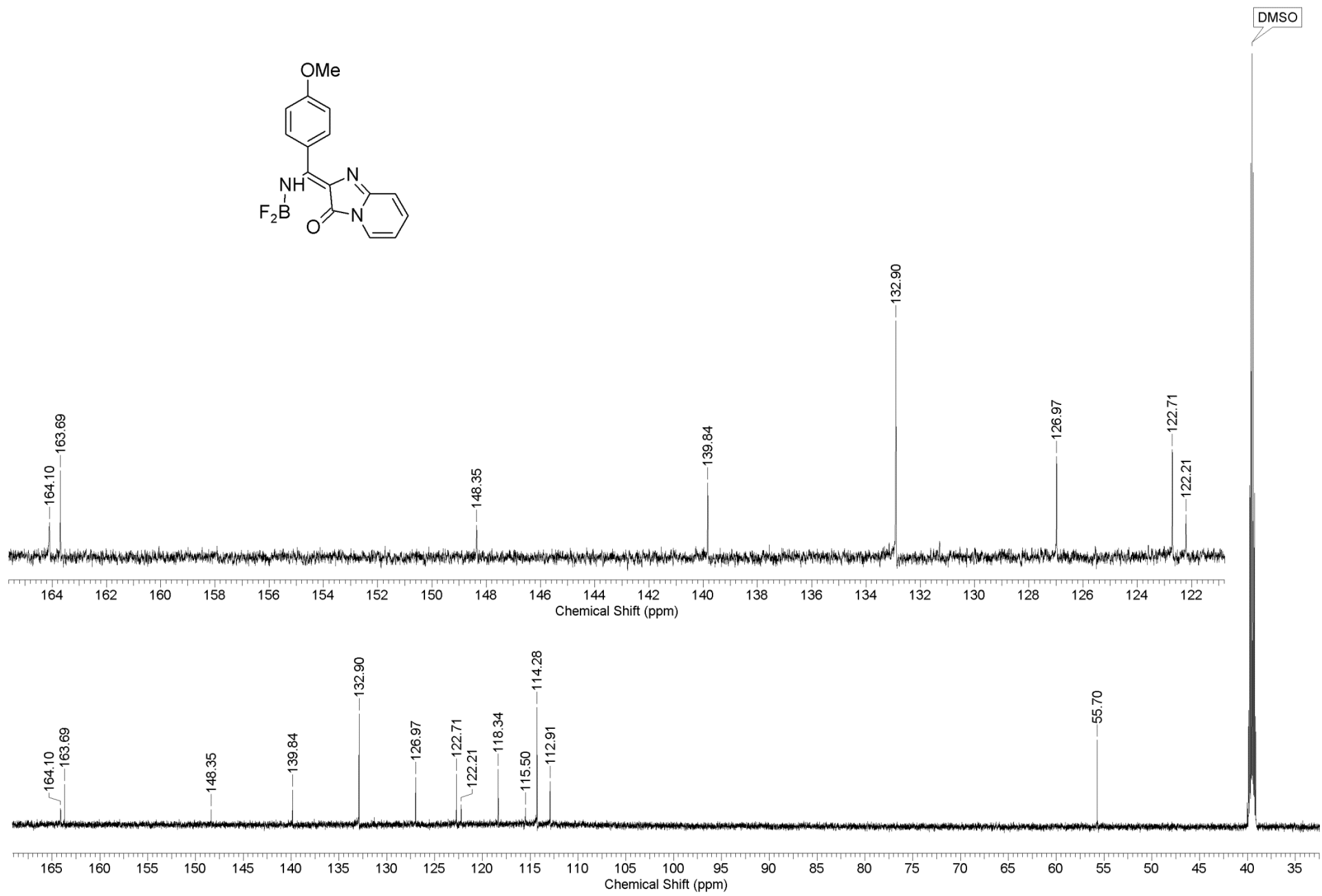


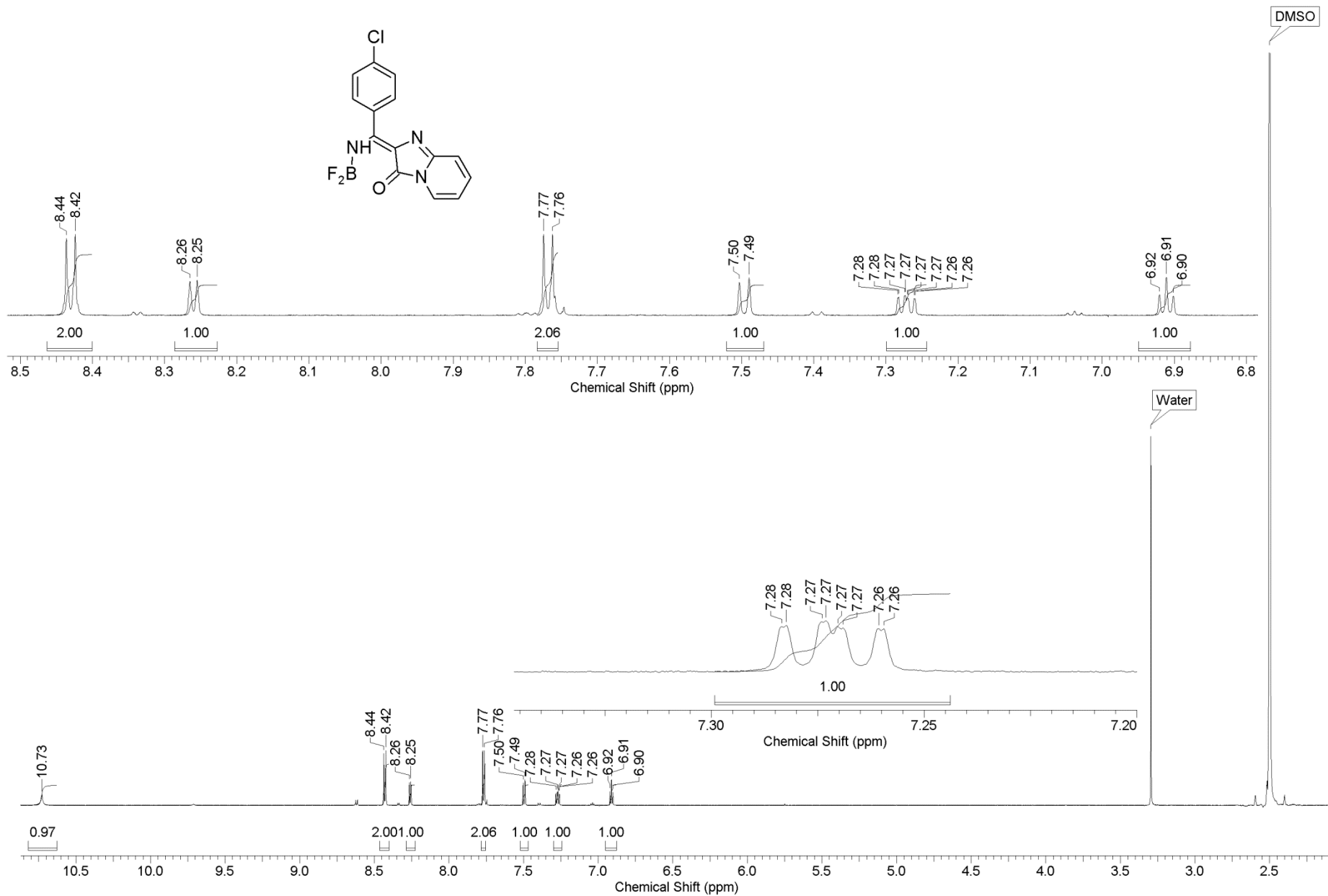


DMSO

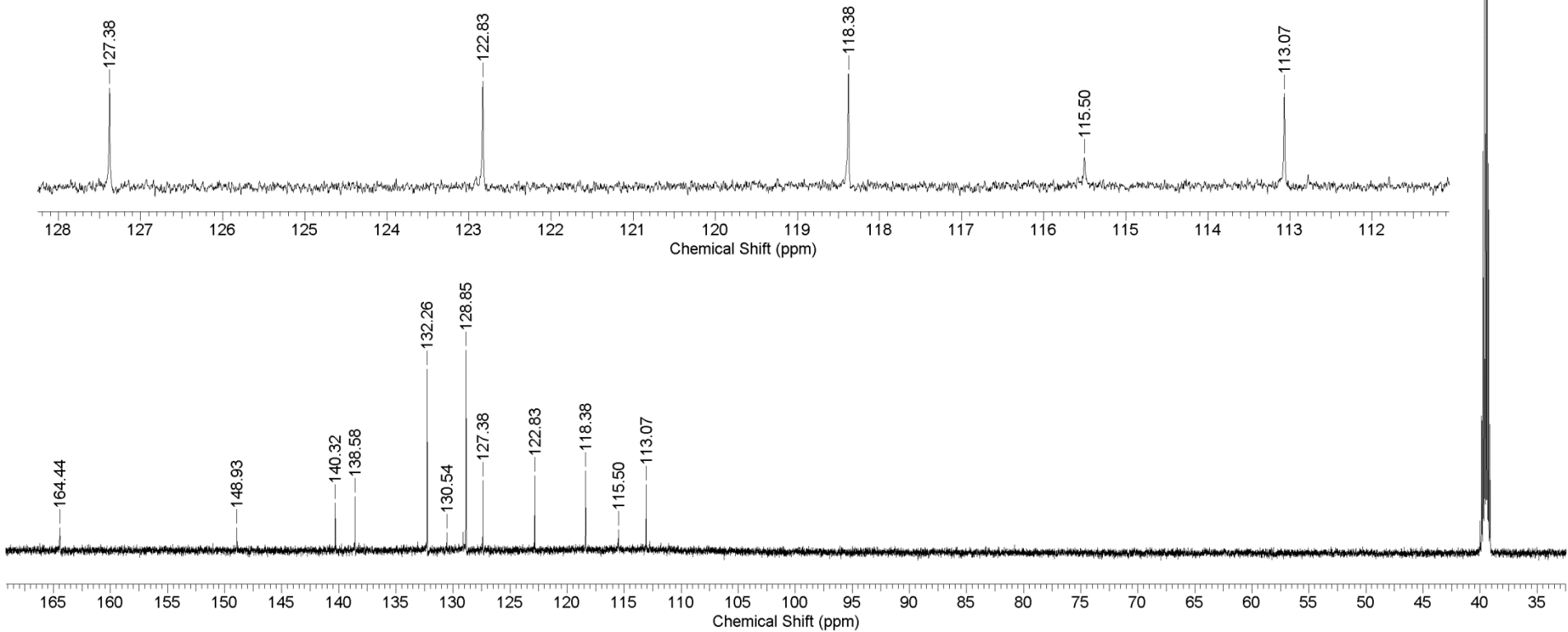
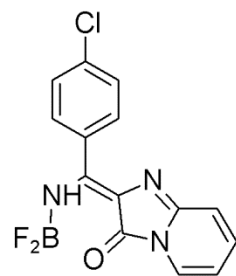


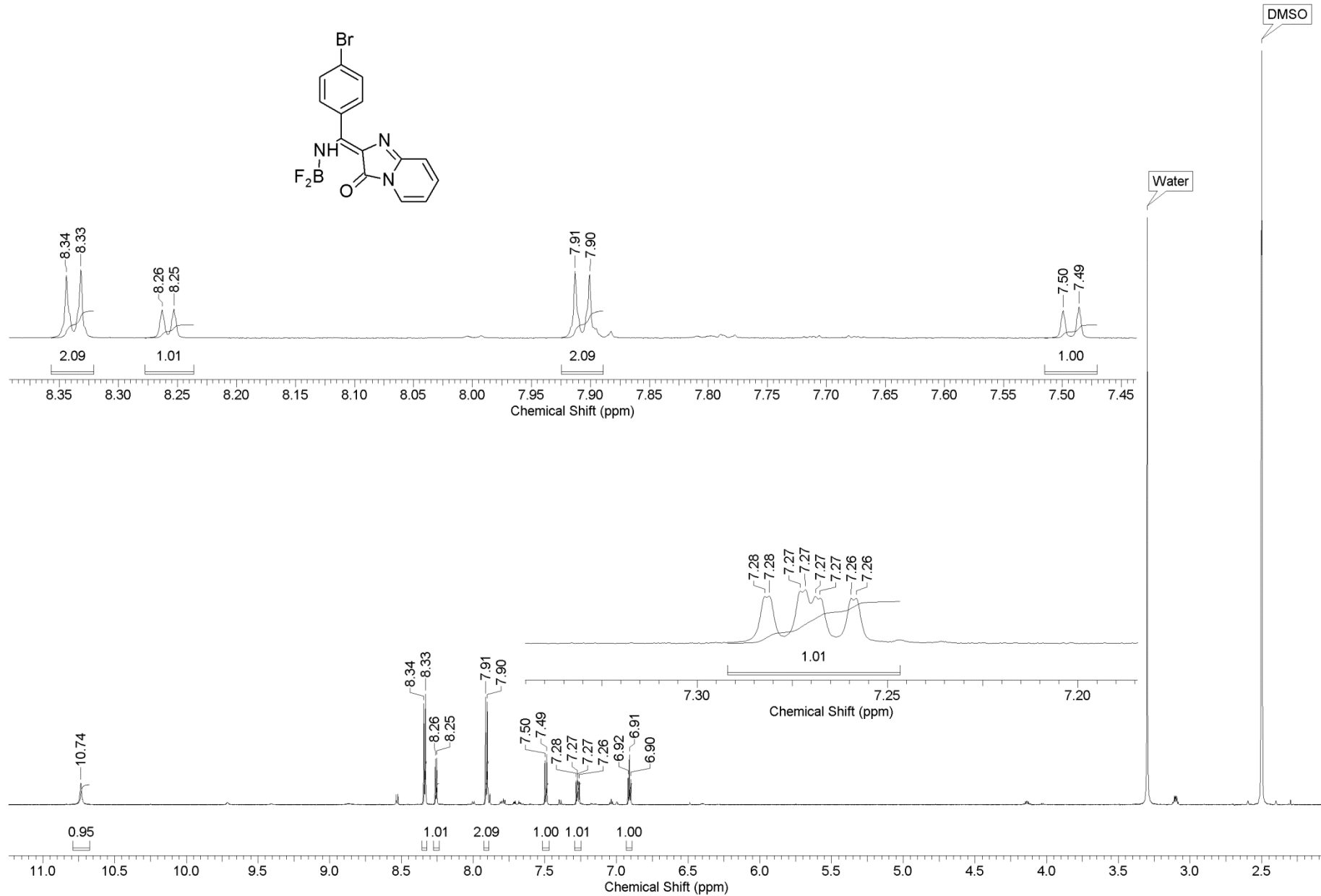
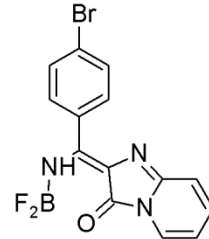




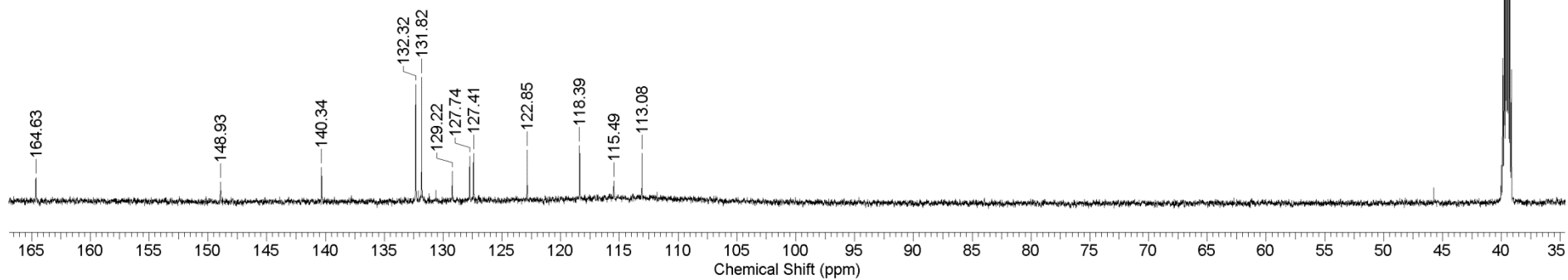
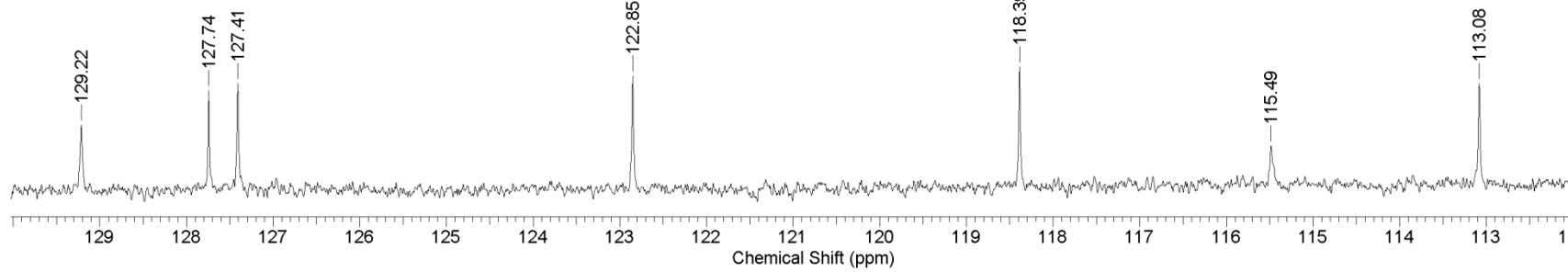
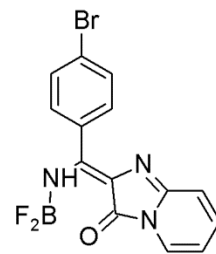


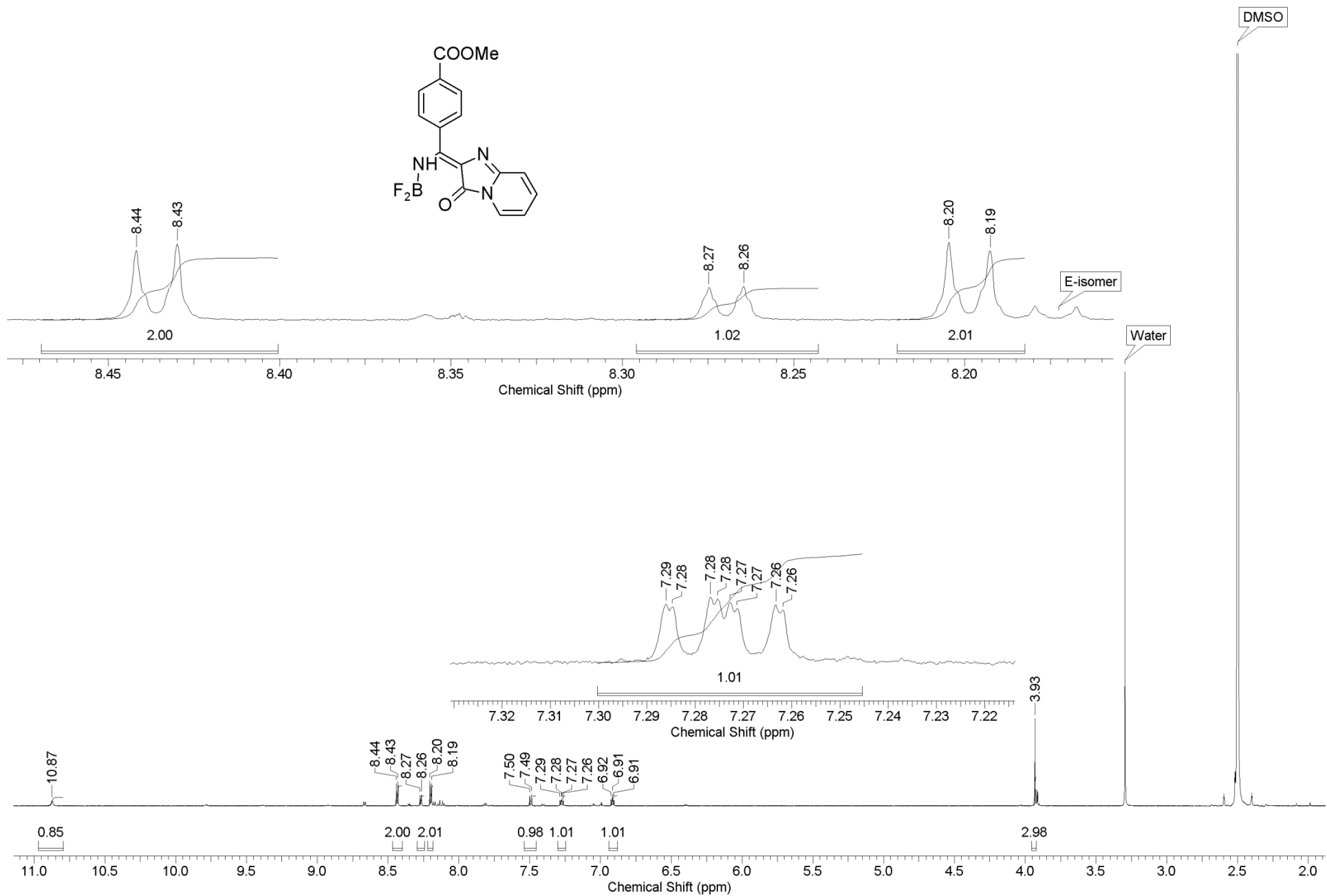
DMSO

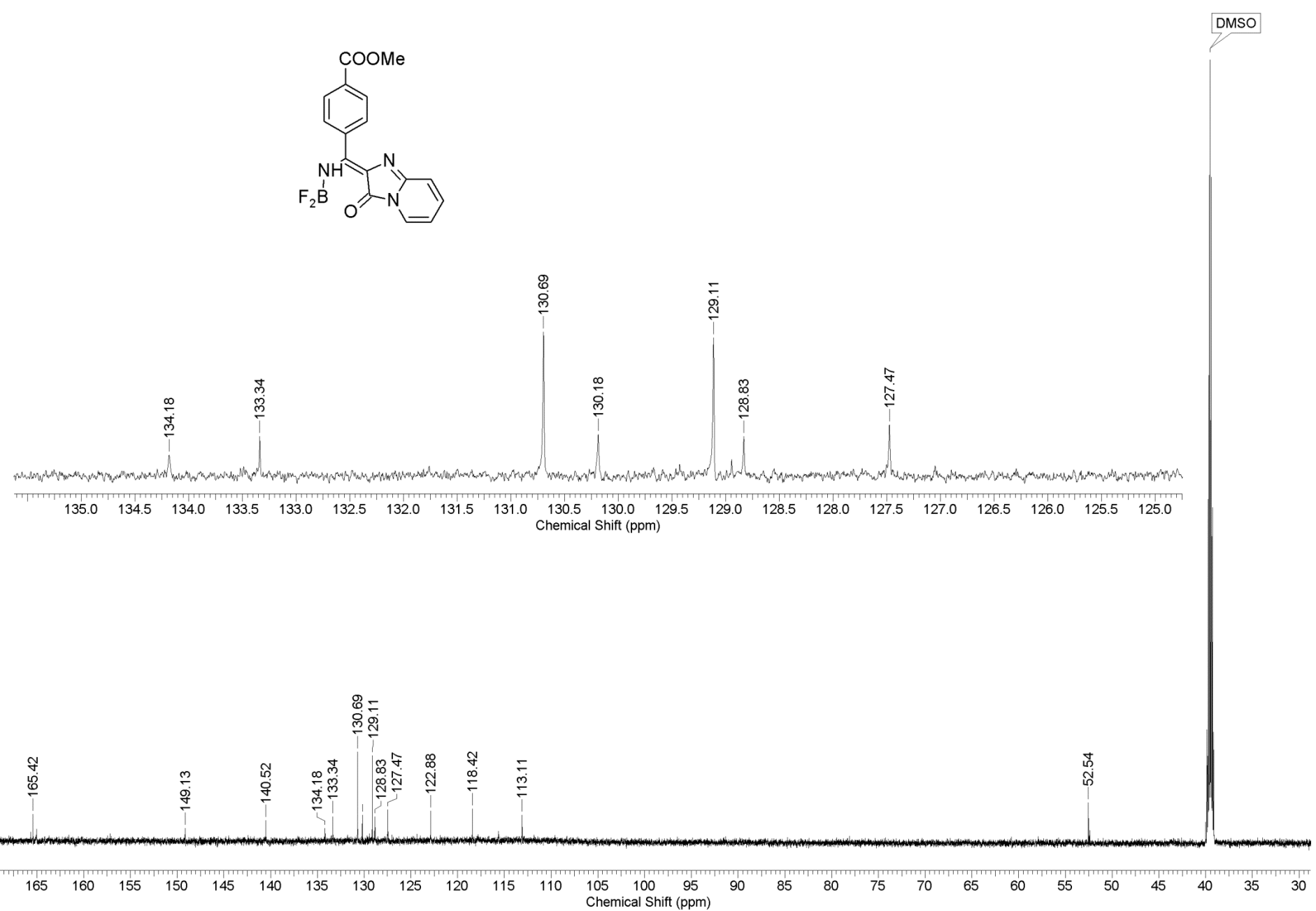




DMSO







5. Computational results

Computational details

The ground-state equilibrium geometry parameters were found at the MP2 level of theory. The (aug)-cc-pVTZ basis set augmented with diffuse functions on oxygen and nitrogen atoms was used. All excited-state calculations were performed using the extended multiconfiguration quasi-perturbation theory XMCQPDT2.¹³ The zeroth-order wave functions were constructed within the complete active space self-consistent field method CASSCF(16,14), where all valence π -type orbitals of the chromophore were included in the active space. The vertical excitation and emission energies were calculated at the XMCQDPT2[7]/SA(7)-CASSCF(16,14)/(aug)-cc-pVTZ level of theory. The equilibrium geometry parameters in the first excited state were obtained using the XMCQDPT2[2]/SA(2)-CASSCF(14,13)/(aug)-cc-pVTZ method with a slightly smaller active space. One orbital was removed from the active space based on the analysis of the occupation numbers of the natural orbitals. All calculations were performed within the Firefly quantum chemistry package.¹⁴

The two-photon absorption properties were calculated using Dalton quantum chemistry program.^{15,16} The ground-state equilibrium geometry parameters obtained previously at the MP2 level of theory were used. The excitation energies and cross-sections were found with time-dependent hybrid exchange–correlation functional TDDFT CAM-B3LYP. The (aug)-cc-pVTZ basis set was used.

¹³ A.A. Granovsky, *J. Chem. Phys.*, 2011, **134**, 214113.

¹⁴ A.A. Granovsky, Firefly, version 8.2.0 <http://classic.chem.msu.su/gran/firefly/index.html>

¹⁵ K. Aidas, C. Angeli, K. L. Bak, V. Bakken, R. Bast, L. Boman, O. Christiansen, R. Cimiraglia, S. Coriani, P. Dahle, E. K. Dalskov, U. Ekström, T. Enevoldsen, J. J. Eriksen, P. Ettenhuber, B. Fernández, L. Ferrighi, H. Fliegl, L. Frediani, K. Hald, A. Halkier, C. Hättig, H. Heiberg, T. Helgaker, A. C. Hennum, H. Hettema, E. Hjertenæs, S. Høst, I.-M. Høyvik, M. F. Iozzi, B. Jansik, H. J. Aa. Jensen, D. Jonsson, P. Jørgensen, J. Kauczor, S. Kirpekar, T. Kjærgaard, W. Klopper, S. Knecht, R. Kobayashi, H. Koch, J. Kongsted, A. Krapp, K. Kristensen, A. Ligabue, O. B. Lutnæs, J. I. Melo, K. V. Mikkelsen, R. H. Myhre, C. Neiss, C. B. Nielsen, P. Norman, J. Olsen, J. M. H. Olsen, A. Østed, M. J. Packer, F. Pawłowski, T. B. Pedersen, P. F. Provasi, S. Reine, Z. Rinkevicius, T. A. Ruden, K. Ruud, V. Rybkin, P. Salek, C. C. M. Samson, A. Sánchez de Merás, T. Saue, S. P. A. Sauer, B. Schimmelpfennig, K. Sneskov, A. H. Steindal, K. O. Sylvester-Hvid, P. R. Taylor, A. M. Teale, E. I. Tellgren, D. P. Tew, A. J. Thorvaldsen, L. Thøgersen, O. Vahtras, M. A. Watson, D. J. D. Wilson, M. Ziolkowski, and H. Ågren, *WIREs Comput. Mol. Sci.*, 2014, **4**, 269–284

¹⁶ Dalton, a molecular electronic structure program, Release Dalton2018.2 (2019), <http://daltonprogram.org>

Table S5. Calculated transition energies, oscillator strengths, and average dipole moments for compound **8a**. Vertical excitation and emission energies were calculated at the XMCQDPT2[2]/SA(2)-CASSCF(16,14)/(aug)-cc-pVTZ level of theory in the MP2/(aug)-cc-pVTZ and XMCQDPT2/CASSCF(14,13)/(aug)-cc-pVTZ geometries, respectively. Oscillator strengths and average dipole moments were calculated as the zeroth order XMCQDPT2 properties.

	Energy, Hartree		Average dipole moment, Debye	
	Ground-state geometry	Excited-state geometry	Ground-state geometry	Excited-state geometry
S₀	-848.6718114	-848.6556788	5.6	5.9
S₁	-848.5487122	-848.5603918	7.0	7.2
	Vertical transition energy, eV (nm)			Oscillator strength
S₀→S₁	3.35 (370)			0.3
S₁→S₀	2.59 (478)			0.2

Table S6. Calculated two-photon absorption properties for compound **8a**. The excitation energies and cross-sections were calculated using TDDFT CAM-B3LYP functional in (aug)-cc-pVTZ basis set. Note that the S₀-S₁ transition energy is overestimated by TDDFT as compared to the XMCQDPT2 results. Also, TDDFT/CAM-B3LYP two-photon absorption strengths are known to be 2-3 times smaller than those obtained using high-level coupled-cluster theory EOM-EE-CCSD for the neutral GFP chromophores ($\sigma=4.90[4.85]$ GM vs. 14.68 GM calculated at the CAM-B3LYP/aug-cc-pVD[T]Z and EOM-EE-CCSD/mod-d-aug-cc-pVDZ levels for the 4-(*p*-hydroxybenzylidene)-imidazolidin-5-one molecule).¹⁷

Two-photon absorption S ₀ →S ₁						
State	Energy, Hartree	2ω, Hartree	ΔE[2ω], eV	Excitation wavelength ω, nm	Polarization	σ, GM
S₀	-850.0550825	0.1485	4.04	614	Linear	5.70
S₁	-849.9066100				Circular	4.91

¹⁷ M.T. P. Beerepoot, D.H. Friese, N.H. List, J. Kongsted, K. Ruud, *Phys. Chem. Chem. Phys.* 2015, **17**, 19306.

Cartesian coordinates of the optimized structures of compound 8a in Å

Ground state (S_0) structure optimized at the MP2/(aug)-cc-pVTZ level of theory

Energy = -848.623647 Hartree

N	-1.663057231800	1.177937832600	-3.297723079600
C	-1.723799953400	2.454878634100	-3.601444474700
C	-2.126608354900	1.111229792300	-1.995849473300
C	-2.462344297200	2.384083623600	-1.525391952700
N	-2.208292506300	3.226285473100	-2.562249887700
H	-1.431483012800	2.890190877900	-4.541695044200
H	-2.330321708300	4.226717769400	-2.544476361800
C	-2.379783720000	-0.003975461800	-1.165439889900
C	-2.254571375800	-1.394348832100	-1.614107420500
C	-2.537155029700	-1.742238799600	-2.940814665000
C	-1.861229698400	-2.382861278300	-0.702221799000
C	-2.450896072800	-3.072820991200	-3.336298329600
C	-1.765972433700	-3.708676219600	-1.110520990800
C	-2.067516897400	-4.056973979700	-2.426075738000
H	-1.589046379700	-2.107296443800	0.308846394400
H	-2.680040327900	-3.341746490700	-4.358067126300

H	-1.448527881800	-4.465729878000	-0.407071521700
O	-2.958513964000	2.733169128600	-0.379220262000
H	-1.995039541000	-5.088430716500	-2.742247650900
N	-2.773753132400	0.277496676200	0.057440492200
H	-3.061567033000	-0.510562556200	0.624585312300
B	-2.797138128000	1.714903856100	0.726622770500
H	-2.820975927100	-0.973322882800	-3.643561965700
F	-1.589815739600	1.919379478500	1.350344319600
F	-3.868694598500	1.787640805000	1.569913621100

First excited state (S1) structure optimized at the XMCQDPT2[2]/SA(2)-CASSCF(14,13)/(aug)-cc-pVTZ level of theory

Energy = -848.560864 Hartree

N	-2.131736091100	1.276869440200	-3.422867693700
C	-2.119425686100	2.598536873700	-3.667254333200
C	-2.302531128600	1.158194935700	-2.080995162000
C	-2.430967114100	2.467430410000	-1.486333599500
N	-2.297656435900	3.346663479600	-2.539038995900
H	-1.973124744700	3.041090520600	-4.639564588100
H	-2.324067998400	4.353930807500	-2.460839590300
C	-2.486702363700	-0.044809164600	-1.260095085600

C	-2.265767101400	-1.398650547500	-1.618976007400
C	-1.856821999200	-1.774494696200	-2.933729491000
C	-2.457492128800	-2.435280405700	-0.657484642800
C	-1.665336873300	-3.114695456400	-3.256032586300
C	-2.264997199000	-3.771040657600	-1.001300972600
C	-1.873789007300	-4.126130025100	-2.302174085400
H	-2.709744289700	-2.188588534900	0.367178974600
H	-1.356494723400	-3.376901756900	-4.260133082900
H	-2.408180094100	-4.537573370600	-0.250396682700
O	-2.621069882200	2.835161327500	-0.277020858300
H	-1.723478871000	-5.165352299900	-2.563059414300
N	-3.088443990800	0.369304149300	-0.083888778500
H	-3.595105571200	-0.346388367300	0.431283967800
B	-2.686297348600	1.644925699500	0.733418675900
H	-1.705354486100	-1.006994007700	-3.679917244900
F	-1.425304604600	1.509856800400	1.255260872400
F	-3.655663626600	1.933391694200	1.644010680800